

A Thesis Submitted for the Degree of PhD at the University of Warwick

Permanent WRAP URL:

<http://wrap.warwick.ac.uk/136484>

Copyright and reuse:

This thesis is made available online and is protected by original copyright.

Please scroll down to view the document itself.

Please refer to the repository record for this item for information to help you to cite it.

Our policy information is available from the repository home page.

For more information, please contact the WRAP Team at: wrap@warwick.ac.uk

**Novel Star-shaped
Polymeric Architectures by
Copper (I) Mediated
Living Radical Polymerisation**

**By
Benjamin Wong**

A thesis submitted for the fulfillment of
the requirements for the degree of
Doctor of Philosophy in Chemistry

University of Warwick
Department of Chemistry

October 2003

Table of Contents

Chapter 1: Introduction and literature review

1.0	Introduction to polymer chemistry.....	1
1.1	Chain growth polymerisation.....	3
1.2	Free radical polymerisation	4
1.3	Free radical initiation and propagation.....	4
1.4	Chain transfer	6
1.5	Free radical termination.....	7
1.6	Characteristics of a free radical polymerisation	8
1.7	Ionic polymerisation systems	9
1.8	Living polymerisation systems	10
1.9	Living radical polymerisation.....	13
1.10	Iniferter systems	14
1.11	Nitroxide mediated polymerisation	15
1.12	Radical addition fragmentation chain transfer polymerisation (RAFT)..	17
1.13	Transition metal mediated living radical polymerisation	19
1.14	Rhodium mediated living radical polymerisation	21
1.15	Palladium mediated living radical polymerisation	22
1.16	Ruthenium mediated living radical polymerisation	22
1.17	Nickel mediated living radical polymerisation.....	25
1.18	Iron mediated living radical polymerisation.....	27
1.19	Copper mediated living radical polymerisation	29
1.20	Star polymers	36

1.21	Cyclodextrins.....	38
1.22	Cyclodextrin inclusion complexes.....	39
1.23	Cyclodextrin derivatives	40
1.24	Industrial uses of cyclodextrins	41
1.25	Summary.....	42
1.26	References	43

Chapter 2: Synthesis and Characterisation of Star Polymers with 21-arms by Copper (I) Mediated Living Radical Polymerisation

2.0	Introduction.....	53
2.1	Chemical Modification of β CD.....	55
2.1.1	Synthesis of heptakis(2,3,6-tri- <i>O</i> -(2-bromo-2-methylpropionyl)- β -cyclodextrin (21-Br-CD) multifunctional initiator for copper (I) mediated living radical polymerisation	56
2.1.1.1	Infra red spectroscopy characterisation of 21-Br-CD.....	57
2.1.1.2	^1H NMR spectroscopy characterisation of 21-Br-CD	58
2.2	Copper (I) mediated living radical polymerisation initiated by 21-Br-CD	58
2.2.1	Suitable Reaction Conditions for the LRP of MMA initiated by 21-Br-CD.....	59
2.2.2	Suitable Reaction Conditions for the LRP of Styrene initiated by 21-Br-CD.....	64
2.3	Molecular Weight Analysis.....	68
2.3.1	Molecular Weight Determination by Low Angle Laser Light Scattering	69

2.3.2	Molecular Weight Determination by Static Light Scattering.....	73
2.4	Conclusions.....	76
2.5	Chapter 2 References.....	77

Chapter 3: Modification of β CD in the Synthesis and Characterisation of
Star Polymers with 14- and 7-arms by Copper (I) Mediated LRP

3.0	Introduction.....	80
3.1	Primary Face Modification of β CD.....	81
3.2	Secondary Face Modification of β CD.....	81
3.3	Protection at the Primary Face for the Synthesis of Heptakis(6- <i>O</i> - <i>tert</i> - butyldimethylsilyl)- β -cyclodextrin.....	82
3.4	Synthesis of Heptakis(2,3-di- <i>O</i> -(2-bromo-2-methylpropionyl)-6- <i>O</i> -(<i>tert</i> - butyldimethylsilyl))- β -cyclodextrin.....	83
3.5	Protection of Both Faces of β CD for the Synthesis of Heptakis(2,3-di- <i>O</i> - acetyl-6- <i>O</i> - <i>tert</i> -butyldimethylsilyl)- β -cyclodextrin.....	86
3.6	Desilylation at the Primary Face.....	88
3.7	Synthesis of Heptakis(2,3-di- <i>O</i> -acetyl-6- <i>O</i> -(2-bromo-2- methylpropionyl))- β -cyclodextrin.....	90
3.8	Copper (I) mediated LRP initiated by 14-Br-CD.....	94
3.8.1	Suitable Reaction Conditions for the LRP of MMA initiated by 14-Br-CD.....	94
3.8.2	Formation of block copolymers.....	101
3.8.3	Suitable Reaction Conditions for the LRP of Styrene initiated by 14-Br-CD.....	107
3.8.4	LRP of <i>n</i> BMA initiated by 14-Br-CD.....	109

3.9	Copper (I) mediated LRP initiated by 7-Br-CD	112
3.9.1	LRP of MMA initiated by 7-Br-CD	113
3.9.2	LRP of PEGMA initiated by 7-Br-CD	116
3.10	Analysis of Polymeric Arms by Hydrolysis of Star Polymers	119
3.11	Conclusions	123
3.12	Chapter 3 References	124

Chapter 4: Preparation of Porous Membranes by Self Organisation Of Star Shaped Polymers formed by LRP

4.0	Introduction	127
4.1	Experimental set-up.....	130
4.2	Star-shaped polymers used in the preparation of porous membranes ...	131
4.3	Porous membrane formation with β CD star-shaped polymers	134
4.3.1	Effect of solvent on membrane formation.....	134
4.3.2	Effect of the rate of airflow on membrane formation.....	139
4.3.3	Effect of temperature and relative humidity on membrane formation	143
4.3.4	Optimum conditions for the formation of porous membranes ..	147
4.4	Formation of pores with polymer blends.....	148
4.4.1	Effect of pore formation with a blend of star and linear polystyrene.....	149
4.5	Effect of molecular weight on the formation of pores.....	154
4.6	Conclusions	161
4.7	Chapter 4 References.....	163

Chapter 5: Further Modifications of Star-shaped β CD Polymers for the Synthesis of Diblock Copolymers

5.0	Introduction	165
5.1	Modification of the ω -Bromo end groups.....	166
5.2	Deprotection of <i>tert</i> -butyl dimethylsilyl groups.....	173
5.3	Modification at the primary face of a 14-armed PMMA star polymer with deactivated chain ends	174
5.4	Living radical polymerisation of a 14-armed PMMA star β CD polymer functionalised at the primary face with alkyl bromide moieties	176
5.5	Conclusions	179
5.6	Chapter 5 References	180

Chapter 6: Experimental

6.0	General Characterisation	181
6.1	Reagents.....	182
6.2	Purification of copper (I) bromide.....	182
6.3	Synthesis of <i>N</i> - ⁿ -pentyl-2-pyridylmethanimine.....	183
6.4	Synthesis of 2-bromoisobutyryl anhydride.....	184
6.5	Synthesis of heptakis(6- <i>O</i> - <i>tert</i> -butyldimethylsilyl)- β -cyclodextrin.....	185
6.6	Synthesis of heptakis(2,3-di- <i>O</i> -(2-bromo-2-methylpropionyl)-6- <i>O</i> -(<i>tert</i> -butyldimethylsilyl))- β -cyclodextrin	186
6.7	Synthesis of heptakis(2,3,6-tri- <i>O</i> -(2-bromo-2-methylpropionyl)- β -cyclodextrin	187
6.8	Synthesis of heptakis(2,3-di- <i>O</i> -acetyl-6- <i>O</i> - <i>tert</i> -butyldimethylsilyl)- β -cyclodextrin	188

6.9	Synthesis of heptakis(2,3-di- <i>O</i> -acetyl)- β -cyclodextrin.....	189
6.10	Synthesis of heptakis(2,3-di- <i>O</i> -acetyl-6- <i>O</i> -(2-bromo-2-methylpropionyl))- β -cyclodextrin	189
6.11	Polymerisation procedure.....	190
6.12	Isolation and purification of polymers	191
6.13	Copper (I) mediated LRP of MMA initiated by heptakis(2,3,6-tri- <i>O</i> -(2-bromo-2-methylpropionyl))- β -cyclodextrin ([M]:[Cu]:[L]:[I] = 500:2:4:1)	191
6.14	Copper (I) mediated LRP of MMA initiated by heptakis(2,3-di- <i>O</i> -(2-bromo-2-methylpropionyl)-6- <i>O</i> -(<i>tert</i> -butyldimethylsilyl))- β -cyclodextrin ([M]:[Cu]:[L]:[I] = 500:4:8:1)	192
6.15	Copper (I) mediated LRP of MMA initiated by heptakis(2,3-di- <i>O</i> -acetyl-6- <i>O</i> -(2-bromo-2-methylpropionyl))- β -cyclodextrin ([M]:[Cu]:[L]:[I] = 500:4:8:1)	192
6.16	Copper (I) mediated LRP of PMMA- <i>b</i> -PBMA initiated by heptakis(2,3-di- <i>O</i> -(2-bromo-2-methylpropionyl)-6- <i>O</i> -(<i>tert</i> -butyldimethylsilyl))- β -cyclodextrin ([M]:[Cu]:[L]:[I] = 500:4:8:1)	193
6.17	Copper (I) mediated LRP of MMA initiated by ethyl-2-bromoisobutyrate followed by dehalogenation of end groups ([M]:[Cu]:[L]:[I] = 100:1:2:1)	194
6.18	Synthesis of (poly(ethylene glycol) methyl ether)-2-bromoisobutyrate (MeOPEG- <i>I</i> ₄₅)	194
6.19	Copper (I) mediated LRP of styrene initiated by MeOPEG- <i>I</i> ₄₅ macroinitiator.....	195
6.20	Hydrolysis of star-shaped PMMA polymers	196

6.21	Hydrolysis of star-shaped polystyrene polymers.....	196
6.22	Copper (I) mediated LRP of MMA initiated by heptakis(2,3-di- <i>O</i> -(2-bromo-2-methylpropionyl)-6- <i>O</i> -(<i>tert</i> -butyldimethylsilyl))- β -cyclodextrin ([M]:[Cu]:[L]:[I] = 500:4:8:1) followed by dehalogenation of end groups.....	197
6.23	Deprotection of <i>tert</i> -butyldimethylsilyl groups from star-shaped PMMA with deactivated end groups	198
6.24	Attempted synthesis of heptakis(2,3-di- <i>O</i> -(poly(methyl methacrylate)-6- <i>O</i> -(2-bromo-2-methylpropionyl))- β -cyclodextrin	198
6.25	Preparation of microporous polymeric membranes.....	199
6.26	Determination of absolute molecular weight of star-shaped polymers using static light scattering (SLS).....	199
6.27	Chapter 6 References.....	201

Table of Figures

Figure 1.1.1 Chain propagation polymerisation of methyl methacrylate initiated by an anion.....	4
Figure 1.3.1 Decomposition of the free radical initiator AIBN by heat / UV	5
Figure 1.4.1 Chain transfer in the radical polymerisation of MMA mediated by a thiol.....	7
Figure 1.5.1 Termination by combination and disproportionation in the free radical.....	8
Figure 1.7.1 Cationic polymerisation of styrene promoted by a Friedel-Crafts catalyst.....	10
Figure 1.8.1 Group transfer polymerisation of methyl methacrylate	13
Figure 1.10.1 Iniferter mediated polymerisation of methyl methacrylate.	15
Figure 1.11.1 Benzoyl peroxide initiated polymerisation of styrene mediated by TEMPO.....	16
Figure 1.11.2 Structure of unimolecular initiator species in the TEMPO mediated polymerisation of styrene	16
Figure 1.12.1 Proposed mechanism for RAFT polymerisation.....	19
Figure 1.13.1 Mechanism of the Kharasch reaction	20
Figure 1.16.1 Active ruthenium based catalysts for the living radical polymerisation of MMA.....	24
Figure 1.17.1 Kharasch addition / polymerisation of CCl ₄ to MMA mediated by [Ni{(CH ₂ NCH ₃) ₂ C ₆ H ₃ }Br].....	25

Figure 1.18.1 FeCp(CO) ₂ I used to mediate living radical polymerisation of styrene ...	28
Figure 1.19.1 4,4'-di(5-nonyl)-2,2'-bipyridine.....	30
Figure 1.19.2 (<i>N</i> -ethyl-2-pyridylmethanimine) Cu(I) BF ₄	31
Figure 1.19.3 Multidentate amines for the Cu(I) based living polymerisation of styrene, MMA and MA	32
Figure 1.19.4 Quadridentate ligand en(Bn)py	33
Figure 1.19.5 Generic structures of typical initiators	34
Figure 1.20.1 Synthesis of a four-arm star polymer from an inorganic core	37
Figure 1.20.2 Synthesis of a pentafunctional initiator with a β -D-glucose core	38
Figure 1.21.1 Chemical structure and approximate geometric dimension of β -cyclodextrin.....	39
Figure 1.22.1 The thermodynamic equilibrium between cyclodextrin (CD) and guest (G) in aqueous solution.....	40
Figure 2.1.1 Synthesis of 2-bromoisobutyric anhydride	56
Figure 2.1.2 Formation of β CD functionalised with 21 2-bromoisobutyryl groups	56
Figure 2.1.3 Infra red spectra of β CD starting material (blue) and 21-Br-CD (red)	57
Figure 2.2.1 Copper (I) mediated living radical polymerisation of MMA with 21-Br-CD initiator	59
Figure 2.2.2 First order kinetic plot for the LRP of MMA in toluene (50 % v/v) at 60 °C initiated by 21-Br-CD and mediated by Cu(I)Br / <i>N</i> -pentyl-2-pyridylmethanimine	63
Figure 2.2.3 Evolution of molecular weight distribution with conversion for the LRP of MMA in toluene (50 % v/v) at 60 °C initiated by 21-Br-CD and mediated by Cu(I)Br / <i>N</i> -pentyl-2-pyridylmethanimine ([M]:[I]:[Cu]:[L] = 500:1:2:4). Dashed line is M _n (theo)	64

Figure 2.2.4 Evolution of molecular weight distribution with conversion for the LRP of styrene in xylene (50 % v/v) at 110 °C initiated by 21-Br-CD and mediated by Cu(I)Br / <i>N</i> -pentyl-2-pyridylmethanimine ([M]:[I]:[Cu]:[L] = 500:1:2:4). Dashed line is M_n (theo)	66
Figure 2.2.5 First order kinetic plot for the LRP of styrene in xylene (50 % v/v) at 110 °C initiated by 21-Br-CD and mediated by Cu(I)Br / <i>N</i> -pentyl-2-pyridylmethanimine	67
Figure 2.3.1 Zimm plot of a 21-armed PMMA star polymer used to obtain absolute molecular weight	74
Figure 3.3.1 Modification of the primary face of β CD with TBDMSCl in the synthesis of heptakis(6- <i>O</i> - <i>tert</i> -butyldimethylsilyl)- β -cyclodextrin	82
Figure 3.4.1 Synthesis of heptakis(2,3-di- <i>O</i> -(2-bromo-2-methylpropionyl)-6- <i>O</i> -(<i>tert</i> -butyldimethylsilyl))- β -cyclodextrin by esterification with 2-bromoisobutyryl anhydride	84
Figure 3.4.2 ^1H NMR spectra of heptakis(2,3-di- <i>O</i> -(2-bromo-2-methylpropionyl)-6- <i>O</i> -(<i>tert</i> -butyldimethylsilyl))- β -cyclodextrin	85
Figure 3.5.1 Reaction scheme for the protection of β CD at the 6-position with TBDMS and at the 2- and 3-positions with acetyl groups	87
Figure 3.6.1 Desilylation at the 6-position of substituted β CD with boron trifluoride etherate	89
Figure 3.6.2 Proposed mechanism for the deprotection of TBDMS ethers with fluoride anion	89
Figure 3.7.1 Synthesis of the seven-armed multifunctional initiator heptakis(2,3-di- <i>O</i> -acetyl-6- <i>O</i> -(2-bromo-2-methylpropionyl))- β -cyclodextrin	91

- Figure 3.7.2** Synthetic strategy for the formation of heptakis(2,3-di-*O*-acetyl-6-*O*-(2-bromo-2-methylpropionyl))- β -cyclodextrin, a seven-armed multifunctional initiator93
- Figure 3.8.1** Evolution of molecular weight distribution with conversion for the LRP of MMA in toluene (50 % v/v) at 60 °C initiated by 14-Br-CD and mediated by Cu(I)Br / *N*-pentyl-2-pyridylmethanimine ([M]:[I]:[Cu]:[L] = 500:1:4:8). Dashed line is M_n (theo)96
- Figure 3.8.2** First order rate plot for the LRP of MMA at 60 °C initiated by 14-Br-CD and mediated by Cu(I)Br / *N*-pentyl-2-pyridylmethanimine ([M]:[Cu]:[L]:[I] = 500:4:8:1) in toluene (50 % v/w)97
- Figure 3.8.3** First order rate plot for the LRP of MMA at 90 °C initiated by 14-Br-CD and mediated by Cu(I)Br / *N*-pentyl-2-pyridylmethanimine ([M]:[Cu]:[L]:[I] = 500:4:8:1) in toluene (50 % v/w)99
- Figure 3.8.4** Evolution of molecular weight distribution with conversion for the LRP of MMA in toluene (50 % v/v) at 90 °C initiated by 14-Br-CD and mediated by Cu(I)Br / *N*-pentyl-2-pyridylmethanimine ([M]:[I]:[Cu]:[L] = 500:1:4:8). Dashed line is M_n (theo)100
- Figure 3.8.5** PMMA-*b*-P*n*BMA diblock copolymer.....102
- Figure 3.8.6** Evolution of molecular weight M_n with conversion for the LRP of PMMA-*b*-*n*BMA initiated by 14-Br-CD PMMA macroinitiator ($M_n \sim 30000 \text{ g mol}^{-1}$) and mediated by Cu(I)Br / *N*-pentyl-2-pyridylmethanimine ([M]:[Cu]:[L]:[I] = 500:4:8:1) in toluene at 60 °C. Dashed line shows M_n (theo)104
- Figure 3.8.7** First order kinetic plot for the LRP of PMMA-*b*-P*n*BMA initiated by 14-Br-CD PMMA macroinitiator ($M_n \sim 30000 \text{ g mol}^{-1}$) in toluene at 60 °C and mediated by Cu(I)Br / *N*-pentyl-2-pyridylmethanimine.....105

Figure 3.8.8 SEC traces for the formation of PMMA- <i>b</i> -P <i>n</i> BMA diblock copolymers formed from a 14-Br-CD PMMA macroinitiator.....	106
Figure 3.8.9 Evolution of molecular weight with conversion for the LRP of styrene initiated by 14-Br-CD in xylene at 100 °C and mediated by Cu(I)Br / <i>N</i> -pentyl-2-pyridylmethanimine ([M]:[I]:[Cu]:[L] = 500:1:4:8). Dashed line shows M_n (theo).....	108
Figure 3.8.10 First order kinetic plot for the LRP of styrene initiated by 14-Br-CD in xylene at 100 °C and mediated by Cu(I)Br / <i>N</i> -pentyl-2-pyridylmethanimine.....	109
Figure 3.8.11 Evolution of molecular weight with conversion for the LRP of <i>n</i> BMA initiated by 14-Br-CD in toluene at 60 °C and mediated by Cu(I)Br / <i>N</i> -pentyl-2-pyridylmethanimine ([M]:[I]:[Cu]:[L] = 500:1:4:8). Dashed line represents M_n (theo).....	111
Figure 3.8.12 First order kinetic plot for the LRP of <i>n</i> BMA in toluene at 60 °C initiated by 14-Br-CD and mediated by Cu(I)Br / <i>N</i> -pentyl-2-pyridylmethanimine ([M]:[I]:[Cu]:[L] = 500:1:4:8).....	112
Figure 3.9.1 Evolution of molecular weight with conversion for the LRP of MMA initiated by 7-Br-CD in toluene at 60 °C and mediated by Cu(I)Br / <i>N</i> -pentyl-2-pyridylmethanimine ([M]:[I]:[Cu]:[L] = 500:1:4:8). Dashed line represents M_n (theo).....	114
Figure 3.9.2 First order kinetic plot for the LRP of MMA in toluene at 60 °C initiated by 7-Br-CD and mediated by Cu(I)Br / <i>N</i> -pentyl-2-pyridylmethanimine ([M]:[I]:[Cu]:[L] = 500:1:4:8).....	115

Figure 3.9.3 Evolution of molecular weight with conversion for the LRP of PEGMA initiated by 7-Br-CD in toluene at 60 °C and mediated by Cu(I)Br / <i>N</i> -pentyl-2-pyridylmethanimine ([M]:[I]:[Cu]:[L] = 50:1:4:8). Dashed line represents M_n (theo).....	117
Figure 3.9.4 First order kinetic plot for the LRP of PEGMA in toluene at 60 °C initiated by 7-Br-CD and mediated by Cu(I)Br / <i>N</i> -pentyl-2-pyridylmethanimine ([M]:[I]:[Cu]:[L] = 50:1:4:8)	118
Figure 3.10.1 Disconnection of polymeric arms from β CD core by hydrolysis of ester linkages in basic conditions	120
Figure 3.10.2 SEC traces of star-shaped PMMA (M_w 129000 g mol ⁻¹) before hydrolysis (left trace) and linear PMMA (M_n 10800 g mol ⁻¹) after hydrolysis (right trace)	122
Figure 4.0.1 Polystyrene-polyparaphenylene block copolymer for the preparation of microporous polymer membranes	127
Figure 4.1.1 Schematic set-up used in the preparation of microporous membranes ...	131
Figure 4.2.1 Synthesis of 1,2,3,4,6-penta- <i>O</i> -(2-bromo-2-methylpropionyl)-D-glucose for the formation of 5-armed star polymers by LRP	132
Figure 4.2.2 Esterification of MeOPEG with 2-bromoisobutryl bromide in THF	133
Figure 4.2.3 Copper (I) mediated LRP of styrene using MeOPEG macroinitiator in xylene.....	133
Figure 4.3.1 Surface morphology of a film of star-shaped polystyrene with 21 arms cast from a 10 g L ⁻¹ toluene solution	135
Figure 4.3.2 Surface morphology of a film of star-shaped polystyrene with 21 arms cast from a 10 g L ⁻¹ dichloromethane solution	136

Figure 4.3.3 Surface morphology of a film of star-shaped polystyrene with 21 arms cast from a 10 g L ⁻¹ carbon disulfide solution. Pore diameter is ~2 μm	138
Figure 4.3.4 Surface morphology of a film of star-shaped polystyrene with 21 arms using an airflow rate of 1500 mL min ⁻¹	140
Figure 4.3.5 Surface morphology of a film of star-shaped polystyrene with 21 arms using an airflow rate of 1000 mL min ⁻¹	141
Figure 4.3.6 Surface morphology of a film of star-shaped polystyrene with 21 arms using an airflow rate of 500 mL min ⁻¹	142
Figure 4.3.7 Pore formation with a 14-armed star polystyrene at relative humidity 69 % (top image), 75 % (middle image) and 82 % (bottom image)	144
Figure 4.3.8 Pore formation with a 21-armed star polystyrene at relative humidity 43 % (top image), 53 % (middle image) and 81 % (bottom image)	146
Figure 4.4.1 Surface morphology of a linear PEG- <i>b</i> -PST block copolymer after film casting from CS ₂ , relative humidity 71 %, 19 °C and airflow rate 500 mL min ⁻¹	150
Figure 4.4.2 Surface morphology of blends of a 21-armed star-shaped polystyrene polymer with 10 % by weight PEG- <i>b</i> -PST (top), 4 % by weight PEG- <i>b</i> -PST (middle) and 1 % by weight PEG- <i>b</i> -PST (bottom)	151
Figure 4.4.3 Chemical structure of dimethylaminoethyl methacrylate (DMAEMA) ..	153
Figure 4.4.4 Pore formation with a 21-armed star polystyrene polymer blended with 2 % by weight PDMAEMA in CS ₂ at 72 % relative humidity, 20 °C and air flow rate 500 mL min ⁻¹	153
Figure 4.5.1 SEM images showing the surface morphology of 21-armed star polystyrene with increasing molecular weight; 18600 g mol ⁻¹ (top), 43000 g mol ⁻¹ (middle) and 79000 g mol ⁻¹ (bottom)	156

Figure 4.5.2 SEM images showing the surface morphology of 14-armed star polystyrene with increasing molecular weight; 18000 g mol ⁻¹ (top), 43000 g mol ⁻¹ (middle) and 79000 g mol ⁻¹ (bottom).....	158
Figure 4.6.1 Synthesis of a fluorescent monomer based on pyrene.....	162
Figure 5.1.1 Chemical structures of α -(trimethylsiloxy)styrene and <i>p</i> -methoxy- α -(trimethylsiloxy)styrene for the quenching of metal-catalysed LRP.....	167
Figure 5.1.2 Dehalogenation of an alkyl halide R'X with trialkyl tin hydride.....	167
Figure 5.1.3 Possible mechanism of reaction of silyl enol ethers with PMMA for the deactivation of chain end.....	169
Figure 5.1.4 Effect of the addition of tri <i>n</i> butyl tin hydride on the LRP of MMA initiated by ethyl-2-bromoisobutyrate.....	170
Figure 5.1.5 Chain extension reaction with MMA of PMMA quenched with Bu ₃ SnH.....	171
Figure 5.1.6 ¹ H NMR spectra of star-shaped PMMA with carbon-hydrogen bonds at the ω -terminal.....	172
Figure 5.1.7 Dehalogenation of a 14-armed PMMA star polymer with Bu ₃ SnH.....	173
Figure 5.2.1 Deprotection of TBDMS groups from a 14-armed PMMA star polymer.....	173
Figure 5.2.2 ¹ H NMR spectra of a 14-armed star PMMA polymer with TBDMS groups deprotected at the primary face.....	174
Figure 5.3.1 Esterification of a 14-armed PMMA star polymer at the primary face with 2-bromoisobutyryl bromide.....	175
Figure 5.3.2 ¹ H NMR spectra of a 14-armed PMMA star polymer with alkyl bromide initiating sites at the primary face of β CD.....	176

Figure 5.4.1 SEC curves for the formation of a diblock star polymer with 14 PMMA
arms at the secondary face and PMMA arms at the primary face.....178

Table of Tables

<p>Table 2.2.1 Evolution of conversion and molecular weight in the LRP of MMA in toluene (50 % v/v) at 60 °C initiated by 21-Br-CD and mediated by Cu(I)Br / <i>N</i>-pentyl-2-pyridylmethanimine ([M]:[I]:[Cu]:[L] = 500:1:4:8). *Conversion determined by gravimetry.....</p>	62
<p>Table 2.2.2 Evolution of conversion and molecular weight in the LRP of styrene in xylene (50 % v/v) at 110 °C initiated by 21-Br-CD and mediated by Cu(I)Br / <i>N</i>-pentyl-2-pyridylmethanimine ([M]:[I]:[Cu]:[L] = 500:1:4:8). *Conversion determined by gravimetry.....</p>	65
<p>Table 2.3.1 Comparison of M_w values determined from SEC and GPC-LALLS experiments of 21-armed star polymers prepared by Cu(I) mediated LRP. *Determined by $[M_n(\text{theo})] \times [M_w/M_n(\text{SEC})]$.....</p>	71
<p>Table 2.3.2 Refractive indices of PMMA and PST used for LALLS experiments..</p>	72
<p>Table 2.3.3 Comparison of molecular weight data obtained by SLS and GPC-LALLS.....</p>	75
<p>Table 3.8.1 Evolution of conversion and molecular weight in the LRP of MMA in toluene (50 % v/v) at 60 °C initiated by 14-Br-CD and mediated by Cu(I)Br / <i>N</i>-pentyl-2-pyridylmethanimine ([M]:[I]:[Cu]:[L] = 500:1:4:8). *Conversion determined by gravimetry.....</p>	95
<p>Table 3.8.2 Evolution of conversion and molecular weight in the LRP of MMA in toluene (50 % v/v) at 90 °C initiated by 14-Br-CD and mediated by Cu(I)Br / <i>N</i>-pentyl-2-pyridylmethanimine ([M]:[I]:[Cu]:[L] = 500:1:4:8). *Conversion determined by gravimetry.....</p>	98

Table 3.8.3 Kinetic data for the synthesis of a diblock copolymer of PMMA- <i>b</i> -P <i>n</i> BMA using 14-armed PMMA as a macroinitiator.....	103
Table 3.8.4 Kinetic data for the LRP of styrene initiated by 14-Br-CD in xylene at 100 °C and mediated by Cu(I)Br / <i>N</i> -pentyl-2-pyridylmethanimine ([M]:[I]:[Cu]:[L] = 500:1:4:8).....	107
Table 3.8.5 Kinetic data for the LRP of <i>n</i> BMA initiated by 14-Br-CD in toluene at 60 °C and mediated by Cu(I)Br / <i>N</i> -pyridyl-2-methanimine ([M]:[I]:[Cu]:[L] = 500:1:4:8).....	110
Table 3.9.1 Evolution of molecular weight for the LRP of MMA initiated by 7-Br-CD and mediated by copper (I) / <i>N</i> -pentyl-2-pyridylmethanimine in toluene at 60 °C ([M]:[I]:[Cu]:[L] = 500:1:4:8). *Conversion determined by gravimetry.....	113
Table 3.9.2 Kinetic data for the LRP of PEGMA initiated by 7-Br-CD in toluene at 60 °C and mediated by copper (I) / <i>N</i> -pentyl-2-pyridylmethanimine ([M]:[I]:[Cu]:[L] = 50:1:4:8). *Conversion determined by ¹ H NMR.....	116
Table 4.3.1 Reaction conditions used to investigate solvent effects in the formation of membranes using a 21-armed star polystyrene ($M_w = 43000 \text{ g mol}^{-1}$, PDI = 1.08).....	135
Table 4.3.2 Reaction conditions used to investigate the effect of varying the rate of airflow in the formation of membranes using a 21-armed star polystyrene ($M_w = 43000 \text{ g mol}^{-1}$, PDI = 1.08).....	139
Table 4.3.3 Reaction conditions used to assess the effect of relative humidity and temperature on pore formation. 10 g L ⁻¹ of 14-armed polystyrene ($M_n = 14000 \text{ g mol}^{-1}$) and 21-armed polystyrene ($M_n = 43000 \text{ g mol}^{-1}$) in CS ₂ with an airflow rate of 1000 mL min ⁻¹ was used.....	143

Table 4.4.1 Experimental conditions used to investigate the effect of the addition of a linear block copolymer to a 21-armed star polystyrene polymer in CS ₂	150
Table 4.5.1 Experimental conditions to investigate the effect of molecular weight on pore formation. A 10 g L ⁻¹ solution in CS ₂ was used in all experiments. *Shoulder peak at high molecular weight observed in SEC trace.....	155
Table 4.5.2 Measurement of average pore diameter of 21-armed polystyrene with differing molecular weights.....	157
Table 4.5.3 Measurement of average pore diameter of 21-armed polystyrene with differing molecular weights. *Heterogeneous pore sizes.....	159
Table 5.4.1 Evolution of molecular weight for the formation of diblock star polymers.....	178

Table of Equations

Equation 1.3.1 Calculation of average kinetic chain length in a free radical polymerisation.....	6
Equation 1.8.1 Derivation of first order kinetics of a living polymerisation.....	12
Equation 2.3.1 Calculation of M_n (theo) where $[M_0]$ and $[I_0]$ are the initial concentrations of monomer and initiator respectively, FW(monomer) and FW(initiator) are the formula weight of monomer and initiator respectively, and f is the initiator functionality.....	68
Equation 2.3.2 Calculation of the Rayleigh factor due to a polymer solute.....	70
Equation 2.3.3 Determination of weight-average molecular weight by LALLS.....	70
Equation 2.3.4 Zimm relationship between molecular weight M , concentration c and Rayleigh ratio R	73

Acknowledgements

I would like to thank my academic supervisor Professor David Haddleton for all the support, encouragement and advice that he has given me during my studies over the last three years. I would also like to thank all the members of the Warwick Polymer Group, past and present, for all the fun that they have provided during my Ph.D studies.

In particular, I would like to thank Dr Kohji Ohno, a post-doctoral research assistant from Kyoto University, for his constant help and advice throughout this project whilst he was working in the Warwick Polymer Group. Many thanks Kohji.

I am grateful to the EPSRC for providing the financial support for this project. Thanks also to Steve York in the Department of Physics for allowing me unlimited use of the scanning electron microscope and to Dr Sagrario Pascual for her help with the membrane structures.

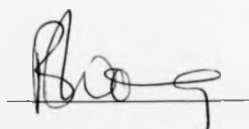
I would also like to acknowledge the University Music Centre, and particularly the University of Warwick Wind Orchestra, for providing weekly distractions to my studies.

Finally, a special thank you to my mum and dad for their support during my Ph. D studies and especially to Emma for putting up with me in the last few months of writing up and her constant nagging for me to get it finished!

Declaration

All experimental work reported within this thesis is original research work performed by the author in the Department of Chemistry, University of Warwick between October 1999 and October 2002. No material contained herein has been submitted for any other degree to this, or any other, institution. Where collaboration has been necessary, the collaborator has been named and the extent of the collaboration made clear.

Results from other authors are referenced in the usual manner throughout the text.



Benjamin Wong

Date: 3/12/03

Abstract

This thesis has investigated the use of copper (I) mediated living radical polymerisation to form well-defined star-shaped polymers with a β -cyclodextrin core using the core-first approach.

Multifunctional initiators based on β -cyclodextrin were synthesised using appropriate protection and deprotection chemistry to precisely pre-determine the functionality. By the careful chemical modification of β -cyclodextrin, multifunctional initiators with precisely 21, 14 and seven initiating sites could be synthesised.

Suitable reaction conditions to provide well-defined star-shaped methyl methacrylate and styrene using copper (I) mediated living radical polymerisation were determined for the multifunctional initiators. The extent of termination reactions by star-star coupling was minimised by using a low concentration of initiating species and employing relatively low reaction temperatures. The molecular weights of the star-shaped polymers were assessed using size exclusion chromatography and light scattering techniques. The linear polymeric arms could be independently assessed by cleaving them from the β -cyclodextrin core and analysing them using size exclusion chromatography.

Highly-ordered porous membrane structures are formed from star-shaped poly(styrene) polymers under certain humid conditions. The optimum conditions for the formation of these honeycomb structures have been investigated and the factors that affect the pore-size have been determined. Functionalisation of the pores were also investigated.

Abbreviations

% wt	% weight
[M ₀]	initial monomer concentration
[M _t]	monomer concentration at time t
[Pol*]	concentration of active species in LRP
2EIBr	ethyl-2-bromoisobutyrate
acac	acetyl acetate
AIBN	azo isobutyryl nitrile
Alk.	alkyl
Ar.	aromatic
ATP	atom transfer polymerisation
ATRC	atom transfer radical cyclisation
ATRP	atom transfer radical polymerisation
βCD	β-cyclodextrin
Bipy	2,2'-dipyridyl
bp.	boiling point
BPO	benzoyl methacrylate
7-Br-CD	heptakis(2,3-di- <i>O</i> -acetyl-6- <i>O</i> -(2-bromo-2-methylpropionyl))-β-cyclodextrin
14-Br-CD	heptakis(2,3-di- <i>O</i> -(2-bromo-2-methylpropionyl)-6- <i>O</i> -(<i>tert</i> -butyldimethylsilyl))-β-cyclodextrin
21-Br-CD	heptakis(2,3,6-tri- <i>O</i> -(2-bromo-2-methylpropionyl))-β-cyclodextrin
CD	cyclodextrin

Conv.	conversion
Cp	cyclopentadiene
CVA	4,4'-azobis-4-cyano valeric acid
DCM	dichloromethane
DEPN	<i>N-tert-butyl-N</i> -[1-diethylphosphono-(2,2-dimethylpropyl)] nitroxide
DMAEMA	dimethyl aminoethyl methacrylate
DMF	<i>N,N</i> -dimethylformamide
DNA	deoxyribose nucleic acid
DP	degree of polymerisation
DRI	differential refractive index
ESR	electron spin resonance
eV	electron volts
f	initiator functionality
FW	formula weight
GPC	gel permeation chromatography
IR	infra red
k_d	rate constant of dissociation
k_p	rate constant of propagation
k_t	rate constant of termination
k_{tr}	rate constant of chain transfer
LALLS	low angle laser light scattering
LRP	living radical polymerisation
M	monomer
MA	methyl acrylate

Me	methyl
MeOPEG	poly(ethylene glycol) methyl ether
MeOPEG-L ₄₅	(poly(ethylene glycol) methyl ether)-2-bromoisobutyrate with 45 repeating units
MHz	mega hertz
Mins.	minutes
MMA	methyl methacrylate
M _n	number average molecular weight
MSC	<i>p</i> -methoxybenzenesulfonyl chloride
M _w	weight average molecular weight
MWD	molecular weight distribution
N _a	Avogadro constant
nBMA	n-butyl methacrylate
NMR	nuclear magnetic resonance
PBA	poly(butyl acrylate)
PDi	polydispersity index
PEG	polyethylene glycol
PEGMA	polyethylene glycol methacrylate
PMMA	poly(methyl methacrylate)
ppm	parts per million
PST	poly(styrene)
Pyr.	pyridyl
R _θ	Rayleigh factor
RAFT	reversible addition fragmentation transfer
SEC	size exclusion chromatography

SEM	scanning electron microscopy
SLS	static light scattering
ST	styrene
TBDMS	<i>tert</i> -butyl dimethylsilyl
TBDMSCl	<i>tert</i> -butyl dimethylsilyl chloride
TBHPO	<i>tert</i> -butyl hydroperoxide
TEMPO	2,2,6,6-tetramethylpiperidinyl-1-oxyl
THF	tetrahydrofuran
TMEDA	tetramethyl ethylenediamine
TMS	tetramethyl silane
TMSCl	trimethylsilyl chloride
UV	ultra violet
v/v	volume / volume
v/w	volume / weight
λ	wavelength

Chapter 1

Introduction and Literature Review

1.0 Introduction to polymer chemistry

The role that polymeric materials play in our everyday lives cannot be underestimated. Indeed, the very existence of life itself is based around natural polymers that include proteins (composed of poly(amino acids)), starch and cellulose. These materials are all formed by the chemical linking of individual units known as monomers and the word polymer is derived from the two Greek words *poly* and *meros*, meaning “many parts”. The advent of synthetic materials has made possible the development of so many devices in everyday use including important advances in information technology. To keep pace with these advances in technology, the polymer chemist plays a key role in helping to meet the growing demands of offering more superior properties to these materials whilst keeping production costs and environmental concerns at a minimum. The exploitation of natural polymeric materials has been known for many centuries where these materials were put to use for clothing and to provide shelter. At this time, little was known about the chemical and molecular structures of these materials and the materials were chosen merely on their physical properties. Scientists first became interested in studying the properties of polymeric materials early in the nineteenth century once natural rubbers had become incorporated into clothing. In 1839, the Goodyear company discovered the vulcanisation process that involved cross-linking polymer chains with disulfide bridges¹ that had the effect of increasing the mechanical strength of the natural rubbers. This process allowed the natural rubbers to have a broader range of applications. In the same year, Simon demonstrated the polymerisation

of styrene² which allowed for the production of synthetic rubbers from styrene / diene mixtures. Also around this time the first commercial thermosetting resin, known as Bakelite, was produced by Baekeland³. Bakelite, used as an electrically insulating material, was formed by a method of polymerisation that involved the condensation of phenols with formaldehyde.

In 1920, Staudinger proposed the idea of chain polymerisation initiated by a radical species. He initially thought that the structures of polymers were large macrocycles where monomers were linked head to tail⁴. The unique properties of these materials were thought to be a direct result of their high molecular weights and an augmentation of the Van der Waals forces that were acting along the length of the polymeric chains⁵. Staudinger was awarded a Nobel Prize in 1953 for his discoveries in the field of macromolecular chemistry. In 1928 Carothers was working on the application of polyesters for their use as fibres at the Du Pont company⁶ before realising that polyamides have a higher melting temperature than polyesters. As a result, the first synthetic polyamide fibres were produced and these novel materials soon replaced the natural materials. Of particular note was the production of the polyamide Nylon 6/6 that was used for such applications as parachutes and ropes in the Second World War. Ziegler discovered, in 1955, that the addition of a transition metal compound to the polymerisation of ethene resulted in the formation of high molecular weight, high density polyethylene at a relatively low temperature and pressure^{7, 8}. As a development of this initiating system, Natta demonstrated the polymerisation of propylene and 1-butene and discovered that the high density and crystalline structures of these poly(olefins) was a result of the stereoregularity conferred by the polymerisation mechanism^{9, 10}. Ziegler and Natta were jointly presented with the Nobel Prize in 1963

in recognition of the significance of their catalytic process for the synthesis of high density linear poly(ethylene) and isotactic poly(propylene).

Nowadays, the development of materials with properties that are not available from natural products is becoming more commonplace and provides continuing challenges to the modern polymer chemist. There are many exciting developments in providing new polymeric materials for applications such as optical display technologies, contact lenses, ink additives for printers, circuit boards and electrically conductive polymers for a host of applications.

This chapter highlights some of the many different methods that are available for the synthesis of polymers and each method has its advantages and disadvantages. The final selection of method chosen for the synthesis of a particular product will be governed by its efficiency and cost.

1.1 Chain growth polymerisation

A special case of chain growth polymerisation occurs when unsaturated vinyl monomers react. In an addition polymerisation there is no elimination of any molecules, unlike in a condensation polymerisation where water is eliminated^{11, 12}. In radical and anionic polymerisation systems, the nucleophilic (initiator) species reacts at the least hindered end of a substituted unsaturated vinyl species to produce a new carbon-carbon bond (Figure 1.1.1). The reactive centre is transferred to the substituted carbon atom at the other end of the double bond and this centre is then able to react with the unsubstituted end of another monomer unit to realise chain propagation.

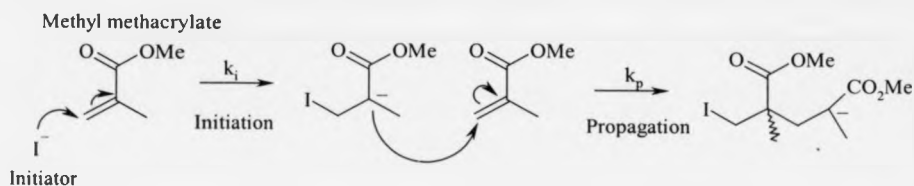


Figure 1.1.1 Chain propagation polymerisation of methyl methacrylate initiated by an anion.

The propagation step of polymerisations initiated by an anion involve the transfer of an electron pair to form a new anion. The propagation step of polymerisations initiated by a radical involves the transfer of a single electron from the initiator. A carbon-carbon bond is then formed by the donation of a single electron from the double bond of the vinyl species leaving a radical on the adjacent carbon atom of the vinyl species.

1.2 Free radical polymerisation

Free radical initiated polymerisations are a common synthetic route to the production of speciality polymers with high molecular weight¹³. The mechanism of free radical polymerisation is well understood and has remained unmodified since it was first reported over sixty years ago¹⁴.

1.3 Free radical initiation and propagation

The homolytic cleavage by photolysis or pyrolysis of an unstable bond forms free radicals. Azo containing compounds such as azoisobutyronitrile (AIBN) (Figure 1.3.1) and 4,4'-azobis-4-cyanovaleric acid (CVA), or peroxides such as dibenzoyl peroxide (BPO) and *tert*-butyl hydroperoxide (TBHPO) are common radical initiators.

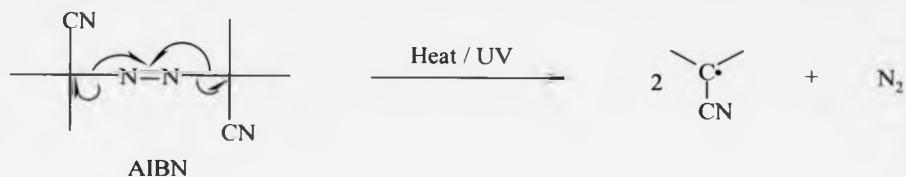


Figure 1.3.1 Decomposition of the free radical initiator AIBN induced by heat / UV.

Free radical species of this type are highly reactive and extremely unstable and hence the lifetime of a free radical is very short. The free radical will readily attack a substituted vinyl monomer resulting in the formation of another radical species. The high reactivity of these radical species mean that chain propagation occurs very rapidly and so polymers with a high molecular weight are produced very quickly. The rate of propagation is proportional to the concentration of the radical and to the concentration of the monomer.

Since the decomposition of the free radical initiators are not instantaneous, the molecules decompose slowly with an associated half life and so polymer chains will propagate at different times. A free radical polymerisation system will contain, at any one time, unreacted monomer, intact initiator, high molecular weight polymer that has ceased propagating, and propagating polymer chains that approach high molecular weights over a very short time. A linear increase of the number average molecular weight (M_n) with conversion is not observed since high molecular weight polymers are formed even at low conversions. The molecular weight is dependant on the concentration and nature of the initiator species (Equation 1.3.1).

$$v = \frac{k_p[M]}{2(fk_d k_t[I])^{1/2}}$$

Where:

v = average kinetic chain length

k_p = rate constant of polymerisation

f = initiator efficiency (fraction of radicals from homolysis that initiate polymerisation)

k_d = rate constant of dissociation of initiator

k_t = rate constant of termination

Equation 1.3.1 Calculation of average kinetic chain length in a free radical polymerisation.

1.4 Chain transfer

Free radical species are very reactive and are able to extract hydrogen atoms from a variety of species including hydrocarbons. If a hydrogen atom is abstracted from a propagating polymer chain, the polymer chain will cease to propagate and the site of abstraction becomes the new site of propagation. This process is known as chain transfer to polymer. Chain transfer can also occur with small molecules in the polymerisation medium and even to monomer in some cases. Chain transfer reduces the average length of each polymer chain but it does not reduce the number of propagating species in the solution. The chain transfer mechanism is important in the production of low molecular weight polymers where chemical additives that promote chain transfer

are used. These chain transfer agents possess a relatively labile [X]-H bond so that chain transfer can readily occur. Chain transfer agents such as thiols¹⁵ (Figure 1.4.1) are being replaced by catalytic additives based on cobalt (II) macrocycles¹⁶ and are used at ppm levels and so do not impart any colour, toxicity or odour to the final polymer.

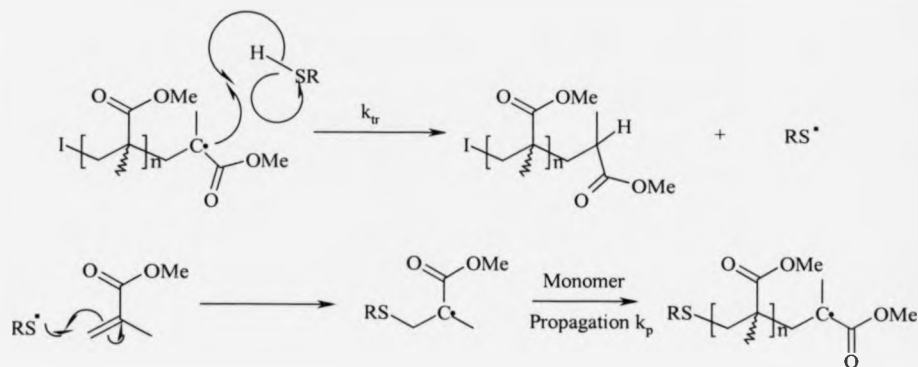


Figure 1.4.1 Chain transfer in the radical polymerisation of MMA mediated by a thiol.

1.5 Free radical termination

When two radical species (polymer or initiator fragment) are close enough to react, a stable covalent bond is formed that cannot be broken under the reaction conditions. Propagation can no longer occur and the polymer chain is deemed a “dead” chain. There are two possible outcomes when two radicals approach each other. In the first scenario, the two radicals can combine to form a single long polymer chain that is formed from the two propagating chains. This is known as termination by combination. In the second scenario, a hydrogen atom can be transferred from one polymer chain to the other polymer chain. This is known as termination by disproportionation (Figure 1.5.1). Termination by disproportionation yields a polymer chain that is terminated by a hydrogen atom and the other polymer chain is terminated with an ω -functionalised double bond. In the free radical polymerisation of MMA, termination by

disproportionation is the prevailing form whereas the polymerisation of styrene, which lacks a labile α -hydrogen atom, has termination by combination as the dominating termination mechanism.

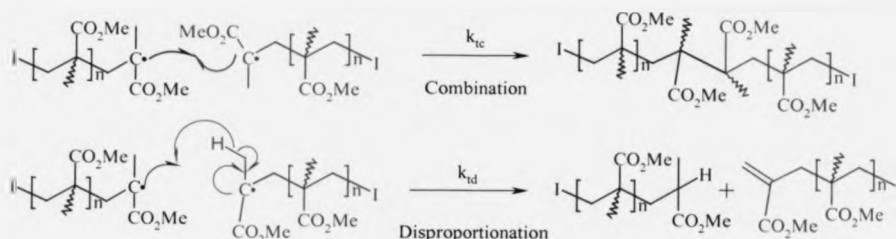


Figure 1.5.1 Termination by combination and disproportionation in the free radical polymerisation of MMA between polymer chain A (blue) and polymer chain B (red).

Both termination by combination and disproportionation occur in a free radical polymerisation and the random process is governed by the concentration of radicals. As a result of these termination processes, a broad molecular weight distribution is observed.

1.6 Characteristics of a free radical polymerisation

Free radical polymerisations are extremely robust and can tolerate a wide variety of functional groups. Almost any molecule possessing a double bond can be polymerised. Polymers functionalised with hydroxyl groups, acid groups or alkyl amines can be obtained by use of appropriate monomers. It is not necessary to have highly pure monomers that need drying and the radical inhibitors that are added to prevent polymerisation during storage do not need to be removed prior to their use. Free radical polymerisations can be carried out in aqueous media since free radicals are tolerant to water. In suspension polymerisations, the monomer and the initiator (that is soluble in the monomer) are suspended as droplets and stabilised by surfactants in the aqueous

media. The behaviour of each droplet can be compared to that of a bulk polymerisation and if the conditions are right, the product is obtained as a solid bead that is isolated by filtration. In the 1920's, the Goodyear Tire and Rubber Company first carried out emulsion polymerisation¹⁷. This process requires a water-soluble initiator to initiate the polymerisation in the aqueous phase. The polymer is obtained as a dispersion of polymeric spheres with a typical diameter of a few hundred nanometers. This is known as a latex and is important in the production of waterborne paints and adhesives. Both suspension and emulsion polymerisation processes are less damaging to the environment compared to solution polymerisation processes and the excellent heat transfer afforded by the aqueous media makes these systems more attractive from a safety standpoint.

1.7 Ionic polymerisation systems

Free radical polymerisations offer a poor degree of control of molecular weight and molecular weight distribution. This is primarily due to the large number of chain termination events that occur between propagating chains in such a process. If the polymerisation is initiated by an ion, termination between two propagating chains will not be able to occur due to charge repulsion and there is no mechanism for combination. A cationic polymerisation system employs an electrophile to initiate the polymerisation of monomers that possess a nucleophilic group. Initiators that have been used in cationic polymerisations include protonic acids¹⁸, Lewis acids (including Friedel-Crafts catalysts)^{19, 20} and iodine²¹. The mechanism of a cationic polymerisation using a Friedel-Crafts catalyst is shown in Figure 1.7.1.

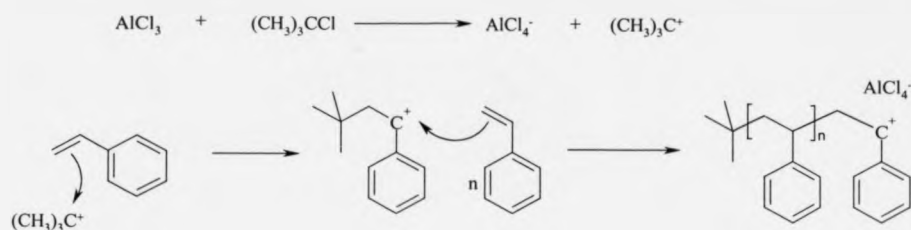


Figure 1.7.1 Cationic polymerisation of styrene promoted by a Friedel-Crafts catalyst.

An anionic polymerisation²² was first reported in the 1940's and a variety of initiators have since been investigated²³ for the polymerisation of monomers bearing an electrophilic substituent. Initiators that have been used in anionic polymerisations include alkali-metal alkyls, Grignard reagents and potassium and lithium in liquid ammonia. Termination of propagating chains is prevented by the repulsion of like charges but chain transfer reactions are dominant due to the transfer of protons from solvent, protic monomers, polymer backbone and impurity. These chain transfer events lead to irreversible termination of the propagating chains. Further side reactions may occur if the monomer possesses multiple sites for nucleophilic attack. The rate of such side reactions and chain transfer events can be reduced relative to the rate of polymerisation if the reaction temperature is reduced.

1.8 Living polymerisation systems

If a polymerisation process proceeds in the absence of any irreversible chain transfer and chain termination reactions then polymer chains will continue to propagate until the supply of all monomer is exhausted. This type of polymerisation process is known as a living polymerisation. In 1956 Szwarc et al. reported the first observation of a polymerisation that had living characteristics²⁴. He demonstrated that the rate of

termination for the polymerisation of styrene using sodium naphthalenide as an anionic initiator system was zero. Furthermore, chain transfer activity was suppressed by the use of highly purified, dry aprotic reagents and so 100 % conversion of styrene to polystyrene was achieved. It was concluded that the lack of chain termination and chain transfer events was due to the charge repulsion between chain ends. A second feed of monomer into this system produced polymers that increased in molecular weight that further demonstrated that the chain ends were not terminated. Elaboration of this type of living polymerisation would create the possibility of complex polymeric architectures including block copolymers. Control over the molecular weight and narrow molecular weight distributions were not always achieved. To overcome this, it was necessary for initiation to be fast relative to the rate of propagation so that all polymer chains begin to grow at the same time (unlike in a free radical polymerisation). If all the chains propagate at the same time and at the same rate then the molecular weight will increase linearly with conversion and narrow molecular weight distributions will be observed. All initiator molecules added to the system will initiate the propagation of one polymer chain and since there are no chain transfer reactions, the average degree of polymerisation (DP) will be equal to the ratio $[\text{Monomer}]:[\text{Initiator}]$. In a living polymerisation system, there is no loss of reactive species during the polymerisation and so first order reaction kinetics are observed as described in Equation 1.8.1.

Rate of polymerisation: $-d[M]/dt = k_p[\text{Pol}^*][M]$

Where k_p = rate constant of propagation and $[\text{Pol}^*]$ is the concentration of active species

Integration gives: $-\ln[M] = k_p[\text{Pol}^*]t + C$

When $t = 0$, $[M] = [M_0]$

Rearrangement gives: $\ln([M_0]/[M_t]) = k_p[\text{Pol}^*]t$

Equation 1.8.1 Derivation of first order kinetics of a living polymerisation.

If the rate of initiation k_i is much greater than the rate of propagation k_p then it will be possible to synthesise polymers with predetermined molecular weights and narrow molecular weight distributions.

The commercial exploitation of living anionic polymerisation systems has so far been limited to the production of styrene and butadiene copolymers used for synthetic rubbers. The need for high purity reagents and low reaction temperatures for the controlled polymerisation of acrylates and methacrylates has prevented living anionic polymerisation having a larger commercial impact.

To overcome the difficulties in the anionic living polymerisation of methacrylates, the Du Pont company^{25, 26} developed group transfer polymerisation. Group transfer polymerisation uses a silyl ketene acetal initiator and the polymerisation is catalysed by either a nucleophile or a Lewis acid. Propagation has been shown to proceed via a concerted mechanism whereby the silane group of the initiator is transferred to the chain end as the new C-C bond is formed (Figure 1.8.1). A wide range of solvents, including DMF, can be used in group transfer polymerisations. Side reactions such as backbiting²⁷ may still occur although the rate of such reactions are decreased due to the concerted nature of the mechanism.

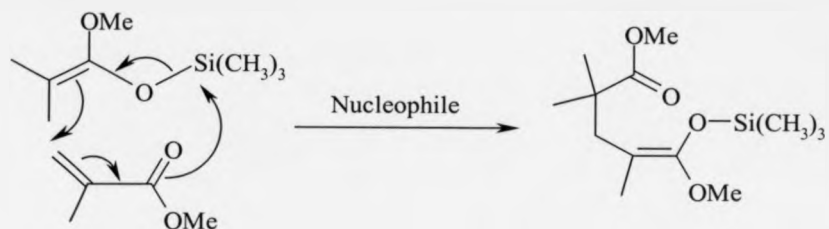


Figure 1.8.1 Group transfer polymerisation of methyl methacrylate.

The exact mechanism of group transfer polymerisation is still in discussion and it is thought that the propagating species is a low concentration of the free anion²⁸. Due to the intolerance of protic functionality in group transfer polymerisation, this process has yet to have a commercial impact.

1.9 Living radical polymerisation

The limited commercial application of living polymerisation systems stem from the need for high purity solvents and reagents, low reaction temperatures, solvents that do not chain transfer and can only exploit a limited variety of monomers. Furthermore, the cost of the initiator and the cost of metal removal in polymers synthesised by group transfer make this process commercially unattractive. Free radical polymerisations on the other hand are very robust, can tolerate a wide range of monomers with different functionalities and can proceed over a wide range of operating conditions but are highly non-selective.

A living radical polymerisation process combines the benefits of a living system with the versatility of a radical process and the reactivity of the radical is reduced. The strategy for controlling the radical polymerisation is to lower the instantaneous concentration of a growing radical species. This is achieved by introducing a covalent dormant species that exists predominantly over, and in fast equilibrium with, the active

radical species. This dynamic and rapid equilibrium minimises the probability of radical bimolecular termination reactions and also gives an equal opportunity of propagation to all polymer chains via the frequent interconversion between the active and dormant chains. In this way, polymers with uniform molecular weight and narrow molecular weight distribution can be produced. The covalent bonds of the dormant species must be activated reversibly and homolytically into the growing radical species by either physical or chemical stimuli.

1.10 Iniferter systems

The first use of the term living radical polymerisation was used by Otsu and Yoshida²⁹ in 1982 to describe iniferter systems that are an extension of the inifer system used by Kennedy et al.³⁰ in the preparation of telechelic polymers via cationic polymerisation. The term iniferters derives from the ability of a compound to *initiate* polymerisation, act as a chain *transfer* agent and *terminate* chains. The initiator incorporates a weak bond that is homolytically activated by either heat or UV light to produce a primary and a secondary radical. The primary radical is stable and is slow to initiate the polymerisation (this is known as the persistent radical) whilst the secondary radical is able to initiate polymerisation and allows chain propagation to occur. Termination reactions between two polymer radicals by combination or disproportionation is reduced when the concentration of iniferter is kept high. Thus, chain transfer and termination by the persistent radical to iniferter is more favourable. Termination of the polymer chains by chain transfer or primary radical, results in a polymer that is ω -functionalised with the persistent radical group. Since this new bond is unstable, it is able to homolytically cleave by either heat or UV light and so propagation can proceed. The absence of irreversible termination reactions renders this process living and the

addition of a second monomer feed allows for further propagation until 100 % monomer conversion to polymer is achieved. However, poor control over molecular weight and molecular weight distribution is observed with these systems because initiation of each polymer chain is slow and does not occur simultaneously.

Efficient iniferter systems have been developed based on the stable organosulfur radical such as the symmetrical dithiuram sulfide³¹ (Figure 1.10.1).

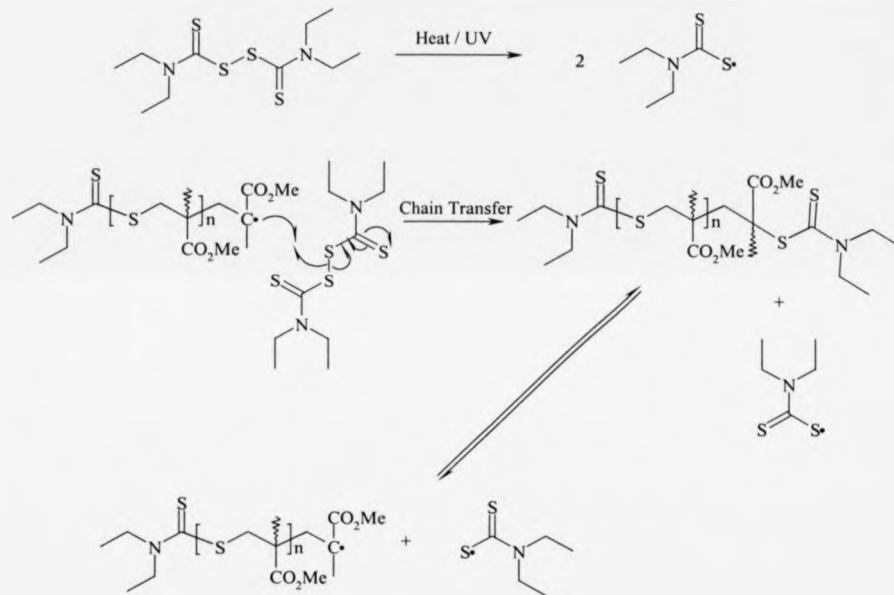


Figure 1.10.1 Iniferter mediated polymerisation of methyl methacrylate.

1.11 Nitroxide mediated polymerisation

As an extension to the stable free radical effect of the iniferter system, Solomon and Rizzardo³² patented the use of nitroxide mediated polymerisations (Figure 1.11.1) to control a radical polymerisation process. Propagating radicals in a nitroxide mediated polymerisation are capped by a stable free radical based on nitroxide such as 2,2,6,6-tetramethylpiperidiny-1-oxyl (TEMPO) (Figure 1.11.2) that is unable to initiate polymerisation itself.

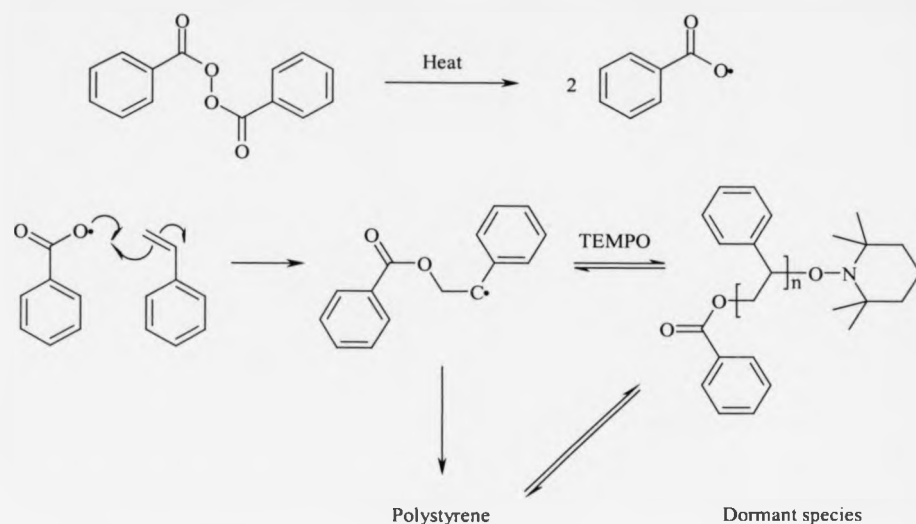


Figure 1.11.1 Benzoyl peroxide initiated polymerisation of styrene mediated by TEMPO.

The C-O bond of the capped species can be homolytically cleaved by heat to allow further free radical propagation and this capped, dormant species can be isolated³³ or used *in situ*³⁴. Fukuda et al.³⁵ and Bon et al.³⁶ have investigated the kinetics of the C-O bond homolysis.

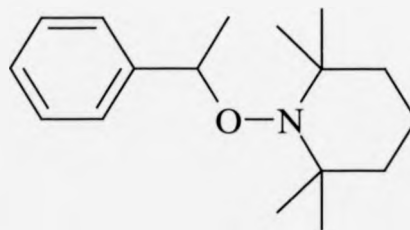


Figure 1.11.2 Structure of unimolecular initiator species in the TEMPO mediated polymerisation of styrene.

Nitroxide mediated polymerisations have been used to prepare polystyrene with a narrow molecular weight distribution ($PDI < 1.5$)³⁷. By modification of the alkyl groups on the nitroxide moiety it has been possible to polymerise acrylates³⁸, dienes³⁹ and vinyl acetate.

Georges et al. achieved well-controlled living polymerisation ($PDI < 1.3$) of styrene using BPO as the radical source together with TEMPO although high temperatures (125 °C) were necessary and only a slow rate of polymerisation was observed⁴⁰. The thermal autoinitiation of styrene by the Mayo⁴¹ process and the disproportionation of the dormant species to an ω -unsaturated species and hydroxyamine complicates the nitroxide mediated polymerisation.

The controlled nitroxide mediated polymerisation of styrenes and 4-vinylpyridine⁴² has not been observed for other monomers such as MMA. Modification of the TEMPO structure at positions other than at the α - position has little effect on the reactivity of the group due to the absence of a delocalised electron system.

However, nitroxide mediated polymerisation is of continued interest due to its ease of use and its absence of any metal species involved. *N-tert-butyl-N*-[1-diethylphosphono-(2,2-dimethylpropyl)] nitroxide (DEPN) has recently been used in the preparation of PST and PBA with a narrow molecular weight distribution⁴³. The nitroxide-mediated polymerisation of acrylic acid has also been recently reported⁴⁴.

1.12 Radical addition fragmentation chain transfer polymerisation (RAFT)

This process is the most recent method to control radical polymerisations and patents were first applied for in 1998^{45, 46}. Dithiocarbamates are used as the mediating species and the process is initiated by a standard free radical initiator such as AIBN that reacts

with the dithiocarbamate. A metastable adduct radical is formed that can be detected by electron spin resonance (ESR) techniques^{47, 48}. This metastable adduct can fragment in two ways to produce a radical and another dithiocarbamate compound. The radical produced is able to initiate polymerisation and propagation occurs similarly to a standard free radical polymerisation. The radical undergoes a chain transfer reaction when it encounters another dithiocarbamate compound (Figure 1.12.1). The growing polymer chain is reversibly capped with the mediator fragment and the dormant and active species are in rapid equilibrium that results in living radical behaviour.

The leaving group R on the sulfur atom has to be a better homolytic leaving group than the polymer chain if good control is to be achieved. The rate of addition / fragmentation should also be fast relative to the rate of polymerisation to ensure that the equilibrium between dormant and active polymer chains is quickly established. Selection of an appropriate X group on the dithiocarbamate is necessary to activate the C=S bond. If the X group contains an alkyl amine functionality, poor control over the polymerisation of styrene, MMA and MA is observed with molecular weight distributions greater than 1.6. However, if the X group contains an aryl amine functionality, better control is observed due to the ability of the nitrogen atom to donate electron density into the sulfide radical system thereby stabilising it and reducing the rate of fragmentation⁴⁹. If the X group is another sulfur atom that contains a good leaving group (R) then the dithiocarbamate mediating group is found at the centre of the two polymer chains and thus serves as a precursor for the synthesis of ABA triblock copolymers⁵⁰. The kinetics and mechanism of the RAFT process is the topic of current research⁵¹⁻⁵⁶.

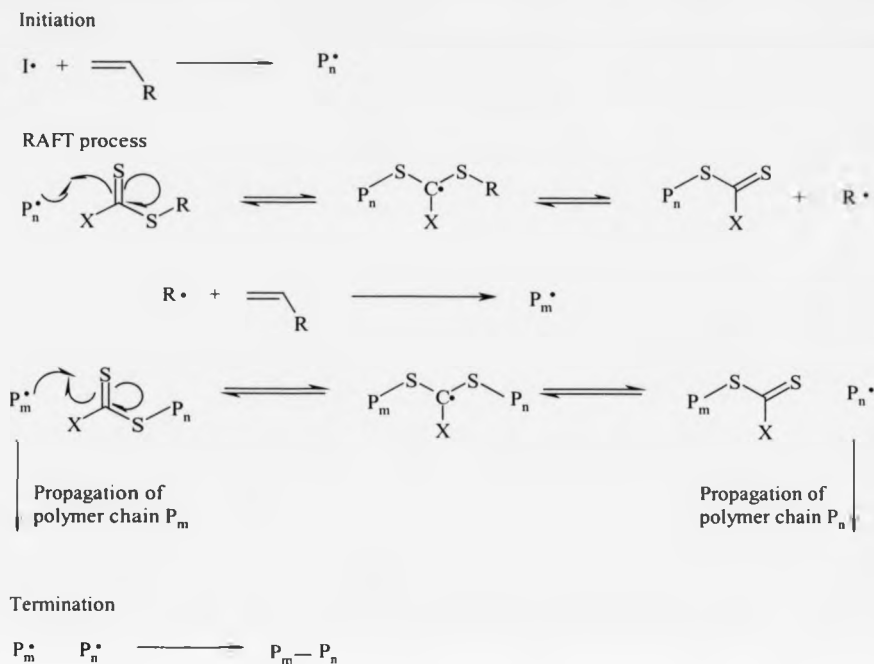


Figure 1.12.1 Proposed mechanism for RAFT polymerisation.

1.13 Transition metal mediated living radical polymerisation

Transition metal mediated living radical polymerisation was first reported almost simultaneously in 1995 by the research groups of Sawamoto⁵⁷ and Matyjaszewski⁵⁸.

The process is based on the Kharasch reaction⁵⁹ where a transition metal that is stabilised by complexing ligands can be oxidised by the transfer of an atom (typically a halogen) from a dormant molecule transforming the latter to an active chain that can undergo polymerisation. In an example of the Kharasch reaction, a weak carbon halogen bond undergoes homolysis in the presence of the transition metal complex and the halogen is transferred to the metal complex. The resulting radical that forms will then undergo addition to the least hindered end of an unsaturated molecule followed by

transfer of the halogen from the metal complex to the other end. This process is known as atom transfer radical addition (ATRA) (Figure 1.13.1).

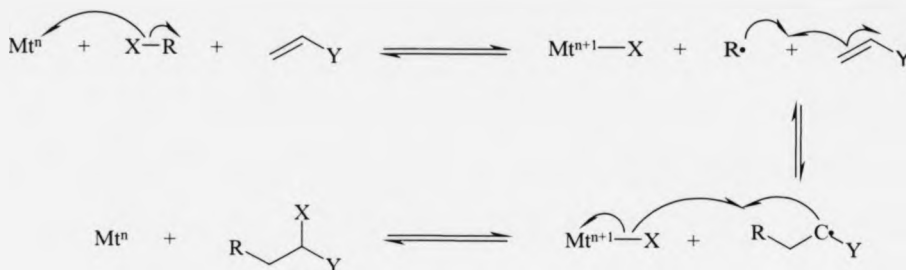


Figure 1.13.1 Mechanism of the Kharasch reaction.

A similar process occurs for intramolecular addition in the formation of ring structures⁶⁰ and this is known as atom transfer radical cyclisation (ATRC).

If the product of addition of R-X also contains a carbon halogen bond that is weakened by the presence of α -electron withdrawing groups, further Kharasch type reactions can occur and this is the principle of the transition metal mediated radical polymerisation of styrenes and (meth)acrylates. This process is referred to as atom transfer radical polymerisation (ATRP). Like other methods of controlled radical polymerisations, the fundamental principle of transition metal mediated living radical polymerisation is to keep the concentration of propagating species low and constant thus minimising bi-radical terminations. In this process, this is achieved by the reversible capping of the propagating species by a halogen atom and establishing a fast equilibrium between the dormant and active species. If the rate of initiation is fast relative to the rate of propagation then all chains will grow at the same time. This can lead to polymers with a narrow molecular weight distribution (typically $\text{PDI} < 1.3$) with M_n determined by the ratio $[\text{M}]:[\text{I}]$.

The initiator used in these systems has a structure that is analogous to that of the monomer that is being polymerised and incorporates a carbon halogen bond that is activated by the transition metal complex. The exact nature of the active catalyst is not well understood and is a topic of current research. Living radical polymerisation has recently been reviewed by Matyjaszewski⁶¹ and Sawamoto⁶².

1.14 Rhodium mediated living radical polymerisation

The reduction of olefins by the Wilkinson's catalyst $\text{RhCl}(\text{PPh}_3)_3$ is well known in organic chemistry and proceeds via a mechanism involving complexation of the substrate to the metal centre. Percec et al. reported that this catalyst was successfully applied to the bulk ATRP of styrene at 130 °C with a *p*-methoxybenzenesulfonyl chloride (MSC) as the initiator⁶³. However, poor control and polymers with high molecular weight distributions ($\text{PDI} = 1.8 - 3.2$) were observed. The molecular weight distributions were found to be lower when the concentration of catalyst was increased but these were still higher than other controlled living radical polymerisations.

In contrast, Teyssie demonstrated the successful ATRP of MMA using 2,2'-dichloroacetophenone⁶⁴ as the initiator in the presence of $\text{RhCl}(\text{PPh}_3)_3$. The PMMA was synthesised with a relatively narrow molecular weight distribution ($\text{PDI} \sim 1.5$) and the polymerisation followed first order kinetics in THF solution. Interestingly, the rate of polymerisation was found to accelerate significantly with a THF / 40 % water solvent system.

Kotani et al. demonstrated the polymerisation of styrene using $[\text{ReO}_2\text{I}(\text{PPh}_3)_2] / \text{Al}(\text{O}^i\text{Pr})_3$ in conjunction with alkyl iodide initiators⁶⁵. The initiating system was almost 100 % efficient and molecular weight distributions of less than 1.5 were observed. The polymerisation was faster than reaction using $\text{RhCl}(\text{PPh}_3)_3$. The system was extended to

the polymerisation of substituted styrenes and similar reaction kinetics were observed for *p*-chlorostyrene and *p*-methylstyrene in toluene at 60 °C. Narrow molecular weight distributions were observed (PDI ~ 1.3)⁶⁶.

1.15 Palladium mediated living radical polymerisation

The first reported use of palladium (0) in polymerisations was by Otsu. He used palladium adsorbed onto carbon black to promote the free radical polymerisation of MMA initiated by chloroform (CHCl₃)⁶⁷. Tsuji reported in 1981 that Pd(OAc)₂ in conjunction with PPh₃ was an efficient promoter of the Kharasch addition of CHCl₃ to olefins with high yields at room temperature⁶⁸. This system was investigated for potential use in the industrial application of living radical polymerisation owing to the stability of the catalyst substituents in water⁶⁹. MMA was polymerised in toluene at 70 °C but the distribution of molecular weights was broad (PDI = 1.6 – 2.3) and the efficiency of the initiator was as low as 30 %. The distribution of molecular weights was improved when the level of PPh₃ was increased but this had the effect of lowering the initiator efficiency to 20 %.

1.16 Ruthenium mediated living radical polymerisation

Living radical polymerisations based on ruthenium complexes are based on the organic reaction of carbon tetrachloride addition across a double bond of an alkene catalysed by [RuCl₂(PPh₃)₃]⁷⁰. The reaction is highly regioselective with the bulky CCl₃ group binding to the least hindered end of the double bond. This degree of control is thought to be afforded by the formation of a radical intermediate that does not escape the co-ordination sphere of the ruthenium^{71, 72}. Living radical polymerisation of MMA is observed when an activating species of methylaluminium bis-(2,6-di-*tert*-

butylphenoxide) is employed and 90 % conversion of MMA is achieved after four hours at 60 °C. First order reaction kinetics were observed and polymers had molecular weights similar to those predicted and low molecular weight distributions ($PDI = 1.3 - 1.4$) were observed⁷³⁻⁷⁶. Styrene was also polymerised by this technique whilst the polymerisation of *N,N*-dimethylacrylamide proceeded at a faster rate at the expense of molecular weight control ($PDI \sim 1.6$)⁷⁷. The effect of additives on the polymerisations showed that hindered Lewis acids such as $Al(O^iPr)_3$, $Ti(O^iPr)_4$ and $Sn(O^iPr)_4$ accelerated the controlled polymerisation whereas metal chlorides such as $TiCl_4$ and $SnCl_4$ were ineffective. It has recently been shown that the addition of amino alcohols can enhance the rate of LRP of MMA with $RuCl_2(PPh_3)_3$. For example, using 2-(diethylamino)ethanol as an additive significantly accelerates the polymerisation (23 h, 91 %, 60 °C) compared to the system without the additive (550 h, 95 %, 80 °C)⁷⁸. The $RuCl_2(PPh_3)_3 / PhCOCHCl_2$ initiating system has been shown to be effective for the living radical polymerisation of MMA in a toluene / water mixture under an inert atmosphere. The addition of $Al(O^iPr)_3$ increased the rate of reaction but the reaction was significantly quicker in the water / toluene mixture than in toluene alone suggesting that complexation of water to the ruthenium catalyst was occurring⁷⁹. Polymerisations mediated by $RuH_2(PPh_3)_4$ proceed at a faster rate when compared with $RuCl_2(PPh_3)_3$ and the addition of a co-catalyst has little effect since the molecular weight distributions are narrow ($PDI < 1.2$)⁸⁰. Good molecular weight control is established by having a fast initiation. When brominated rather than chlorinated α -haloesters are used and the dimeric initiator $(CO_2Me)CH_2C(CH_3)(CO_2Me)Br$ is employed, polymers of narrow distribution are observed.

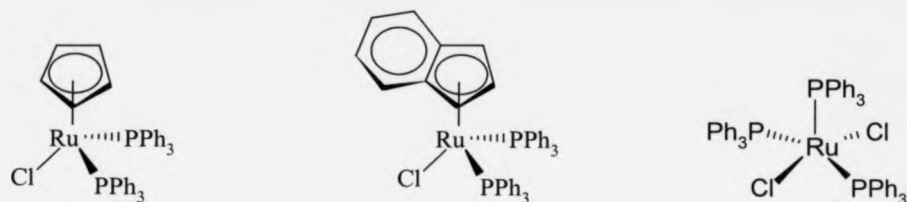


Figure 1.16.1 Active ruthenium based catalysts for the living radical polymerisation of MMA.

The living radical polymerisation of MMA and styrene promoted by ruthenium “half sandwich” type cyclopentadienyl complexes (Figure 1.16.1) has also been reported using CHCl_2COPh as the initiator with an $\text{Al}(\text{O}^i\text{Pr})_3$ activator. Ruthenium indenyl complexes were even more active and did not require a co-catalyst to mediate smooth polymerisation. Polymers produced by this initiating system had very low molecular weight distributions ($\text{PDI} < 1.15$)^{81, 82}.

Heterogeneous ruthenium mediated polymerisation of MMA has also been performed using a solid support system without the use of a co-catalyst. 2-Aminopropyl silica was used in conjunction with $\text{RuCl}_2(\text{PPh}_3)_3$ and reaction rates were relatively fast (91 % conversion after four hours) although the molecular weight distributions of the final polymers (~ 1.5) were larger than the corresponding homogeneous reaction with $\text{Al}(\text{O}^i\text{Pr})_3$. The isolated polymer was successfully used to reinitiate polymerisation to confirm that living polymerisation had occurred. Basic aluminium oxide and silica gel were investigated as cheaper solid supports but it was concluded that the amino functionality was necessary to form the active catalyst⁸³.

1.17 Nickel mediated living radical polymerisation

The living radical polymerisation of MMA and ⁿBMA promoted by $[\text{Ni}\{(\text{CH}_2\text{NCH}_3)_2\text{C}_6\text{H}_3\}\text{Br}]$ was first reported by Teyssie⁸⁴ as an extension to its efficient activity for promoting the Kharasch addition of perhaloalkanes to MMA⁸⁵ (Figure 1.17.1).

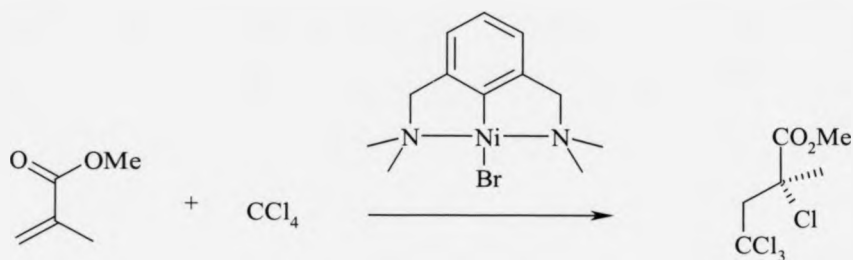


Figure 1.17.1 Kharasch addition / polymerisation of CCl_4 to MMA mediated by $[\text{Ni}\{(\text{CH}_2\text{NCH}_3)_2\text{C}_6\text{H}_3\}\text{Br}]$.

The polymerisation of MMA initiated by CCl_4 in toluene at $80\text{ }^\circ\text{C}$ produced polymers with a narrow molecular weight distribution ($\text{PDI} < 1.2$) and 80 % monomer conversion was achieved after 22 hours. Molecular weight increased with conversion but experimental values deviated from theoretical values with increasing conversion. When stabilised organic bromides such as ethyl-2-bromoisobutyrate (2EIBr) were used in place of the CCl_4 initiators, molecular weight values were significantly higher than the theoretical values and initiator efficiencies were 60 % and 40 % for 2EIBr and bromoisobutyrophenone respectively in toluene at $80\text{ }^\circ\text{C}$. Size exclusion chromatography (SEC) experiments using a differential refractive index (DRI) and ultra violet (UV) detector showed that the UV active bromoisobutyrophenone was fully incorporated in the polymer chain.

Since the nickel complex is stable in water, the suspension polymerisation of MMA initiated by 2EIBr was investigated. High conversions were obtained with a unimodal molecular weight distribution ($M_n = 60\,000\text{ g mol}^{-1}$, $\text{PDI} = 1.7$) and an initiator efficiency of 40 %. In contrast, a similar reaction in the absence of the nickel catalyst resulted in poor control ($\text{PDI} = 6.5$).

Sawamoto et al. investigated the polymerisation of MMA mediated by the Ni (II) analogue of their Ru (II) based system⁸⁶. The initiator used was CCl_3Br in conjunction with $\text{NiBr}_2(\text{PPh}_3)_3$ and $\text{Al}(\text{O}^i\text{Pr})_3$ as an activator and good control was observed ($\text{PDI} = 1.4$ at 90 % conversion). Slower rates of polymerisation were observed when the CCl_4 initiator was used and polymers with a bimodal molecular weight distribution were produced. Similar results were obtained when mixed halide systems were used. The failure of the chloride containing systems is due to the greater strength of the Ni-Cl bond thereby differing from the previously described Ru (II) systems that promote living radical polymerisation independently of the halogen atoms employed.

The same group also showed that the $\text{NiBr}_2(\text{PBu}_3)_3 / \text{Al}(\text{O}^i\text{Pr})_3$ system is efficient in the living radical polymerisation of MMA, methyl acrylate (MA) and n-butyl acrylate (BA) at higher temperatures (up to 120 °C) and at faster rates (90 % conversion in 2.5 hours) than the less thermally stable $\text{NiBr}_2(\text{PPh}_3)_3$. Polymers with a narrow molecular weight distribution ($\text{PDI} \sim 1.2$) were observed⁸⁷. The addition of a second feed of monomer to the system as conversion approached 100 % resulted in continued polymerisation unlike $\text{NiBr}_2(\text{PPh}_3)_3$ that experienced considerable slowing. Polymers with the lowest molecular weight distribution ($\text{PDI} \sim 1.1$) were obtained when the higher molecular weight bromoester functionalised MMA dimer was used as the initiator.

1.18 Iron mediated living radical polymerisation

The use of iron complexes for their use in living radical polymerisation was reported almost simultaneously by the groups of Matyjaszewski⁸⁸ and Sawamoto⁸⁹ in 1997. Sawamoto demonstrated that $\text{FeCl}_2(\text{PPh}_3)_2$ could successfully mediate the polymerisation of MMA initiated by CCl_4 (PDI ~ 1.4). The activator $\text{Al}(\text{O}^i\text{Pr})_3$ accelerated the rate of reaction although it was not necessary as in the case for the equivalent Ru (II) system.

Matyjaszewski used a FeX_2 system (where X = Cl or Br) complexed with various ligands including substituted bipyridines, trialkylamines, trialkyl phosphines and trialkyl phosphates for the polymerisation of styrene and MMA with good control (PDI ~ 1.2). High rates of polymerisation for styrene were observed when a $\text{FeBr}_2/\text{P}(\text{}^n\text{Bu})_3$ catalyst system was used. Polymers with narrow molecular weight distributions were observed when fast initiating molecules such as *p*-toluenesulfonyl and 2EIBr were employed.

In 1998 Teyssie demonstrated the controlled polymerisation of MMA with an $\text{FeCl}_3/\text{PPh}_3$ system initiated by the free radical initiator 2,2'-azobis-iso-butylnitrile (AIBN)⁹⁰. The use of AIBN as an initiator avoided the need for halogenated initiators that are potentially toxic and can be expensive. Molecular weight was found to increase with monomer conversion and the concentration of active species remained constant once the correct equilibrium between Fe (II) and Fe (III) had been attained. Low molecular weight distributions (PDI < 1.4) were observed and the incorporation of the CN fragment in the polymer from AIBN was confirmed by ^{13}C NMR. By changing the initiator to 4,4'-azobis-4-cyanovaleric acid, using similar reaction conditions, yielded polymers with a carboxylic acid ω -functionalisation⁹¹. Grubbs et al. have reported the use of a ferrous halide complexed by 1,3-diisopropyl-4,5-dimethylimidazol-2-

ylidene⁹². This iron catalyst was found to be highly reactive and efficient in the LRP of MMA and styrene. The high activity and efficiency of the catalyst was attributed to the high electron donacity of the ligand.

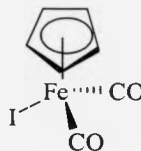


Figure 1.18.1 $\text{FeCp(CO)}_2\text{I}$ used to mediate living radical polymerisation of styrene.

The use of a novel half metallocene Fe (II) complex (Figure 1.18.1) for the living polymerisation of styrene initiated by the iodo analogue of 2EIBr was presented by Sawamoto et al.⁹³. When $\text{Al(O}^i\text{Pr)}_3$ or $\text{Ti(O}^i\text{Pr)}_3$ were used as activators, well-controlled but very slow polymerisations were observed (90 % conversion after 12 days for example) using toluene at 60 °C. Increasing the reaction temperature to 80 °C had the effect of increasing the rate of polymerisation without affecting the degree of control. Faster rates of polymerisation were observed without an activator (this is not observed with other metal complexes) but results in the synthesis of oligomers. Other Fe (II) complexes of the type FeLX(CO)_2 were investigated [$\text{X} = \text{I, Br; L} = \eta^5\text{-C}_5\text{H}_5, \eta^5\text{-C}_5\text{Me}_5$] but these were found not to have any improvement over the original complex⁹⁴. Fast reaction rates for the living radical polymerisation of styrene were observed using bi-metallic complexes of the type $\text{Fe}_2\text{Cp}_2(\text{CO})_4$ (100 % conversion after 33 hours in dioxane solution at 80 °C) and an activating co-catalyst was not required. Recently, the living radical polymerisation of MMA has been reported where neither an organic halide nor a radical initiator is required⁹⁵. In this system, FeCl_3 undergoes a redox reaction with tetraethyl thiuram disulfide to form the active FeCl_2 catalyst and the

halogenated initiator species $\text{Et}_2\text{NCS}_2\text{Cl}$ *in situ*. The polymerisation of MMA proceeded at a very fast rate (40 % conversion after eight minutes in anisole at 100 °C) and the molecular weight increased linearly with conversion where theoretical and actual values were almost identical. Molecular weight distributions were below 1.5. The same living polymerisation characteristics were observed using Fe (III) tri(diethyldithiocarbamate) in the polymerisation of MMA⁹⁶.

1.19 Copper mediated living radical polymerisations

Copper based systems for living radical polymerisations were amongst the first transition metal systems to be reported and became known as atom transfer radical polymerisations. This process was an extension of the atom transfer radical addition system already described. In 1995, Wang and Matyjaszewski demonstrated the bulk polymerisation of styrene using the initiator 1-phenethyl chloride and $\text{Cu(I)Br} / 2,2'$ -bipyridine (bipy) as the mediating species⁵⁸. Using this system, it was possible to obtain polymers with a narrow molecular weight distribution ($\text{PDI} \sim 1.5$) and molecular weights that increased linearly with conversion. As an extension to this work, the copper based system was used for the bulk and solution polymerisation of other monomers including methyl acrylate, butyl acrylate and methyl methacrylate and the effect of several organic halides ($X = \text{Br}, \text{Cl}$) and $\text{Cu(I)Cl} / \text{Cu(I)Br}$ systems were investigated⁹⁷. Analysis of the stereochemical information obtained from ^{13}C NMR spectra of PMMA led the authors to propose that the initiating species was a free radical since the PMMA showed similar stereochemistry to that synthesised by a free radical process. Polymerisations using bipy were heterogeneous since these complexes were not fully soluble. Homogeneous polymerisation of MMA⁹⁸ and styrene⁶³ occurred

using 4,4'-alkyl substituted bipyridines (Figure 1.19.1) and these systems led to polymers with a lower molecular weight distribution than the unsubstituted bipy.

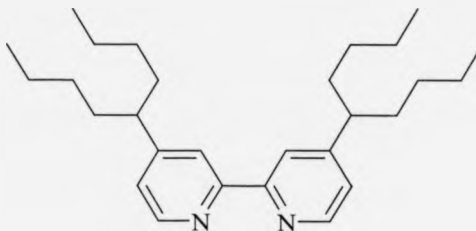


Figure 1.19.1 4,4'-di(5-nonyl)-2,2'-bipyridine.

The synthesis of substituted bipyridines is not trivial and so the use of alternative solubilising ligands for Cu (I) have been investigated. Haddleton et al. investigated the use of *N*-alkyl-2-pyridylmethanimine complexes for the homogeneous polymerisation of methacrylates⁹⁹⁻¹⁰¹. Ligands of this type are readily synthesised by the condensation reaction of 2-pyridine carboxaldehyde with an amine. The wide variety of amines available means that the length of the alkyl chain on the ligand can be varied and so the solubility of the ligand can be varied. Additionally, functionality can be incorporated on the hydrocarbon tail¹⁰².

Several alkyl substituted pyridylmethanimines were successful in promoting the living radical polymerisation of MMA. Straight chain alkyls showed faster reaction rates while the use of branched alkyl ligands showed broader molecular weight distributions. These ligands have also provided an improvement on atom transfer radical cyclisation reactions such as that of α,α,α -trichloroallylacetate. *N*-pentyl-2-pyridylmethanimine showed a rate enhancement over the established CuCl / bipy and tetramethyl ethylenediamine (TMEDA) systems¹⁰³.

The crystal structure (Figure 1.19.2) of the isolated CuL_2BF_4 shows a tetrahedral copper centre and this is the first time that a structurally characterised Cu (I) complex was used in the polymerisation of MMA, rather than the formation of a complex *in situ*. To date there is no evidence to suggest that the isolated structure resembles the structure of the active catalyst that mediates the polymerisation¹⁰⁴.

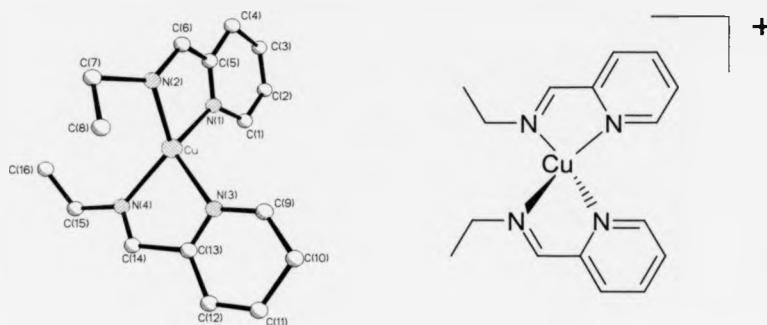


Figure 1.19.2 (*N*-ethyl-2-pyridylmethanimine) Cu(I) BF_4 .

Commercially available multidentate amines (Figure 1.19.3) that are less expensive than bipy have been investigated to assess their complexation with copper and their suitability to promote living radical polymerisation. The absence of a delocalised electron system in these ligands means that a less obvious coloration of the final polymer is observed.

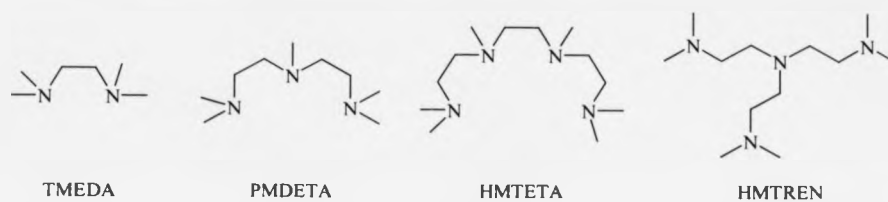


Figure 1.19.3 Multidentate amines for the Cu(I) based living polymerisation of styrene, MMA and MA.

Homogeneous solutions of CuBr are produced by these amine ligands for the bulk polymerisation of styrene¹⁰⁵ and methyl acrylate and in anisole solution for MMA. These ligands yield products with narrow molecular weight distributions ($PD_i = 1.3$ for styrene, 1.2 for MMA and 1.1 for MA) and M_n increases linearly with conversion in accordance with the values calculated by the ratio $[M]:[I]$. The use of HMTREN in a heterogeneous system has been optimised for the polymerisation of butyl acrylate, styrene and MMA¹⁰⁶ but the polymerisation of MMA was not as well-controlled using HMTREN and maximum conversions of only ~10 % were observed.

More recently, Johnson et al. investigated the use of nine quadridentate nitrogen donor ligands for the polymerisation of MMA initiated by 2EIBr. The best molecular weight control was observed using the catalyst $[Cu\{en(Bn)py\}Cl]BPh_4$ (Figure 1.19.4). Using this catalyst, PMMA with a molecular weight distribution of <1.1 and a conversion of ~90 % after 90 minutes in anisole solution at 80 °C was produced¹⁰⁷. The rate of polymerisation was decreased when bulk was added to the pyridine ring and less control over the molecular weight observed. Slower rates of polymerisation were also observed when fluorinated benzene rings were investigated although the degree of control was unaffected.

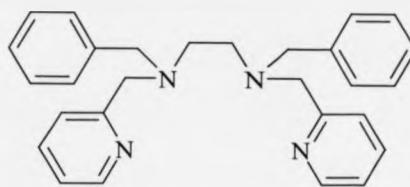


Figure 1.19.4 Quadridentate ligand en(Bn)py.

Haddleton et al. also reported the use of fluorinated ligands in an attempt to recycle the catalytic complex. An equivolume mixture of perfluoromethyl cyclohexane and toluene was used as the polymerisation solvent that is only miscible at the reaction temperature of 90 °C. Since the catalytic complex is only soluble in the fluoruous phase, homogenous catalysis can be achieved during the reaction and the catalyst can then be separated from the product at room temperature. Good control over polymerisations were observed after three consecutive recycles of the catalyst and a low amount of residual catalyst was observed in the final product¹⁰⁸.

Efficient living radical polymerisation mediated by the oxidised form of the transition metal was first reported by Matyjaszewski. This process was described as “Reverse Atom Transfer Radical Polymerisation” and when a system initiated by AIBN was used with Cu(II)/dNbipy as a catalyst, high initiator efficiencies were observed for the polymerisation of styrene and methyl acrylate. The polymerisation of MMA with this system produced products with broader molecular weight distributions ($PDI \sim 1.4$)¹⁰⁹. The function of the initiator in copper mediated living radical polymerisation is of primary importance as fast initiation and minimal side reactions are required to give good control over molecular weight. Since living radical polymerisation is tolerant to a wide variety of functional groups, initiator molecules that bear functional groups have

been used to synthesise polymers with α -functionality. This allows the synthesis of a variety of polymeric architectures. Efficient initiators for copper mediated living radical polymerisation are generally alkyl halides (R-X) with either inductive or resonance stabilised substituents. The structure of the initiator is often analogous to that of the monomer (Figure 1.19.5).

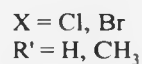
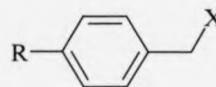
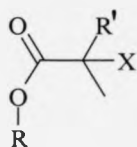


Figure 1.19.5 Generic structures of typical initiators.

The facile reaction of almost any alcohol with either 2-bromoisobutyryl bromide or 2-chloroisobutyryl chloride yields a functionalised molecule that is able to initiate a copper mediated living radical polymerisation^{110, 111}. Sugar compounds¹¹², cholesterol and dye moieties are just some of the compounds that have been functionalised to initiate polymerisation. Molecules that possess more than one hydroxyl group can also be functionalised and used to initiate polymerisation and interesting polymeric architectures including star polymers and hyper-branched macromolecules can be synthesised¹¹³.

Sulfonyl halides have also been shown to be efficient initiators due to their low tendency to dimerise and were described as “universal initiators”¹¹⁴. The S-Cl bond in the sulfonyl halide is relatively weak (weaker than the C-Cl bond) and consequently initiation is faster than propagation that is necessary for well-controlled

polymerisations. Sulfonyl halide initiators have been successfully employed with various monomers including styrene, methacrylates and acrylates¹¹⁵.

Functional monomers such as 2-hydroxyethyl acrylate¹¹⁶, glycidyl acrylate¹¹⁷, (meth)acrylamide¹¹⁸, substituted styrenes⁶⁶ and acrylonitrile¹¹⁹ have all been polymerised in a controlled manner. The homopolymerisation of vinyl acetate, isobutene and *N*-(cyclohexyl)maleimide is difficult but is possible by copolymerisation with monomers such as methyl acrylate, acrylonitrile and styrene¹²⁰. The well-controlled formation of bio-polymers based on nucleoside derivatised monomers has also been reported where a system containing secondary hydroxyl, primary, secondary and tertiary amido, silyl ether and ester linkages was used¹²¹. These developments at the polymer-biology interface are very important in the synthesis of possible deoxyribo nucleic acid (DNA) interacting therapies and there is the possibility of using templated synthesis to create artificial DNA analogues¹²². Templated polymerisation has already been realised in a free radical polymerisation where poly(5'-acryloyluridine) selectively homopolymerised the complementary monomer 5'-acryloyladenosine in the presence of 5'-acryloyluridine. These monomers can also be polymerised on a solid silica support thereby facilitating the separation of the products from the reagents. Moreover, the product can be used for subsequent templated polymerisation and again be separated from the new product.

The tolerance of functional groups to copper mediated living radical polymerisation may also have a beneficial effect on the polymerisation. As an example, the addition of low levels of phenol, traditionally added as an inhibitor, have the effect of increasing the rate of polymerisation of MMA without decreasing the control of the reaction¹²³. It is thought that the complexation of the phenol to the copper centre modifies the structure of the copper catalyst and makes it more active.

1.20 Star Polymers

The control over molecular weight and functionality that is obtained by living radical polymerisation methods allows for the synthesis of a range of materials with interesting topologies. Polymeric materials containing separate polymeric 'arms' can be synthesised that include graft, brush and star polymers^{113, 124}. Well-defined dendrimers also exhibit a high degree of branching¹²⁵. Differences in architecture between these various topologies can provide a wide variation in the final properties of these materials.

Star polymers can be synthesised by the 'core first' approach whereby a multifunctional molecule is used to initiate polymerisation. This method allows star polymers to be formed with a predetermined number arms that corresponds to the number of initiating groups on the initiator. The first example of a star polymer synthesised by living radical polymerisation employed hexakis(bromomethyl)benzene to yield a star polymer incorporating six polystyrene arms radiating from a central core¹²⁶. Many other multifunctional initiators have since been employed to synthesise star polymers with varying numbers of arms. Inorganic heterocyclic cores such as cyclotetrasiloxanes (Figure 1.20.1) and cyclotriphosphazenes have been modified to be used as tetra- and hexa-functional initiators respectively¹²⁷.

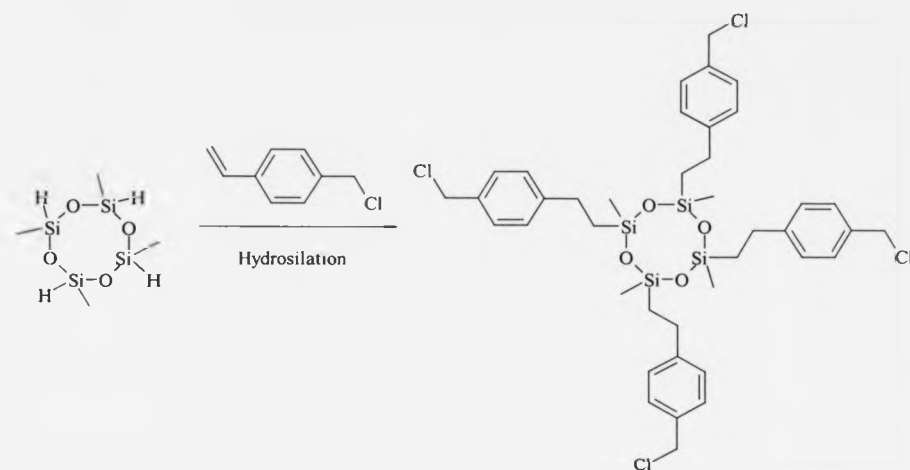


Figure 1.20.1 Synthesis of a four-arm star polymer from an inorganic core.

The formation of star polymers incorporating four, six and eight arms has been reported where the central core is a modified calixarene. In these experiments, MMA and ⁿbutyl acrylate were polymerised by living radical polymerisation and well-defined star polymers were formed. Good control over the polymerisation was confirmed by good agreement between the theoretical and measured molecular weights of the arms once the arms had been cleaved from the central core¹²⁸. Haddleton et al. have reported the esterification of β -D-glucose to form a pentafunctional initiator (Figure 1.20.2) to produce star PMMA and PST with five arms¹¹².

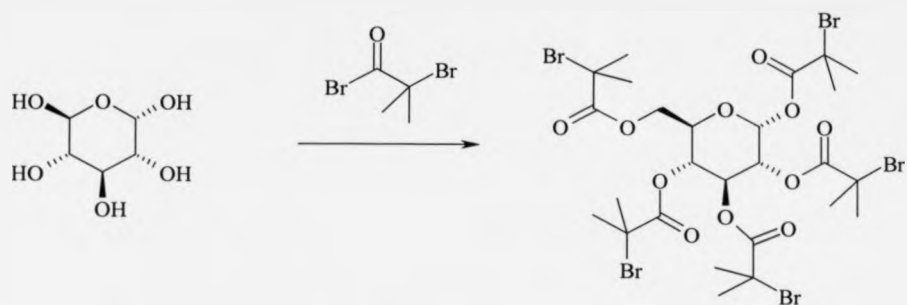


Figure 1.20.2 Synthesis of a pentafunctional initiator with a β -D-glucose core.

1.21 Cyclodextrins

The initial report of the family of compounds that became known as the cyclodextrins was made by Villiers in 1891¹²⁹. These compounds are formed by the degradation of the amylose fraction of starch by glucosyltransferases and results in one or several turns of the amylose helix being hydrolysed and their ends joining together. This produces cyclic oligosaccharides that are known as the cyclodextrins. The glucosyltransferases are not very specific and so a family of these macrocyclic cyclodextrins are produced that incorporate a differing number of glucopyranose units¹³⁰. The most common of these cyclodextrins are α -, β - and γ -cyclodextrin that contain six, seven and eight glucopyranose units respectively. These compounds are all crystalline, homogenous and nonhygroscopic. The glucose units of the cyclodextrins are linked by α -(1-4) linkages as in glucose and adopt a 4C_1 chair conformation. As a consequence of the 4C_1 conformation of the glucopyranose units, all the secondary hydroxyl groups are found on one of the two edges of the ring and all the primary hydroxyl groups are located on the other edge. In reality, the ring is bucket-shaped (Figure 1.21.1) and the cavity of the molecule is lined by the hydrogen atoms and the glycosidic oxygen bridges.

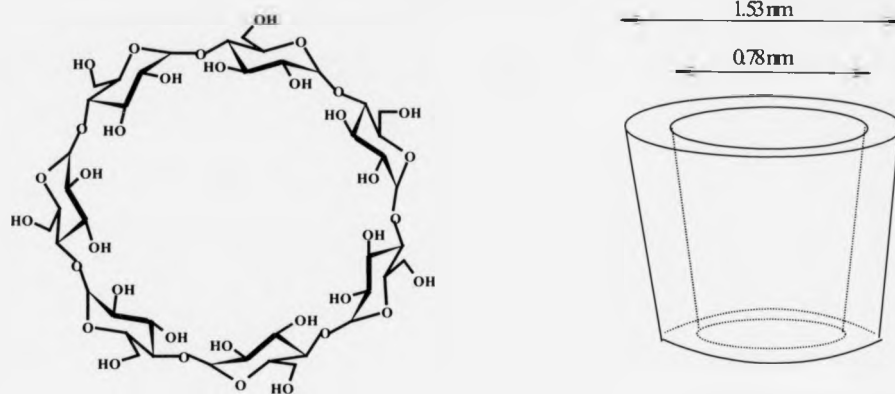


Figure 1.21.1 Chemical structure and approximate geometric dimension of β -cyclodextrin.

The distribution of hydrophilic and hydrophobic groups of the molecule is very important. The hydrophilic hydroxyl groups are found at the rims of the structure thus rendering the molecule soluble in aqueous media whereas the hydrophobic portion is found inside the cavity. The term 'microheterogeneous environment'¹³¹ was coined to describe the ability of a cyclodextrin to provide a hydrophobic matrix in an aqueous solution.

1.22 Cyclodextrin Inclusion Complexes

In an aqueous environment the slightly apolar cavity of a cyclodextrin molecule is occupied by water molecules and this is energetically unfavourable due to polar-apolar interactions. Consequently, these water molecules are readily substituted by appropriate 'guest' molecules that are less polar than water. The unique structural properties of the cyclodextrin cavity mean that inclusion complexes can be formed with a variety of guest molecules including noble gases, paraffins, alcohols, carboxylic acids, aromatic

dyes and benzene derivatives¹³⁰⁻¹³⁵. The cyclodextrin in an aqueous solution is described as the 'host' molecule and the substitution of the high-enthalpy water molecules provide the driving force for complex formation by the 'guest' molecule. Typically, the host:guest ratio is 1:1. In solution, a thermodynamic equilibrium between dissociated and associated species is established and is expressed by the complex stability constant K_a (Figure 1.22.1).



$$K_a = \frac{[\text{CD} \cdot \text{G}]}{[\text{CD}][\text{G}]}$$

Figure 1.22.1 The thermodynamic equilibrium between cyclodextrin (CD) and guest (G) in aqueous solution.

1.23 Cyclodextrin derivatives

The number of possible chemical modifications to the cyclodextrins is unlimited due to the number of substitutable hydroxyl groups (18, 21 and 24 hydroxyl groups for α -, β - and γ -cyclodextrin respectively). Over 1500 derivatives have been described that can be classified into carriers for biologically active substances¹³⁶, enzyme models¹³⁷, separating agents¹³⁸, catalysts¹³⁹ and additives¹⁴⁰. Many of these derivatives involve complicated synthesis resulting in expensive products. If a cyclodextrin derivative is to be industrially produced, its synthesis should ideally be a one-pot and simple process and the final derivative should be non-toxic and its complex-forming capacity should be retained. Among the industrially produced derivatives of cyclodextrin are methylated, hydroxyalkylated and acetylated cyclodextrins^{141, 142}.

1.24 Industrial uses of cyclodextrins

The cyclodextrins are used to obtain certain benefits that result from complexation with other molecules. These benefits include the control of solubility of a guest molecule, stabilisation against the effects of heat, light and oxidation, masking of unwanted physiological effects and reduction of volatility.

An example of where cyclodextrins can control the solubility of a compound is in the additives of canned orange slices. The compound hesperidin is found in the juice of some oranges and this imparts an undesirable cloudiness to the juice of the canned orange slices. Addition of β -cyclodextrin to the orange juice causes solubilisation of the hesperidin resulting in a more desirable clear juice¹⁴³. Additionally, solubilisation of the hesperidin masks the bitter flavour of this compound.

The stabilisation effects of cyclodextrin can be exemplified by the compound nicardipine that is sensitive to light and decomposes when exposed to light.

Complexation of nicardipine with methylated β -cyclodextrin results in a 10-fold decrease of photodegradation¹⁴⁴.

The off taste that results from coatings on tins and cans can be reduced or eliminated using cyclodextrins in the coating. The off tastes are caused by aldehydes and ketones containing 6-18 carbons. Analysis of the cyclodextrin-containing coatings show that these aldehydes and ketones are withheld in the coating and so do not impart the undesirable flavours to the contents of the tin or can¹⁴⁵.

Cyclodextrins can be used to complex compounds to reduce their volatility. An example is in the production of silane resins that are made using a 1,5-cyclooctadieneplatinum catalyst. The catalyst causes the reaction to proceed immediately but if the catalyst is complexed to cyclodextrin, this extends the shelf life of the silicone to over seven months since complexation prevents the catalysis and reaction. The catalyst can be

released by heating the complex to 150 °C and the subsequent curing process can be achieved in 30 minutes¹⁴⁶.

1.25 Summary

In this chapter the author has outlined some of the different systems that are employed in controlled / living polymerisations. Well-defined homo- and co- polymers can be realised using living radical techniques and this route is more industrially viable than the original anionic systems due to the tolerance of trace impurities, water and monomer functionality. Good control for the polymerisation of substituted styrenes, 4-vinylpyridine and acrylates can be achieved using nitroxide-mediated polymerisations although reaction rates are slow. Methacrylates readily undergo termination by disproportionation with the nitroxide radical due to the presence of the α -hydrogen atom on the methacrylate.

The development of the RAFT process has been shown to give good control in the polymerisation of MMA, styrene, butyl acrylate and methacrylic acid. However, the synthesis of the RAFT agents is not trivial and problems associated with odour and toxicity may limit their commercial use.

This thesis is mainly concerned with copper mediated living radical polymerisation as it has been shown to be a good promoter of well-controlled polymerisations for a variety of monomers. Furthermore, the metal catalyst is inexpensive, a wide variety of ligands can be synthesised in trivial reactions and a co-catalyst is not required. This thesis demonstrates the effectiveness of copper catalysts to produce well-defined complex polymeric architectures that would be impossible using conventional methods.

1.26 Chapter 1 References

- 1 W. R. Moore and J. Trego, *J. Appl. Polym. Sci.*, 1961, **5**, 299.
- 2 E. Simon, *Liebigs Ann. Chem.*, 1839, **31**, 265.
- 3 'Phenolic Resins' in 'Encyclopedia of Polymer Science and Engineering', ed. H. F. Mark, N. M. Bikales, C. G. Overberger, and G. Menges, Wiley Interscience 1988.
- 4 H. Staudinger, *Chem. Ber.*, 1920, **53**, 1073.
- 5 H. Staudinger, *Chem. Ber.*, 1924, **57**, 1203.
- 6 W. R. Carothers, *J. Am. Chem. Soc.*, 1928, **51**, 2548.
- 7 K. Ziegler, E. Holzkamp, H. Breil, and H. Martin, *Angew. Chem.*, 1955, **67**, 426.
- 8 K. Ziegler, *Angew. Chem.*, 1964, **76**, 545.
- 9 G. Natta, *Science*, 1965, **147**, 261.
- 10 G. Natta, P. Pino, P. Corradini, F. Danusso, E. Mantica, G. Mazzanti, and G. Moraglio, *J. Am. Chem. Soc.*, 1954, **77**, 1708.
- 11 G. Odian, 'Principles of Polymerization', John Wiley & Sons Inc. 1991.
- 12 R. J. Young, 'Introduction to Polymers', Chapman and Hall 1981.
- 13 G. Moad and D. H. Solomon, 'The Chemistry of Free Radical Polymerization', Pergamon 1995.
- 14 P. J. Flory, 'Principles of Polymer Chemistry', Cornell University Press 1953.
- 15 J. P. A. Heuts, L. M. Muratore, and T. P. Davis, *Macromol. Chem. Phys.*, 2000, **201**, 2780.
- 16 Y. Y. Li and B. B. Wayland, *Chem. Commun.*, 2003, 1594.

- 17 D. C. Blakely, 'Emulsion Polymerisation- Theory and Practice', Applied Science, London 1975.
- 18 J. P. Kennedy and E. Marechal, 'Carbocationic Polymerization', Wiley Interscience 1982.
- 19 A. Gandini and H. Cheradame, *Adv. Polym. Sci.*, 1980, **35**, 1.
- 20 H. Egret, J. P. Couvercelle, J. Bellenev, and C. Bunel, *Eur. Polym. J.*, 2002, **38**, 1953.
- 21 A. F. Johnson and R. N. Young, *J. Polym. Sci. Symp.*, 1976, **56**, 211.
- 22 H. L. Hsieh and J. Smid, 'Recent Advances in Anionic Polymerization', Elsevier 1987.
- 23 S. Bywater, 'Anionic Polymerization', ed. H. F. Mark, N. M. Bikales, C. G. Overberger, and G. Menges, Wiley Interscience 1985.
- 24 M. Szwarc, M. Levy, and R. Milkovich, *J. Am. Chem. Soc.*, 1956, **18**, 2656.
- 25 A. H. E. Muller, *Makromolekulare Chemie-Macromol. Symp.*, 1990, **32**, 87.
- 26 D. Y. Sogah, W. R. Hertler, O. W. Webster, and G. M. Cohen, *Macromolecules*, 1987, **20**, 1473.
- 27 W. J. Brittain and I. B. Dicker, *Macromolecules*, 1989, **22**, 1054.
- 28 S. Bywater, *Makromolekulare Chemie-Macromol. Symp.*, 1993, **67**, 339.
- 29 T. Otsu and M. Yoshida, *Polym. Bull. (Berlin)*, 1982, **7**, 197.
- 30 J. P. Kennedy, *J. Macromol. Sci. Chem.*, 1979, **A13**, 695.
- 31 S. R. Turner and R. W. Blevins, *Macromolecules*, 1990, **23**, 1856.
- 32 D. H. Solomon, E. Rizzardo, and E. Cacioli, *Eur. Pat. Appl. EP135280*, 1985, **102**, 221335q.

- 33 S. A. F. Bon, 'Debut: Collected Studies on Nitroxide-Mediated Controlled Radical Polymerization', Technische Universiteit, Eindhoven, 1998.
- 34 R. P. N. Veregin, M. K. Georges, P. M. Kazmaier, and G. K. Hamer, *Macromolecules*, 1993, **26**, 5316.
- 35 A. Goto and T. Fukuda, *Macromol. Chem. Phys.*, 2000, **201**, 2138.
- 36 S. A. F. Bon, G. Chambard, and A. L. German, *Macromolecules*, 1999, **32**, 8269.
- 37 M. K. Georges, R. P. N. Veregin, P. M. Kazmaier, and G. K. Hamer, *Macromolecules*, 1993, **26**, 2987.
- 38 D. Benoit, V. Chaplinski, R. Braslau, and C. J. Hawker, *J. Am. Chem. Soc.*, 1999, **121**, 3904.
- 39 D. Benoit, E. Harth, P. Fox, R. M. Waymouth, and C. J. Hawker, *Macromolecules*, 2000, **33**, 363.
- 40 M. K. Georges, R. P. N. Veregin, P. M. Kazmaier, G. K. Hamer, and M. Saban, *Macromolecules*, 1994, **27**, 7228.
- 41 F. R. Mayo, *J. Am. Chem. Soc.*, 1968, **90**, 1289.
- 42 A. Fischer, A. Brembilla, and P. Lochon, *Macromolecules*, 1999, **32**, 6069.
- 43 D. Benoit, S. Grimaldi, S. Robin, J. P. Finet, P. Tordo, and Y. Gnanou, *J. Am. Chem. Soc.*, 2000, **122**, 5929.
- 44 L. Couvreur, C. Lefay, J. Belleney, B. Charleux, O. Guerret, and S. Magnet, *Macromolecules*, 2003, **36**, 8260.
- 45 T. P. Le, G. Moad, E. Rizzardo, and S. H. Thang, *PCT Int. Appl. WO 9801478 A1 980115*, 1998.

- 46 T. P. Le, G. Moad, E. Rizzardo, and S. H. Thang, *PCT Int. Appl. WO 9801478 A1 980115*, 1998.
- 47 F. M. Calitz, M. P. Tonge, and R. D. Sanderson, *Macromolecules*, 2003, **36**, 5.
- 48 D. G. Hawthorne, G. Moad, E. Rizzardo, and S. H. Thang, *Macromolecules*, 1999, **32**, 5457.
- 49 R. T. A. Mayadunne, E. Rizzardo, J. Chiefari, Y. K. Chong, G. Moad, and S. H. Thang, *Macromolecules*, 1999, **32**, 6977.
- 50 R. T. A. Mayadunne, E. Rizzardo, J. Chiefari, J. Krstina, G. Moad, A. Postma, and S. H. Thang, *Macromolecules*, 2000, **33**, 243.
- 51 C. Barner-Kowollik, M. L. Coote, T. P. Davis, L. Radom, and P. Vana, *J. Polym. Sci. Pol. Chem.*, 2003, **41**, 2828.
- 52 G. Moad, R. T. A. Mayadunne, E. Rizzardo, M. Skidmore, and S. H. Thang, in 'Kinetics and mechanism of RAFT polymerization', 2003.
- 53 G. Moad, R. T. A. Mayadunne, E. Rizzardo, M. Skidmore, and S. H. Thang, *Macromol. Symp.*, 2003, **192**, 1.
- 54 A. R. Wang and S. P. Zhu, *J. Polym. Sci. Pol. Chem.*, 2003, **41**, 1553.
- 55 R. T. A. Mayadunne, J. Jeffery, G. Moad, and E. Rizzardo, *Macromolecules*, 2003, **36**, 1505.
- 56 P. Vana, J. F. Quinn, T. P. Davis, and C. Barner-Kowollik, *Aust. J. Chem.*, 2002, **55**, 425.
- 57 M. Kato, M. Kamigaito, M. Sawamoto, and T. Higashimura, *Macromolecules*, 1995, **28**, 1721.
- 58 J. S. Wang and K. Matyjaszewski, *J. Am. Chem. Soc.*, 1995, **117**, 5614.
- 59 Kharasch, Engelmann, and Mayo, *J. Org. Chem.*, 1937, **2**, 288.

- 60 J. Iqbal, B. Bhatia, and N. K. Nayyar, *Chem. Rev.*, 1994, **94**, 519.
- 61 K. Matyjaszewski and J. H. Xia, *Chem. Rev.*, 2001, **101**, 2921.
- 62 M. Kamigaito, T. Ando, and M. Sawamoto, *Chem. Rev.*, 2001, **101**, 3689.
- 63 V. Percec, B. Barboiu, A. Neumann, J. C. Ronda, and M. Y. Zhao, *Macromolecules*, 1996, **29**, 3665.
- 64 G. Moineau, C. Granel, P. Dubois, R. Jerome, and P. Teyssie, *Macromolecules*, 1998, **31**, 542.
- 65 Y. Kotani, M. Kamigaito, and M. Sawamoto, *Macromolecules*, 1999, **32**, 2420.
- 66 Y. Kotani, M. Kamigaito, and M. Sawamoto, *Macromolecules*, 2000, **33**, 6746.
- 67 T. J. Otsu, *Polym. Sci., Polym. Chem. Ed.*, 1968, **6**, 3075.
- 68 J. Tsuji, K. Sato, and H. Nagashima, *Chem. Lett.*, 1981, 1169.
- 69 P. Lecomte, I. Drapier, P. Dubois, P. Teyssie, and R. Jerome, *Macromolecules*, 1997, **30**, 7631.
- 70 H. Matsumoto, T. Nakano, K. Takasu, and Y. Nagai, *Tetrahedron Lett.*, 1973, **51**, 5147.
- 71 H. Matsumoto, T. Nakano, K. Takasu, and Y. Nagai, *J. Org. Chem.*, 1978, **43**, 1734.
- 72 W. J. Bland, R. Davis, and J. L. A. Durrant, *J. Organomet. Chem.*, 1985, **280**, 397.
- 73 S. Hamasaki, C. Sawauchi, M. Kamigaito, and M. Sawamoto, *J. Polym. Sci. Pol. Chem.*, 2002, **40**, 617.
- 74 K. Y. Baek, M. Kamigaito, and M. Sawamoto, *J. Polym. Sci. Pol. Chem.*, 2002, **40**, 2245.

- 75 K. Y. Baek, M. Kamigaito, and M. Sawamoto, *J. Polym. Sci. Pol. Chem.*, 2002, **40**, 1937.
- 76 K. Y. Baek, M. Kamigaito, and M. Sawamoto, *J. Polym. Sci. Pol. Chem.*, 2002, **40**, 1972.
- 77 M. Senoo, Y. Kotani, M. Kamigaito, and M. Sawamoto, *Macromol. Symp.*, 2000, **157**, 193.
- 78 T. Ando, C. Sawauchi, M. Ouchi, M. Kamigaito, and M. Sawamoto, *J. Polym. Sci. Pol. Chem.*, 2003, **41**, 3597.
- 79 T. Nishikawa, M. Kamigaito, and M. Sawamoto, *Macromolecules*, 1999, **32**, 2204.
- 80 H. Takahashi, T. Ando, M. Kamigaito, and M. Sawamoto, *Macromolecules*, 1999, **32**, 6461.
- 81 T. Ando, M. Kamigaito, and M. Sawamoto, *Macromolecules*, 2000, **33**, 5825.
- 82 H. Takahashi, T. Ando, M. Kamigaito, and M. Sawamoto, *Macromolecules*, 1999, **32**, 3820.
- 83 D. M. Haddleton, D. J. Duncalf, D. Kukulj, and A. P. Radigue, *Macromolecules*, 1999, **32**, 4769.
- 84 C. Granel, P. Dubois, R. Jerome, and P. Teyssie, *Macromolecules*, 1996, **29**, 8576.
- 85 D. M. Grove, G. V. Koten, and A. H. M. Verschuuren, *J. Mol. Cat.*, 1989, **45**, 169.
- 86 H. Uegaki, M. Kamigaito, and M. Sawamoto, *J. Polym. Sci. Pol. Chem.*, 1999, **37**, 3003.

- 87 H. Uegaki, Y. Kotani, M. Kamigaito, and M. Sawamoto, *Macromolecules*, 1998, **31**, 6756.
- 88 K. Matyjaszewski, M. L. Wei, J. H. Xia, and N. E. McDermott, *Macromolecules*, 1997, **30**, 8161.
- 89 T. Ando, M. Kamigaito, and M. Sawamoto, *Macromolecules*, 1997, **30**, 4507.
- 90 G. Moineau, P. Dubois, R. Jerome, T. Senninger, and P. Teyssie, *Macromolecules*, 1998, **31**, 545.
- 91 M. Baumert and R. Mulhaupt, *Macromol. Chem. Rap. Commun.*, 1997, **18**, 787.
- 92 J. Louie and R. H. Grubbs, *Chem. Commun.*, 2000, 1479.
- 93 Y. Kotani, M. Kamigaito, and M. Sawamoto, *Macromolecules*, 1999, **32**, 6877.
- 94 Y. Kotani, M. Kamigaito, and M. Sawamoto, *Macromolecules*, 2000, **33**, 3543.
- 95 X. P. Chen and K. Y. Qiu, *Chem. Commun.*, 2000, 233.
- 96 X. P. Chen and K. Y. Qiu, *Chem. Commun.*, 2000, 1403.
- 97 J. S. Wang and K. Matyjaszewski, *Macromolecules*, 1995, **28**, 7901.
- 98 R. B. Grubbs, C. J. Hawker, J. Dao, and J. M. J. Frechet, *Angew. Chem., Int. Ed. Engl.*, 1997, **36**, 270.
- 99 V. Darcos and D. M. Haddleton, *Eur. Polym. J.*, 2003, **39**, 855.
- 100 A. P. Narrainen, S. Pascual, and D. M. Haddleton, *J. Polym. Sci. Pol. Chem.*, 2002, **40**, 439.
- 101 D. M. Haddleton, D. J. Duncalf, D. Kukulj, M. C. Crossman, S. G. Jackson, S. A. F. Bon, A. J. Clark, and A. J. Shooter, *Eur. J. Inorg. Chem.*, 1998, 1799.
- 102 X. S. Wang, F. L. G. Malet, S. P. Armes, D. M. Haddleton, and S. Perrier, *Macromolecules*, 2001, **34**, 162.

- 103 A. J. Clark, D. J. Duncalf, R. P. Filik, D. M. Haddleton, G. H. Thomas, and H. Wongtap, *Tetrahedron Lett.*, 1999, **40**, 3807.
- 104 T. Pintauer, B. McKenzie, and K. Matyjaszewski, in 'Toward structural and mechanistic understanding of transition metal-catalyzed atom transfer radical processes', 2003.
- 105 X. L. Wan and S. K. Ying, *J. Appl. Polym. Sci.*, 2000, **75**, 802.
- 106 J. Queffelec, S. G. Gaynor, and K. Matyjaszewski, *Macromolecules*, 2000, **33**, 8629.
- 107 R. M. Johnson, C. Ng, C. C. M. Samson, and C. L. Fraser, *Macromolecules*, 2000, **33**, 8618.
- 108 D. M. Haddleton, S. G. Jackson, and S. A. F. Bon, *J. Amer. Chem. Soc.*, 2000, **122**, 1542.
- 109 J. H. Xia and K. Matyjaszewski, *Macromolecules*, 1997, **30**, 7692.
- 110 K. Ohno, B. Wong, and D. M. Haddleton, *J. Polym. Sci. Pol. Chem.*, 2001, **39**, 2206.
- 111 N. Ayres, D. M. Haddleton, A. J. Shooter, and D. A. Pears, *Macromolecules*, 2002, **35**, 3849.
- 112 D. M. Haddleton, D. Kukulj, E. J. Kelly, and C. Waterson, *Abstr. Pap. Am. Chem. Soc.*, 1999, **217**, 202.
- 113 K. Matyjaszewski, *Polym. Int.*, 2003, **52**, 1559.
- 114 V. Percec, H. J. Kim, and B. Barboiu, *Macromolecules*, 1997, **30**, 6702.
- 115 V. Percec, A. D. Asandei, F. Asgarzadeh, B. Barboiu, M. N. Holerca, and C. Grigoras, *J. Polym. Sci. Pol. Chem.*, 2000, **38**, 4353.

- 116 S. Coca, C. B. Jasieczek, K. L. Beers, and K. Matyjaszewski, *J. Polym. Sci. Pol. Chem.*, 1998, **36**, 1417.
- 117 N. V. Tsarevsky, T. Sarbu, B. Gobelt, and K. Matyjaszewski, *Macromolecules*, 2002, **35**, 6142.
- 118 M. Teodorescu and K. Matyjaszewski, *Macromol. Rapid Commun*, 2000, **21**, 190.
- 119 C. B. Tang, T. Kowalewski, and K. Matyjaszewski, *Macromolecules*, 2003, **36**, 1465.
- 120 S. Coca and K. Matyjaszewski, *Polym. Prepr.*, 1996, **40(2)**, 338.
- 121 A. Marsh, A. Khan, D. M. Haddleton, and M. J. Hannon, *Macromolecules*, 1999, **32**, 8725.
- 122 A. Marsh, A. Khan, M. Garcia, and D. M. Haddleton, *Chem. Commun.*, 2000, 2083.
- 123 D. M. Haddleton, A. J. Clark, M. C. Crossman, D. J. Duncalf, A. M. Heming, S. R. Morsley, and A. J. Shooter, *Chem. Commun.*, 1997, 1173.
- 124 M. H. Stenzel and T. P. Davis, *J. Polym. Sci. Pol. Chem.*, 2002, **40**, 4498.
- 125 D. A. Tomalia and J. M. J. Frechet, *J. Polym. Sci. Pol. Chem.*, 2002, **40**, 2719.
- 126 J. S. Wang, D. Greszta, and K. Matyjaszewski, *Polym. Mater. Sci.*, 1995, **73**, 416.
- 127 J. Pyun and K. Matyjaszewski, *Chem. Mat.*, 2001, **13**, 3436.
- 128 J. Ueda, M. Kamigaito, and M. Sawamoto, *Macromolecules*, 1998, **31**, 6762.
- 129 A. Villiers, *Compt. Rend.*, 1891, **112**, 536.
- 130 J. Szejtli, 'Cyclodextrin Technology', Kluwer Academic Publishers: Dordrecht 1988.

- 131 F. Cramer, 'Einschlussverbindungen', Springer-Verlag: Heidelberg 1954.
- 132 D. Duchêne, Cyclodextrin and their Industrial Uses, 1987.
- 133 W. Saenger, *Angew. Chem., Int. Ed. Engl.*, 1980, **19**, 344.
- 134 K. Harata, in 'Comprehensive Supramolecular Chemistry', ed. J. L. Atwood, J. E. D. Davies, and D. D. MacNicol, Oxford, 1996.
- 135 K. H. Fromming and J. Szejtli, 'Cyclodextrin in Pharmacy', Kluwer Academic Publishers, Dordrecht 1994.
- 136 E. G. Argyris, E. Acheampong, G. Nunnari, M. Mukhtar, K. J. Williams, and R. J. Pomerantz, *J. Virol.*, 2003, **77**, 12140.
- 137 M. Fernandez, A. Fragoso, R. Cao, M. Banos, and R. Villalonga, *Enzyme Microb. Technol.*, 2002, **31**, 543.
- 138 L. A. Kartsova and N. V. Komarova, *J. Anal. Chem.*, 2003, **58**, 972.
- 139 S. P. Kim, A. G. Leach, and K. N. Houk, *J. Org. Chem.*, 2002, **67**, 4250.
- 140 H. Ikeda, A. Matsuhisa, and A. Ueno, *Chem.-Eur. J.*, 2003, **9**, 4907.
- 141 R. Cao, A. Fragoso, E. Almirall, and R. Villalonga, *Supramol. Chem.*, 2003, **15**, 161.
- 142 M. Singh, R. Sharma, and U. C. Banerjee, *Biotechnol. Adv.*, 2002, **20**, 341.
- 143 S. V. Singh, R. K. Jain, A. Gupta, and A. S. Dhatt, *J. Food Sci. Technol.-Mysore*, 2003, **40**, 247.
- 144 R. Pomponio, R. Gotti, C. Bertucci, and V. Cavrini, *Electrophoresis*, 2001, **22**, 3243.
- 145 W. S. Bobo, U.S Patent 5,177,129, 1993.
- 146 D. Steinborn and H. Junicke, *Chem. Rev.*, 2000, **100**, 4283.

Chapter 2**Synthesis and Characterisation of Star Polymers with
21-arms by Copper (I) Mediated Living Radical Polymerisation****2.0 Introduction**

The synthesis of star polymers by transition metal mediated living radical polymerisation has been investigated by a number of research groups¹⁻¹⁰. There are two general synthetic approaches to the formation of star polymers. The first is known as the arms-first method¹¹⁻¹⁴ whereby linear polymeric arms are formed by living polymerisation. Star formation then occurs in one of two ways: a difunctional comonomer can be used to provide cross-linking through propagation or the reaction can be quenched by the addition of a multifunctional coupling agent that connects a precise number of arms to a central core. The second approach to star polymer formation is known as the core-first method¹⁵⁻¹⁸ and this method involves the use of a multifunctional initiator that reacts with the monomer units. The core-first method results in star polymers with well-defined structures in terms of both number of arms and length of arms. Furthermore, the polymerisation consists solely of stars in the absence of linear polymers. The synthesis of star polymers is of interest because of the materials' properties that include a lower viscosity, a high degree of chain end functionality and different hydrodynamic properties compared to their linear analogues. These properties give rise to interesting applications and provide an opportunity to assess structure-property relationships.

Recently, free radical polymerisation has been applied to the synthesis of star polymers with pendant saccharide units¹⁹ and living radical polymerisation used in the grafting of glycopolymers to a solid surface²⁰. Hence, the multiple functionalities observed in saccharide molecules provide a route to the synthesis of a host of star polymers. The living radical polymerisation of simple saccharide molecules including glucose²¹ and sucrose²² has previously been reported and this has provided the impetus to investigate star polymer formation based on more complex saccharide molecules that have a higher number of potentially polymerisable arms. The wide range of available saccharide molecules means that star polymers with any number of discrete arms can be realised. The synthesis of such star polymers using living radical polymerisation methods offers advantages over other methods such as ionic living processes. In an ionic living process, the number of arms that each star possesses may be limited due to the increasing number of ion pairs that are required for an increasing number of initiating sites. This will lead to problems associated with stability and solubility and so star polymers with more than four arms, prepared by anionic living polymerisation, are difficult to obtain. Similar restrictions apply to the synthesis of star polymers by cationic polymerisation. The synthesis of star polymers by conventional free radical polymerisation leads to crosslinked materials due to radical recombination reactions. Conversely, living radical polymerisation techniques provide a gateway to the synthesis of complex macromolecular architectures due to the simplicity of the experimental procedures involved and the versatility of applicable monomers. Well-defined structures can be synthesised in a variety of media using this polymerisation technique. Cyclodextrin was selected as a suitable substrate for the formation of star polymers due to its interesting cyclic structure, hydrophobic cavity and its many primary and secondary hydroxyl groups. With appropriate chemical modification of β -cyclodextrin

(β CD) it is possible to synthesise a multifunctional initiator with predetermined functionality that is suitable for living radical polymerisation. Furthermore, β CD is readily available and inexpensive.

2.1 Chemical Modification of β CD

The modification of CD's provides a challenge to the synthetic chemist due to the presence of the hydrophobic cavity and the large number of hydroxyl groups. There are a total of 21 hydroxyl groups in β CD, 14 of which are the secondary hydroxyl groups located at the 2- and 3-positions of the glucopyranose unit and seven are primary hydroxyl groups located at the 6-position. For the β CD to be employed as a multifunctional initiator for the formation of star polymers, it is necessary to modify these hydroxyl groups with an appropriate functionality. Since hydroxyl groups are nucleophilic in nature, any initial reaction involves electrophilic attack at these positions. A weak base or a basic solvent is required to neutralise the acid that is formed when the electrophile reacts with the β CD. Cyclodextrins are stable under basic conditions whereas they decompose in the presence of a strong acid²³.

2.1.1 Synthesis of Heptakis(2,3,6-tri-*O*-(2-bromo-2-methylpropionyl)- β -cyclodextrin (21-Br-CD) Multifunctional Initiator for Copper (I) Mediated Living Radical Polymerisation

The synthesis of initiators for living radical polymerisations employing a copper (I) / pyridylmethanimine catalytic system usually proceeds by the condensation of 2-bromoisobutyrylbromide with an appropriate alcohol. However, the direct esterification of β CD with 2-bromoisobutyrylbromide was unsuccessful and led to a crude black mixture. It was thought that this reagent was too reactive towards β CD which has a larger number of hydroxyl groups. The milder reagent 2-bromoisobutyric anhydride was subsequently synthesised (Figure 2.1.1) and the esterification of the 21-hydroxyl groups of β CD was accomplished by reaction with this less reactive reagent over three days (Figure 2.1.2).

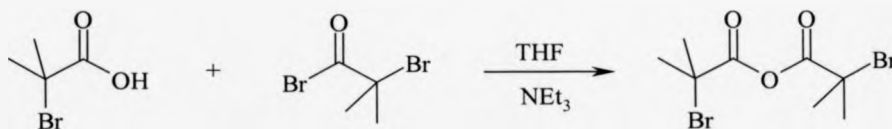


Figure 2.1.1 Synthesis of 2-bromoisobutyric anhydride.

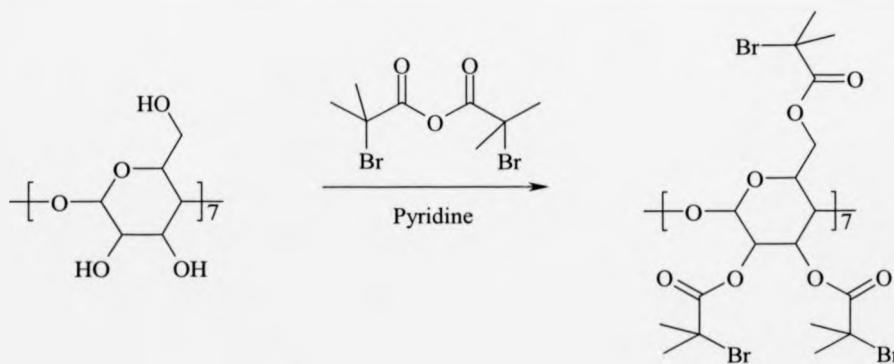


Figure 2.1.2 Formation of β CD functionalised with 21 2-bromoisobutyryl groups.

Since β CD is hydrophilic it was necessary to dry the starting materials, including the β CD, prior to esterification to avoid any side reactions between water and the anhydride. The β CD was dried *in vacuo* at 80 °C over phosphorous pentoxide. The 21-armed multifunctional β CD initiator, 21-Br-CD, was purified by flash chromatography and characterised by infra red and nuclear magnetic resonance spectroscopy.

2.1.1.1 Infra red spectroscopy characterisation of 21-Br-CD

Infra red (IR) spectroscopy was used to confirm that esterification of the β CD had occurred. Figure 2.1.3 shows the IR spectrum of the β CD starting material (blue trace) with the characteristic OH stretch of the hydroxyl groups at 3300 cm^{-1} . The IR spectra of the final product is shown in the same figure (red trace) where the appearance of the carbonyl stretch of the ester is visible at 1700 cm^{-1} and the OH stretch of the starting material has disappeared. This indicates that all of the 21 hydroxyl groups of β CD have reacted with the 2-bromoisobutyric anhydride.

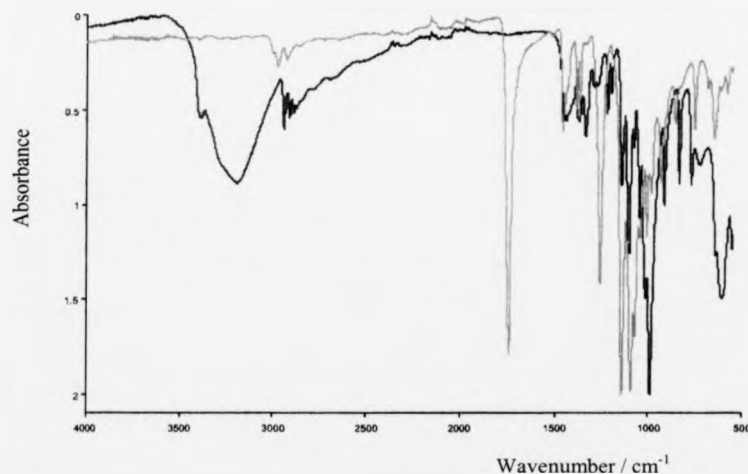


Figure 2.1.3 Infra red spectra of β CD starting material (blue) and 21-Br-CD (red).

2.1.1.2 ¹H NMR spectroscopy characterisation of 21-Br-CD

The ¹H NMR spectra of 21-Br-CD in deuterated chloroform shows two sets of signals. The signals between 3.5-5.0 ppm correspond to the 49 hydrogen atoms associated with the backbone of βCD and the singlet observed at 1.81 ppm corresponds to the 126 hydrogen atoms associated with the methyl groups of the 2-bromoisobutyric anhydride.

2.2 Copper (I) Mediated Living Radical Polymerisation Initiated by 21-Br-CD

The living radical polymerisation (LRP) of methyl methacrylate (MMA) and styrene (ST) using 21-Br-CD to form a star polymer with 21 discrete arms (Figure 2.2.1) was investigated. Copper (I) bromide was used as a catalyst and *N*-ⁿ-pentyl-2-pyridylmethanimine was employed as a ligand in a ratio of 1 to 2 to ensure solubility of the copper catalyst and to maintain the copper (I) / copper (II) equilibrium in the reaction solvent.

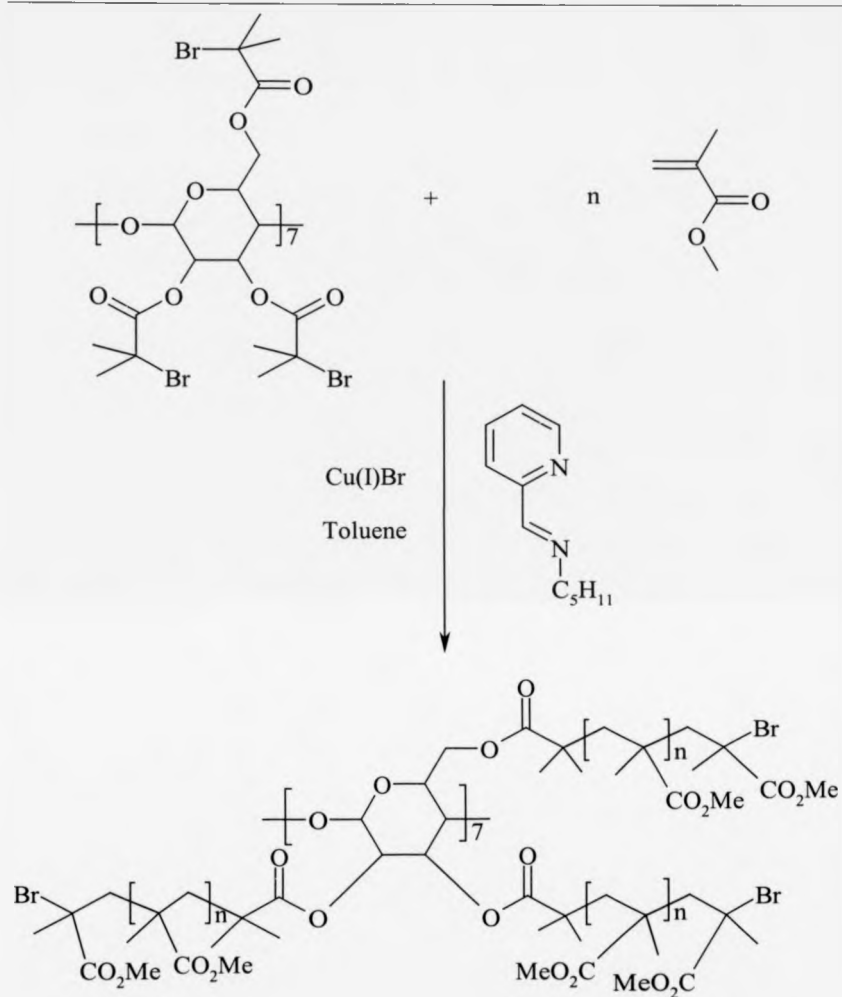


Figure 2.2.1 Copper (I) mediated living radical polymerisation of MMA with 21-Br-CD initiator.

2.2.1 Suitable Reaction Conditions for the LRP of MMA Initiated by 21-Br-CD

Initially, a polymerisation system had to be developed that provided linear first order kinetic plots that are evidence of a living polymerisation process. Suitable reaction conditions for living polymerisation using 21-Br-CD as a multifunctional initiator were investigated. Due to the high number of initiation sites in close proximity on the 21-Br-CD molecule, it was necessary to work at high dilutions to minimise the possibility of any irreversible coupling reactions between adjacent polymer chains and between adjacent star polymers. The living radical polymerisation of linear PMMA initiated by ethyl-2-bromoisobutyrate (2EIBr) typically proceeds at 90 °C and the ratio of [MMA]:[2EIBr]:[ligand]:[Cu(I)Br] is typically 100:1:2:1²⁴. These same ratios were employed when investigating the use of 21-Br-CD as the initiator. Star polymers with a narrow molecular weight distribution were synthesised and the monomer conversion, determined by gravimetric analysis, was found to be 30 % after 30 minutes. At higher conversions (81 % after two hours) however, the size exclusion chromatogram (SEC) showed the presence of a shoulder on the main peak in the higher molecular mass region. This shoulder peak was tentatively attributed to the irreversible coupling between two star polymers.

For living radical polymerisation to be achieved, it was necessary to suppress these coupling reactions at higher conversions so that chain end functionality could be maintained at the completion of a reaction. This would provide opportunity for the isolated star polymer to be used as a macroinitiator in the synthesis of AB type block copolymers. To suppress the coupling reactions, the concentration of the 21-Br-CD initiator was lowered and the effect of the polymerisation where the ratio [MMA]:[21-Br-CD] was lowered to 500:1 was investigated. Polymerisations with this ratio proceeded much slower and conversions of only 34 % were observed after a reaction time of two hours compared with 81 % conversion when the ratio [MMA]:[21-Br-CD] was 100:1. Although star polymers with a narrow molecular weight distribution were observed by SEC, the shoulder at the high molecular mass end of the SEC trace was still observed.

To further suppress the effects of irreversible star-star coupling, which renders the polymer chains 'dead', the reaction temperature was lowered from 90 °C to 60 °C. It has previously been reported that MMA can be polymerised at temperatures as low as 15 °C²⁵ and Qin et al. have shown that MMA can polymerised in a living manner at 60 °C²⁶. In other studies, Percec et al. have stated that the polymerisation of MMA does not occur at temperatures as low as 33 °C using a copper (I)/substituted bipyridine catalyst and an arene sulfonyl initiator²⁷. Typically, living radical polymerisations are carried out at temperatures above 80 °C so as to achieve acceptable rates of polymerisation.

Table 2.2.1 shows the evolution of molecular weight with conversion when the polymerisation temperature was lowered to 60 °C.

Time (minutes)	Conversion* (%)	M _n (SEC)	M _n (theo)	PDI
60	6.5	27600	72040	1.13
120	9.4	44800	102770	1.11
180	12.6	65200	136980	1.07
240	14.9	79100	160750	1.07
300	17.2	90800	184700	1.07
360	19.5	112000	209370	1.06

Table 2.2.1 Evolution of conversion and molecular weight in the LRP of MMA in toluene (50 % v/v) at 60 °C initiated by 21-Br-CD and mediated by Cu(I)Br / *N*-pentyl-2-pyridylmethanimine ([M]:[I]:[Cu]:[L] = 500:1:4:8). *Conversion determined by gravimetry.

Polymerisations carried out at 60 °C in toluene with a ratio of [MMA]:[21-Br-CD]:[ligand]:[Cu(I)Br] at 500:1:2:1 showed smooth reaction kinetics and a first order kinetic plot showed a linear increase of molecular weight over time (Figure 2.2.2). This indicated that the concentration of active species remained approximately constant over the course of the polymerisation. Good control over the molecular weight could be attained since the molecular weight increased linearly with increasing conversion (Figure 2.2.3). Furthermore, the molecular weight distribution remained low throughout the reaction. The SEC traces showed that coupling reactions between star polymers were suppressed to less than a few percent.

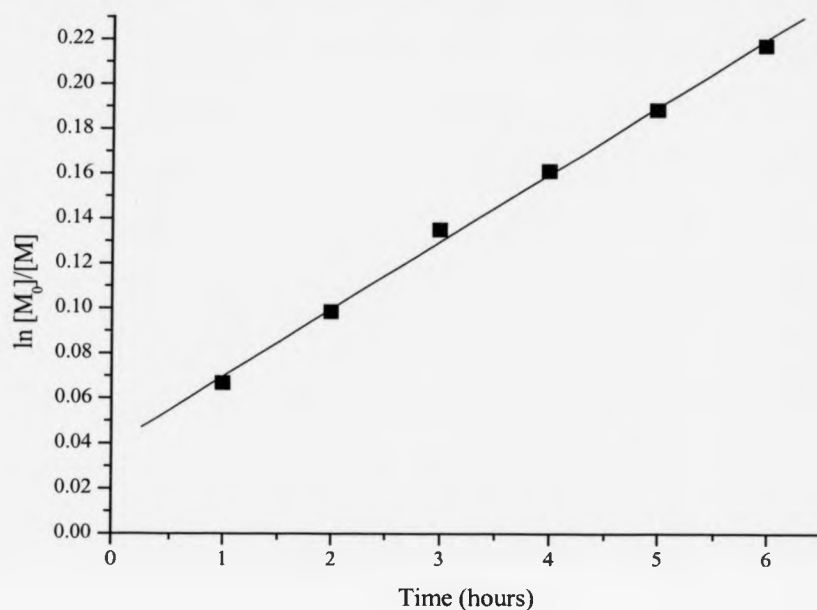


Figure 2.2.2 First order kinetic plot for the LRP of MMA in toluene (50 % v/v) at 60 °C initiated by 21-Br-CD and mediated by Cu(I)Br / *N*-pentyl-2-pyridylmethanimine.

It is noticeable from Figure 2.2.3 that the observed molecular weight obtained by SEC shows a large deviation from the theoretical molecular weight calculated from the conversion and the ratio of the initial concentrations of monomer and initiator. The theoretical molecular weight is much higher than those obtained experimentally. It is thought that this difference is a consequence of the unique architectural differences between linear and star-shaped polymers that alter the hydrodynamic volume of these structures.

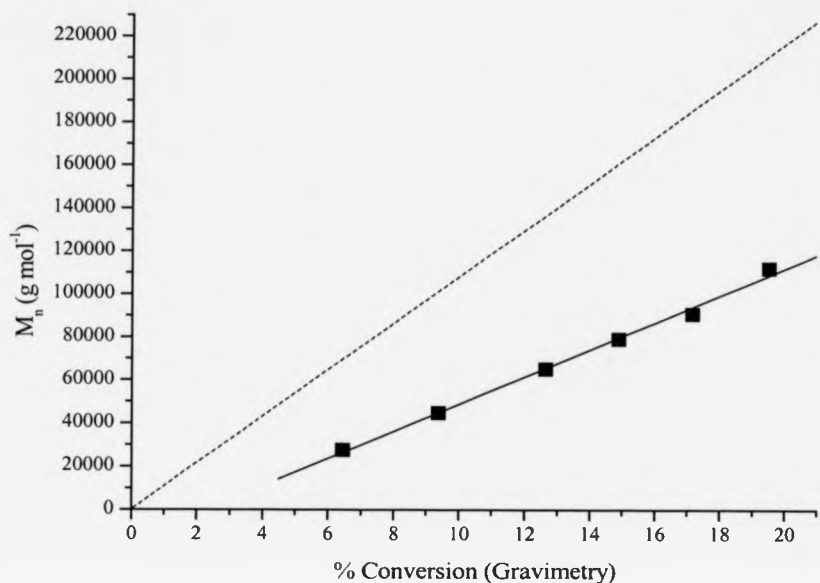


Figure 2.2.3 Evolution of molecular weight distribution with conversion for the LRP of MMA in toluene (50 % v/v) at 60 °C initiated by 21-Br-CD and mediated by Cu(I)Br / *N*-pentyl-2-pyridylmethanimine ([M]:[I]:[Cu]:[L] = 500:1:2:4). Dashed line is M_n (theo).

2.2.2 Suitable Reaction Conditions for the LRP of ST Initiated by 21-Br-CD

Reaction temperatures higher than that for MMA are usually required for the LRP of styrene if similar rates of polymerisation are to be achieved. The higher temperatures are required as the carbon-halogen bond activation energy in the styrene systems is greater than the carbon-halogen bond activation energy in the MMA systems. The optimum temperature for the LRP of styrene with a copper (I) bromide / alkyl pyridylmethanimine catalyst has been reported by Haddleton et al. as being 110 °C²⁸. Matyjaszewski et al. have shown that copper (I) chloride / alkyl bipyridine systems can

polymerise styrene at 130 °C if similar reaction rates to the analogous copper (I) bromide systems are to be observed²⁹. The reaction temperature can be lowered to 80-90 °C if a more efficient catalyst is used^{30, 31}. The controlled living radical polymerisation of PMMA using the 21-armed multifunctional initiator occurred smoothly when a low concentration of initiator was employed ($[M]:[I] = 500:1$) and so this same ratio was employed when investigating the LRP of styrene using 21-Br-CD. The polymerisation temperature was set at 110 °C and the evolution of molecular weight with conversion is summarised in Table 2.2.2.

Time (minutes)	Conversion* (%)	M_n (SEC)	M_n (theo)	PDI
60	3.4	3970	41300	1.01
120	3.6	6480	43500	1.04
180	5.2	12600	60870	1.06
240	6.2	19700	72230	1.07
300	7.2	26900	82960	1.08
360	8.6	36400	98320	1.09
420	9.9	44900	112680	1.09

Table 2.2.2 Evolution of conversion and molecular weight in the LRP of styrene in xylene (50 % v/v) at 110 °C initiated by 21-Br-CD and mediated by Cu(I)Br / *N*-pentyl-2-pyridylmethanimine ($[M]:[I]:[Cu]:[L] = 500:1:4:8$). *Conversion determined by gravimetry.

Good control over the molecular weight was observed after two hours (Figure 2.2.4) and this observation was backed up by the low molecular weight distributions that were

observed during the polymerisation. Initially, the rate of reaction was slow (Figure 2.2.5) but once the system has reached equilibrium first order kinetics were observed and no irreversible termination was apparent. Although these reaction conditions gave good control over the polymerisation of styrene, this was accompanied by a low polymer conversion.

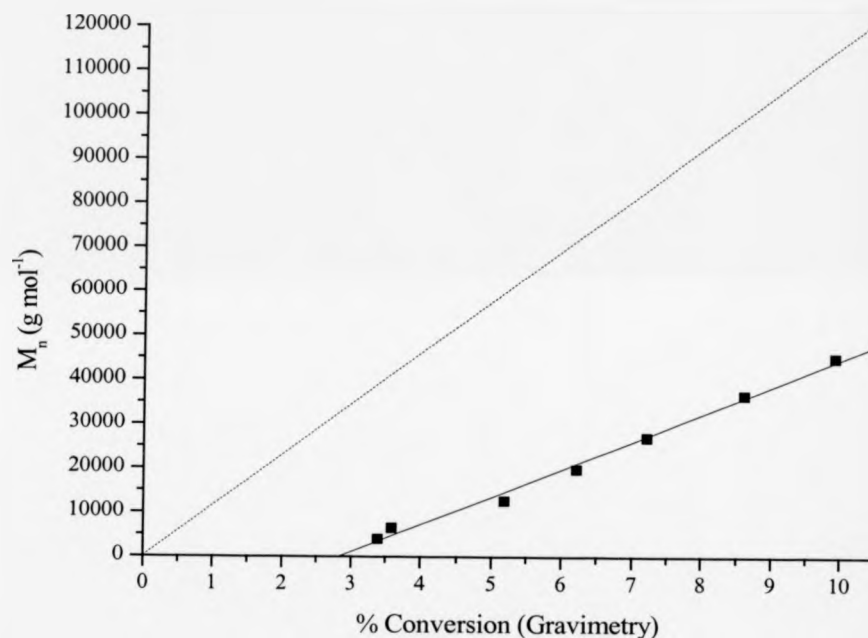


Figure 2.2.4 Evolution of molecular weight distribution with conversion for the LRP of styrene in xylene (50 % v/v) at 110 °C initiated by 21-Br-CD and mediated by Cu(I)Br / *N*-pentyl-2-pyridylmethanimine ([M]:[I]:[Cu]:[L] = 500:1:2:4). Dashed line is M_n (theo).

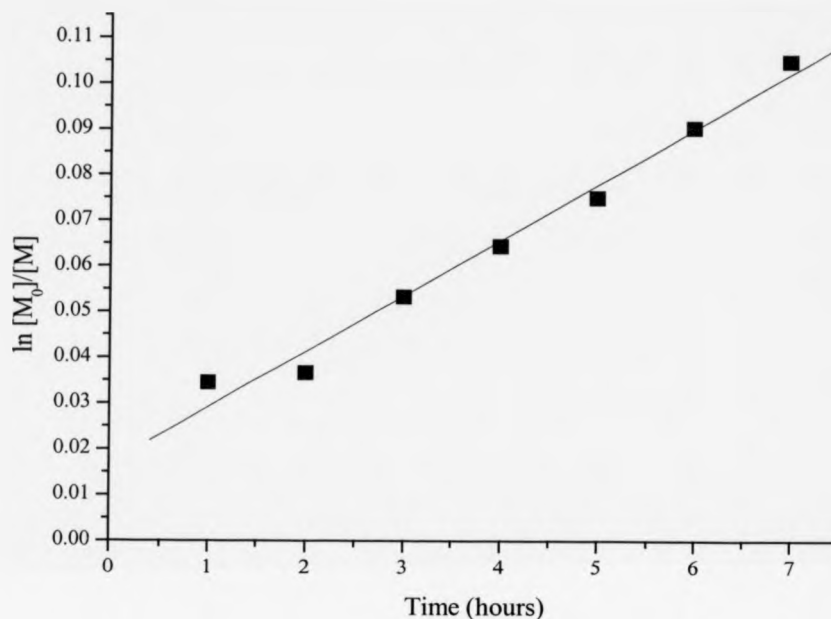


Figure 2.2.5 First order kinetic plot for the LRP of styrene in xylene (50 % v/v) at 110 °C initiated by 21-Br-CD and mediated by Cu(I)Br / *N*-pentyl-2-pyridylmethanimine.

These results demonstrate that star-shaped polystyrene polymers with 21-arms can be prepared in a controlled fashion using copper (I) mediated living radical polymerisation, albeit with low conversions. Low concentrations of the initiator are thought necessary to suppress the effects of irreversible termination reactions.

2.3 Molecular Weight Analysis

The number average molecular weights of the star polymers were determined by size exclusion chromatography (SEC) and found to be much lower than the theoretical molecular weight M_n (theo). Equation 2.3.1 shows how M_n (theo) was calculated.

$$M_n \text{ (theo)} = ([M_0]/[I_0] \times f \times \text{FW(monomer)} \times \text{conversion}) + \text{FW(initiator)}$$

Equation 2.3.1 Calculation of M_n (theo) where $[M_0]$ and $[I_0]$ are the initial concentrations of monomer and initiator respectively, FW(monomer) and FW(initiator) are the formula weight of monomer and initiator respectively, and f is the initiator functionality.

The difference between the molecular weight of the star polymers observed by SEC and the theoretical value was not thought to be due to the incompleteness of the initiation reaction. The difference was attributed to the differences in hydrodynamic volume between star-shaped and linear polymers. The SEC was calibrated with linear PMMA standards. The analysis of samples of star polymers against linear standards does not give a true value for the molecular weight of the stars. During an SEC measurement polymers are fractionated according to their hydrodynamic volume. The sizes of star polymer molecules are generally smaller than that of linear polymers with equivalent molecular weight³². This is due to the ability of a star polymer to coil when in solution and so its hydrodynamic volume is reduced. A linear polymer with the same molecular weight will not coil to the same extent as a star polymer and so its hydrodynamic volume will be greater. As a consequence, the star polymers, with their lower hydrodynamic volume, will remain in the pores of the SEC column for longer. Hence,

the true molecular weight of the star polymers cannot be obtained where a set of linear polymer standards is used to establish the relationship between the elution volume and the molecular weight. As a result of the differences in hydrodynamic volume between star and linear polymers, the SEC underestimates the actual molecular weight of the stars. Hence the direct interpretation of SEC results is only applicable to linear homopolymers where the calibrating materials and the test samples are of a similar chemical type. Others have also observed differences between experimental values determined by SEC and theoretical values^{33, 34}. ^1H NMR spectroscopy can be used to estimate the molecular weight of polymers. This can be achieved by comparing the signals arising from the vinyl proton of the MMA monomer with the methyl groups of the 21-Br-CD initiator. However, due to the low concentration of initiator used in these reactions ($[\text{MMA}]:[\text{21-Br-CD}] = 500:1$) the use of ^1H NMR to determine molecular weight was not appropriate.

2.3.1 Molecular Weight Determination by Low Angle Laser Light Scattering

An alternative method of determining the weight-average molecular weight M_w of a star polymer directly without the need for column calibration is by light scattering methods. In a low-angle laser light-scattering (LALLS) experiment, the light scattered from a polymer solution at a single low angle is measured. The combination of LALLS and SEC will give information on the molecular weight of the star polymer as calculated from the excess Rayleigh factor R_θ and the polymer concentration c . The Rayleigh factor R_θ is the fraction of light scattered relative to the incident beam at a defined angle θ . When dealing with a solution, only the scattering from the solute, dR_θ , is of interest and so the scattering due to the solvent must be subtracted (Equation 2.3.2).

$$dR_{\theta} = R_{\theta} (\text{solution}) - R_{\theta} (\text{solvent})$$

Equation 2.3.2 Calculation of the Rayleigh factor due to a polymer solute.

In a LALLS experiment, the molecular weight M_w is given by Equation 2.3.3.

$$\frac{Kc}{dR_{\theta}} = \frac{1}{M_w}$$

Where K is the optical constant:

$$K = \frac{2\pi^2 n^2 (dn/dc)^2}{N_a \lambda^4}$$

n = refractive index of pure solvent

dn/dc = change in refractive index of the solution with polymer concentration

λ = wavelength of the incident light

N_a = Avogadro's constant

Equation 2.3.3 Determination of weight-average molecular weight by LALLS.

The molecular weight can therefore be determined by measuring the concentration of the eluting species. In practice this is achieved by connecting a concentration detector in series with the LALLS photometer. At each elution volume the concentration c and Rayleigh factor dR_{θ} of the eluting species can be measured and so the molecular weight M_w can be determined.

The accuracy of a GPC-LALLS experiment increases as the molecular weight and concentration of the polymer increases. This is because the amount of light scattered is directly proportional to the product of the molecular weight and solute concentration.

The weight-average molecular weights of a selection of 21-armed star polymers are shown in Table 2.3.1.

Polymer	M _w (SEC)	M _w /M _n (SEC)	M _w (GPC-LALLS)	M _w (theo) [*]
PMMA	62700	1.06	104000	106000
PMMA	27400	1.10	35800	39800
PST	55700	1.45	202000	135000
PST	33500	1.16	68000	55400

Table 2.3.1 Comparison of M_w values determined from SEC and GPC-LALLS experiments of 21-armed star polymers prepared by Cu(I) mediated LRP. *Determined by [M_n (theo)] x [M_w/M_n (SEC)].

The measurement of weight-average molecular weights using the LALLS method shows good agreement with the theoretical weight-average molecular weights calculated from the product of the molecular weight distribution obtained by SEC and the theoretical number-average molecular weight. The molecular weights determined by LALLS are much higher than those obtained by SEC. The agreement between the theoretical weight-average molecular weight and the weight-average molecular weight determined by LALLS is more pronounced with the 21-armed PMMA stars. The higher molecular weight distributions of the 21-armed polystyrene stars may have lead to complications in measuring the weight-average molecular weight by LALLS. The measurement of the absolute molecular weight of the star polymers by the LALLS method appears to give a much better agreement with the theoretical values when compared to the data obtained using the SEC method independently.

In order to obtain accurate light scattering data using the LALLS method, it was necessary to isolate and purify the star polymers prior to undertaking a LALLS experiment. This enabled the exact concentration of the star polymer in the solvent to be determined which is vital to obtain accurate LALLS data. As a result, kinetic experiments could not be performed using the molecular weight data obtained from LALLS since the precise concentration of polymer at a given time could not be calculated.

Samples of polystyrene stars scatter the incident light to a greater extent than samples of PMMA stars. This is because the refractive index increment dn/dc of polystyrene is greater than that of PMMA (Table 2.3.2) and so, according to Equation 2.3.3, can be expected to scatter the light to a greater extent.

Polymer	dn/dc	λ (nm)	Solvent
PMMA	0.086	633	THF
PST	0.192	633	THF

Table 2.3.2 Refractive indices of PMMA and PST used for LALLS experiments.

The use of the LALLS method to measure the absolute molecular weight of the isolated star polymers has been shown to be a good method for this purpose. The results of the LALLS experiments are consistent with the star polymers having a more compact and coiled structure in the THF solution compared to linear analogues that would be expected to assume a more random coil structure in the THF solution.

2.3.2 Molecular Weight Determination by Static Light Scattering

An alternative method of determining the absolute molecular weight of star polymers is to use size intensity measurements by means of static light scattering (SLS) techniques. In this method, the intensity of scattered light from a polymer solution as a function of scattering angle and solute concentration can be used to determine the molecular weight. In 1948, Zimm³⁵ derived the relationship between the concentration and intensity of scattered light (Equation 2.3.4).

$$\frac{Kc}{R} = \frac{1}{MP_{\theta}} + 2A_2c$$

Where K is the optical constant previously described

R is the Rayleigh ratio and dependent on the intensity of scattered light

P_{θ} is the particle scattering function that depends on particle shape

A_2 is the second virial coefficient

Equation 2.3.4 Zimm relationship between molecular weight M , concentration c and Rayleigh ratio R .

Zimm proposed a special graphing technique, now called a Zimm plot, to deduce the molecular weight of the polymer sample. A Zimm plot shows concentration over Rayleigh ratio as a series of measurements made at different angles and different concentrations to form a grid. A double extrapolation to zero concentration and zero angle can be calculated and the intercept on the vertical axis is proportional to the reciprocal of the weight-average molecular weight.

Static light scattering techniques are very sensitive to dirt and dust in the sample and so great care was taken in preparing the samples. Four concentrations (0.25 – 2.00 g L⁻¹) of star-shaped poly(methyl methacrylate) in THF were accurately prepared in a laminar

air-flow cabinet to reduce the contamination of dust. The four concentrations of polymer solution along with all solvents were also filtered twice through $0.02 \mu\text{m}$ membrane filters to ensure that all dust was excluded and solutions left to stand overnight to ensure complete solvation. The SLS experiments were performed over twelve angles between 30° and 140° with 60 separate one-second intensity measurements being made at each angle before averaging for each angle. Once each of the twelve angles for each of the four polymer concentrations had been measured, a Zimm plot was constructed. An example of one of these Zimm plots is shown in Figure 2.3.1.

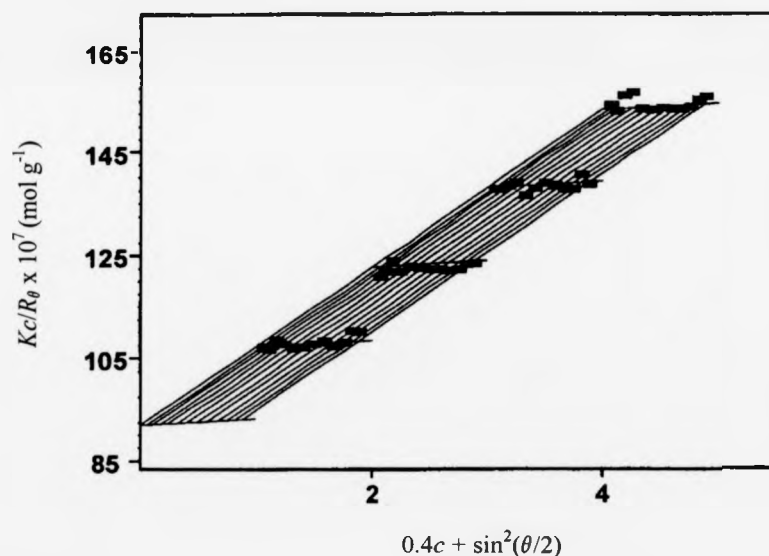


Figure 2.3.1 Zimm plot of a 21-armed PMMA star polymer used to obtain absolute molecular weight.

The more concentrated polymer samples scatter light to a greater extent and so the intensity of the scattered light is greater at higher concentrations whereas the intensity of scattered light is lower for lower concentrations of polymer samples. The extrapolation of the Zimm plot to zero concentration and zero angle gives the reciprocal of the weight-average molecular weight and a good agreement between molecular weights obtained by SLS and LALLS was observed (Table 2.3.3).

Polymer	M_w (SLS)	M_w (GPC-LALLS)
PMMA	109000	104000
PMMA	38300	35800
PST	225000	202000
PST	80000	68000

Table 2.3.3 Comparison of molecular weight data obtained by SLS and GPC-LALLS.

The determination of the absolute molecular weight of star-shaped polymers by light scattering methods therefore provides evidence that star-shaped polymers have been formed. In the SEC experiments, the lower hydrodynamic volumes of the star-shaped polymers mean that they remain in the pores of the SEC columns for longer and this is why SEC appears to underestimate the true size of the polymers. In light scattering experiments such as SLS however, the star-shaped polymers are not separated according to their size and their molecular weight can be obtained more directly.

2.4 Conclusions

The synthesis of well-defined star polymers containing 21 arms by the core first approach has been realised. This is the first time that such star polymers, incorporating a β CD core, have been prepared by copper mediated LRP. The precise organic synthesis of the β CD derivative to form the novel multifunctional initiator was essential if the number of arms were to be predetermined. Despite the high molecular weight of this initiator, it was still possible to purify the initiator by column chromatography and it could be fully characterised. Suitable reaction conditions required for living radical polymerisation of MMA and styrene were investigated. Due to the high concentration of initiating species on the β CD molecule it was necessary to use a low concentration of the initiator to prevent any irreversible coupling reactions between star polymers. Smooth reaction kinetics were observed when the ratio of the monomer to initiating group was found to be 500:1. Lower reaction temperatures also contributed to a suppression of star-star coupling thus producing well-defined polymers with a low molecular weight distribution. The molecular weights of the star polymers as determined by SEC were found to be much lower than the theoretical molecular weights calculated from the monomer conversion and initial concentration of the initiator. This was attributed to the differences in hydrodynamic volumes between linear polymers (which are used to calibrate the SEC systems) and the sample of star polymer. More accurate weight-average molecular weight data was obtained using light scattering methods such as low angle laser light scattering (LALLS) and static light scattering experiments (SLS). Using these light scattering methods gave molecular weight values that were closer to those predicted by theory.

2.5 Chapter 2 References

- 1 B. Wong, K. Ohno, and D. M. Haddleton, *Abstr. Pap. Am. Chem. Soc.*, 2001, **221**, 533.
- 2 K. Y. Baek, M. Kamigaito, and M. Sawamoto, *J. Polym. Sci. Pol. Chem.*, 2002, **40**, 2245.
- 3 K. Y. Baek, M. Kamigaito, and M. Sawamoto, *J. Polym. Sci. Pol. Chem.*, 2002, **40**, 1972.
- 4 C. Celik, G. Hizal, and U. Tunca, *J. Polym. Sci. Pol. Chem.*, 2003, **41**, 2542.
- 5 K. Ishizu, J. Park, T. Shibuya, and A. Sogabe, *Macromolecules*, 2003, **36**, 2990.
- 6 T. Kakuchi, A. Narumi, T. Matsuda, Y. Miura, N. Sugimoto, T. Satoh, and H. Kaga, *Macromolecules*, 2003, **36**, 3914.
- 7 K. Kanki and T. Masuda, *Macromolecules*, 2003, **36**, 1500.
- 8 K. Matyjaszewski, *Macromolecular Symposia*, 2003, **195**, 25.
- 9 D. R. Robello, A. Andre, T. A. McCovick, A. Kraus, and T. H. Mourey, *Macromolecules*, 2002, **35**, 9334.
- 10 M. H. Stenzel and T. P. Davis, *J. Polym. Sci. Pol. Chem.*, 2002, **40**, 4498.
- 11 M. Morton, T. D. Helminiak, S. D. Gadkary, and F. Bueche, *J. Polym. Sci.*, 1962, **57**, 471.
- 12 K. Huber, W. Burchard, and L. J. Fetters, *Macromolecules*, 1984, **17**, 541.
- 13 N. Hadjichristidis, A. Guyot, and L. J. Fetters, *Macromolecules*, 1978, **11**, 668.
- 14 D. M. Haddleton and M. C. Crossman, *Macromol. Chem. Phys.*, 1997, **198**, 871.
- 15 P. Lutz and P. Rempp, *Macromol. Chem. Phys.*, 1988, **189**, 1051.
- 16 S. Jacob, I. Majoros, and J. P. Kennedy, *Macromolecules*, 1996, **29**, 8631.

- 17 H. Shohi, M. Sawamoto, and T. Higashimura, *Makromol. Chem. Phys.*, 1992, **193**, 2027.
- 18 T. Fujimoto, S. Tani, K. Takano, M. Ogawa, and M. Nagawawa, *Macromolecules*, 1978, **11**, 673.
- 19 T. Miyata and K. Nakamae, *Trends Polym. Sci.*, 1997, **5**, 198.
- 20 M. Ejaz, K. Ohno, Y. Tsujii, and T. Fukuda, *Macromolecules*, 2000, **33**, 2870.
- 21 D. M. Haddleton, R. Edmonds, A. M. Heming, E. J. Kelly, and D. Kukulj, *New J. Chem.*, 1999, **23**, 477.
- 22 M. H. Stenzel-Rosenbaum, T. P. Davis, V. K. Chen, and A. G. Fane, *Macromolecules*, 2001, **34**, 5433.
- 23 D. French, D. W. Knapp, and J. H. Pazur, *J. Am. Chem. Soc.*, 1950, **72**, 5150.
- 24 D. M. Haddleton, C. B. Jasieczek, M. J. Hannon, and A. J. Shooter, *Macromolecules*, 1997, **30**, 2190.
- 25 D. M. Haddleton, D. Kukulj, D. J. Duncalf, A. M. Heming, and A. J. Shooter, *Macromolecules*, 1998, **31**, 5201.
- 26 D. Q. Qin, S. H. Qin, X. P. Chen, and K. Y. Qiu, *Polymer*, 2000, **41**, 7347.
- 27 V. Percec, B. Barboiu, A. Neumann, J. C. Ronda, and M. Y. Zhao, *Macromolecules*, 1996, **29**, 3665.
- 28 S. Perrier, D. Berthier, I. Willoughby, D. Batt-Coutrot, and D. M. Haddleton, *Macromolecules*, 2002, **35**, 2941.
- 29 K. Matyjaszewski, T. E. Patten, and J. H. Xia, *J. Am. Chem. Soc.*, 1997, **119**, 674.
- 30 J. H. Xia and K. Matyjaszewski, *Macromolecules*, 1997, **30**, 7697.

-
- 31 K. Matyjaszewski, M. L. Wei, J. H. Xia, and S. G. Gaynor, *Macromolecular Chemistry and Physics*, 1998, **199**, 2289.
- 32 B. H. Zimm and W. H. Stockmayer, *J. Chem. Phys.*, 1949, **17**, 1301.
- 33 K. A. Davis and K. Matyjaszewski, *Macromolecules*, 2000, **33**, 4039.
- 34 K. A. Davis, B. Charleux, and K. Matyjaszewski, *J. Polym. Sci. Pol. Chem.*, 2000, **38**, 2274.
- 35 B. Zimm, *J. Chem. Phys.*, 1948, **16**, 1099.

Chapter 3Modification of β CD in the
Synthesis and Characterisation of
Star Polymers with 14- and 7-arms by Copper (I) Mediated LRP**3.0 Introduction**

The work described in the previous chapter showed that under appropriate reaction conditions, all 21 hydroxyl groups of a β CD molecule could be chemically modified to yield 21-Br-CD. This modified β CD can subsequently be used as a multifunctional initiator in copper (I) mediated LRP for the synthesis of well-defined star polymers possessing 21 discrete arms. As an extension to the transformation of all the hydroxyl groups, it is possible to exploit the differing chemical reactivities of the primary and secondary hydroxyl groups of β CD to obtain derivatives where the number and exact positions of modifications are ascertained and pure compounds with unambiguous structures are obtained. To this end, there have been a large number of CD derivatives synthesised and these have been reviewed¹. The selective modification of CDs can be divided into three categories: (1) the 'clever' method, where the chemistry of CD is exploited to get the desired product; (2) the 'long' method, where a number of protection and deprotection steps are necessary to selectively reach the positions that would otherwise not be selectively accessible; (3) the 'sledgehammer' method, where CD is indiscriminately reacted to give a mixture of products and the desired product is painstakingly separated by chromatography. The primary hydroxyl groups located at the 6-position of the CDs are the most basic whereas the secondary hydroxyl groups at the 2- and 3-positions are the most acidic^{2, 3}. Thus, under normal circumstances, a mild

electrophilic reagent will attack at the 6-position in preference to the 2- and 3-positions. More reactive reagents will attack the hydroxyl groups less selectively. By exploiting the differing reactivities of these hydroxyl groups it is possible to selectively modify the primary and secondary faces of β CD to synthesise derivatives that may be used as multifunctional initiators for LRP.

3.1 Primary Face Modification of β CD

A strategy to synthesise a β CD derivative that can be employed as a multifunctional initiator for the formation of star polymers with 14 discrete arms will involve exploiting the reactivity of the primary hydroxyl groups. Once these seven primary hydroxyl groups are protected, the remaining 14 secondary hydroxyl groups are available to be transformed into initiating units. Permodification (modification of all the hydroxyl groups at one site) at the primary face is relatively easier than mono-, di-, or trisubstitution because symmetrical substitution is achieved when the reaction is allowed to run for a longer time.

3.2 Secondary Face Modification of β CD

The secondary face of the CDs are more crowded than the primary face since there are twice the number of hydroxyl groups. Hydrogen bonding can occur between the hydroxyl groups at the 2- and 3-positions which makes them more rigid and less flexible compared to those at the 6-position. These factors make the secondary face less reactive and harder to functionalise than the primary face. During the course of a reaction, as the degree of substitution increases, the secondary side becomes even more crowded and so any attacking groups are directed towards the primary face thus

decreasing the selectivity. This further provides the necessity for the protection of the primary side so that initiator formation is directed selectively at the secondary face.

3.3 Protection at the Primary Face for the Synthesis of Heptakis(6-*O*-*tert*-butyldimethylsilyl)- β -cyclodextrin

The most popular reagent used to produce modifications at the primary face is *tert*-butyldimethylsilyl chloride (TBDMSCl). This reagent is more selective than trimethylsilyl chloride (TMSCl) since TMSCl also attacks at the secondary face. The protection of the primary face with TBDMSCl in pyridine at room temperature yields the 6-substituted derivative (Figure 3.3.1) as the major product. The silyl ethers of CD are good protecting groups due to their ease of removal⁴⁻⁶.

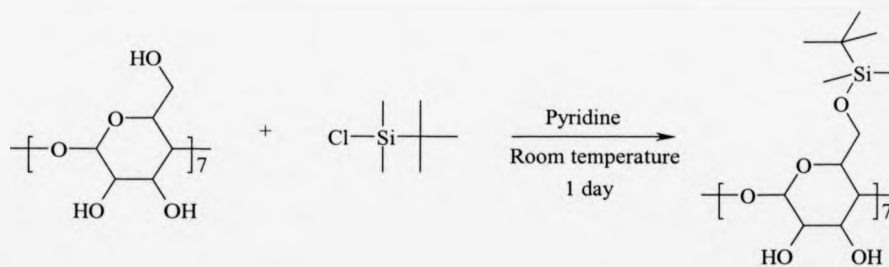


Figure 3.3.1 Modification of the primary face of β CD with TBDMSCl in the synthesis of heptakis(6-*O*-*tert*-butyldimethylsilyl)- β -cyclodextrin.

The silylation reaction was carried out at room temperature to avoid previously reported incidences of reactivity at the secondary side when higher reaction temperatures were used⁷. The selection of pyridine as both a solvent and a base also conferred greater regioselectivity towards the primary side in contrast to when imidazole in *N,N*-dimethylsilyl chloride was used. The treatment of β CD with an excess of TBDMSCl gave 85 % yield of heptakis(6-*O*-*tert*-butyldimethylsilyl)- β -cyclodextrin after flash chromatography. The product was characterised by ¹H and ¹³C NMR spectroscopy to verify that silylation had occurred at all seven hydroxyl groups at the primary face. The seven-fold symmetry of heptakis(6-*O*-*tert*-butyldimethylsilyl)- β -cyclodextrin was proved by the ¹³C NMR spectra which showed the presence of only six skeleton carbon signals. This indicated a symmetric pattern of substitution.

3.4 Synthesis of Heptakis(2,3-di-*O*-(2-bromo-2-methylpropionyl)-6-*O*-(*tert*-butyldimethylsilyl))- β -cyclodextrin

Following the successful protection of the seven primary hydroxyl groups with TBDMS, the 14 secondary hydroxyl groups are available for chemical modification. To synthesise appropriate initiators for their use in copper (I) mediated LRP, it is necessary to transform these hydroxyl groups to a 2-bromo-2-methylpropionyl functionality. From the previous chapter, direct esterification of CDs with 2-bromoisobutyrylbromide was unsuccessful since this reagent was too reactive. The milder reagent 2-bromoisobutyryl anhydride was employed in the esterification of heptakis(6-*O*-*tert*-butyldimethylsilyl)- β -cyclodextrin (Figure 3.4.1).

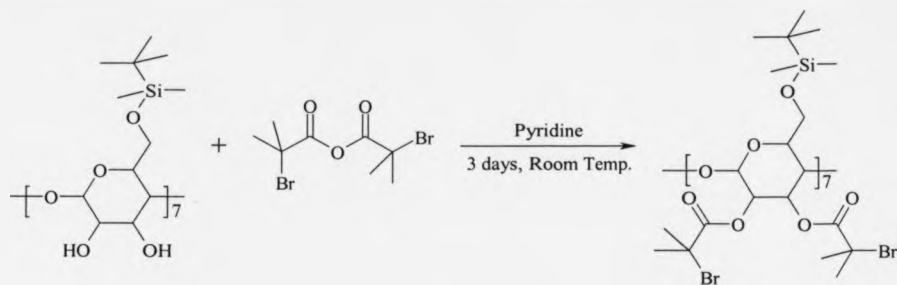


Figure 3.4.1 Synthesis of heptakis(2,3-di-O-(2-bromo-2-methylpropionyl)-6-O-(tert-butyl dimethylsilyl))- β -cyclodextrin by esterification with 2-bromoisobutyryl anhydride.

A long reaction time was required to ensure that the esterification reaction was complete. Following an aqueous work-up to remove any inorganic species, flash chromatography was used to purify the final compound. Analysis of the IR spectra showed that the OH stretches associated with the secondary hydroxyl groups at 3000 cm^{-1} had completely disappeared and a new absorption at 1720 cm^{-1} was observed that corresponded to the carbonyl stretch of the initiating group. The ^1H NMR spectra (Figure 3.4.2) showed the appearance of a signal at 1.91 ppm that was twice the integral at 0.03 ppm associated with methyl groups on the silyl protecting group. The signal at 1.91 ppm arises from the incorporation of 14 initiating units on the core of the protected β CD. Furthermore, the signal at 1.89 ppm arising from free 2-bromoisobutyryl anhydride had disappeared.

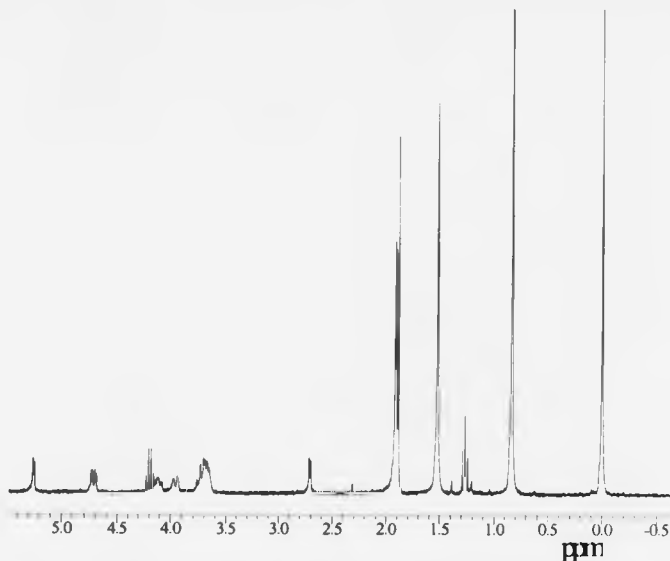


Figure 3.4.2 ^1H NMR spectra of heptakis(2,3-di-*O*-(2-bromo-2-methylpropionyl)-6-*O*-(*tert*-butyldimethylsilyl))- β -cyclodextrin.

The small discrepancy between the calculated and observed values in the elemental analysis of this compound was attributed to the difficulty in obtaining accurate values for such high molecular weight molecules ($\text{FW} > 4000 \text{ g mol}^{-1}$).

This compound, possessing 14 discrete initiating sites, was subsequently used as a multifunctional initiator in copper (I) mediated LRP for the formation of star polymers possessing 14 arms.

3.5 Protection of Both Faces of β CD for the Synthesis of Heptakis(2,3-di-*O*-acetyl-6-*O*-*tert*-butyldimethylsilyl)- β -cyclodextrin

The strategy required to form a multifunctional initiator that is capable of yielding star polymers with seven discrete arms radiating from a β CD core involves an additional protection and deprotection step at the secondary and primary face respectively. It was thought that the direct esterification of β CD with 2-bromoisobutyryl anhydride would not be regioselective towards the primary face and partial esterification at the 2- and 3-positions would occur that would be too laborious to separate by chromatographic methods. Hence, the strategy that was followed to accomplish a seven-armed multifunctional initiator involved protecting all 21 hydroxyl groups of β CD followed by deprotection at the primary face to yield a molecule with seven free hydroxyl groups that could be transformed into initiator groups. It was necessary for the protecting groups at the primary face to be easily and selectively deprotected to form the species with seven free hydroxyl groups. Since TBDMS is the most popular protecting group at the primary side due to its ease of attachment and ease of removal, this protecting group was employed.

There are a number of protecting groups available for the protection at the secondary side of CD. These include the tosylation of 6-silylated CD in pyridine with tosyl chloride at elevated temperatures^{8, 9}. However, tosylation gives low yields because of the tendency to form 2,3-epoxy derivatives in the basic medium. Sulfonates can be used to protect the secondary side of 6-silylated CDs but these reactions are very sensitive to moisture¹⁰. Alkylation and benzylation of 6-silylated CDs can be achieved by reacting the hydroxyl groups with appropriate alkyl and benzyl halides respectively in basic

conditions^{11, 12}. Acetylation of 6-silylated CDs with acetic anhydride also provides a route to the protection of the hydroxyl groups at the secondary face of β CD.

Figure 3.5.1 shows the reaction scheme that was used to prepare β CD protected at the primary face with TBDMS and at the secondary face with acetyl groups.

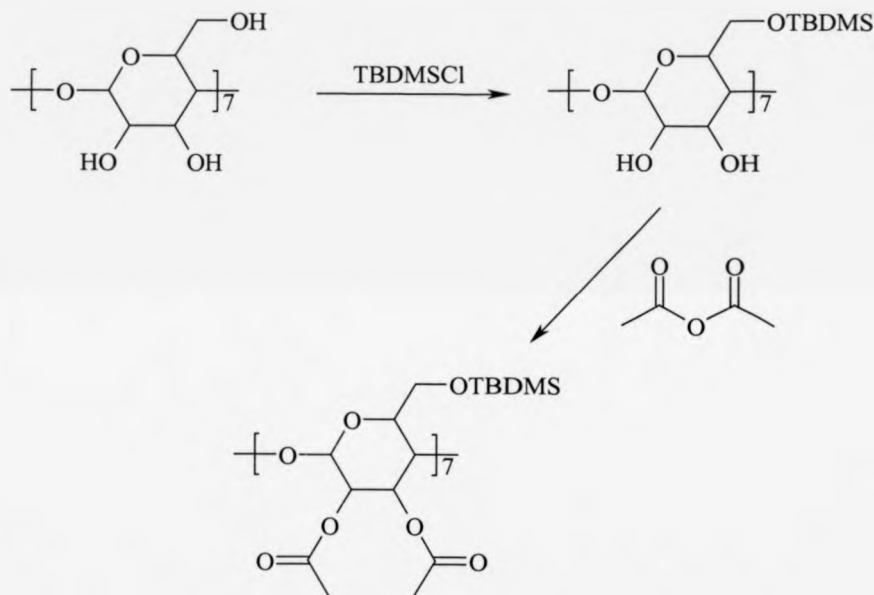


Figure 3.5.1 Reaction scheme for the protection of β CD at the 6-position with TBDMS and at the 2- and 3-positions with acetyl groups.

The synthesis of the 6-silylated β CD was carried out as described in Section 3.3 above. The acetylation of this compound was achieved by reaction with acetic anhydride in pyridine at room temperature over three days. Although this reaction has previously been reported at 100 °C over four hours⁴, the reaction was carried out at room temperature to avoid the possibility of the TBDMS protecting group from cleaving.

A catalytic amount of 4-(dimethylamino)pyridine was added to the reaction and the product was purified by column chromatography.

The ^1H NMR spectra of heptakis(2,3-di-*O*-acetyl-6-*O*-*tert*-butyldimethylsilyl)- β -cyclodextrin showed the appearance of two signals at 2.20 and 2.21 ppm corresponding to the protons on the methyl group of the acetyl unit at the 2- and 3-position of the secondary face. Analysis of the ^{13}C NMR spectra also showed the appearance of two signals at 171.0 and 169.2 ppm that correspond to the carbonyl carbons of the acetyl unit.

3.6 Desilylation at the Primary Face

For the seven hydroxyl groups at the primary face to be regenerated, the TBDMS groups are required to be deprotected. This can be achieved by several routes. Attempts at desilylation with tetrabutylammonium fluoride¹³ in oxolane at room temperature resulted in the formation of a mixture of deacetylated products¹⁴. Desilylation in a mixture of water, acetic acid and oxolane has also been reported as unsuccessful¹³ since most of the starting material was recovered unchanged after reaction at room temperature for 20 hours. More recently, cleavage of the TBDMS group by chloride ions has been reported¹⁵ for more base-sensitive substrates since the fluoride anion is strongly basic. Deprotection using ultrasonic cleavage in methanol/carbon tetrachloride has also been reported¹⁶. The use of boron trifluoride etherate in dichloromethane for successful desilylation has previously been reported¹⁷ and this procedure was subsequently adopted (Figure 3.6.1).

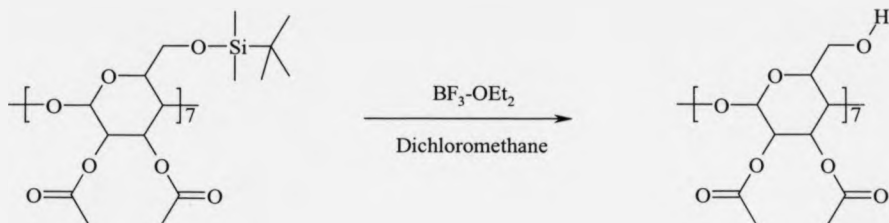


Figure 3.6.1 Desilylation at the 6-position of substituted β CD with boron trifluoride etherate.

The high affinity of silicon towards fluoride ions provides the driving force for the reaction between TBDMS ethers and fluoride ions. The mechanism is thought to proceed via the corresponding alkoxide and TBDMS-F followed by the addition of water to give the alcohol (Figure 3.6.2) but this mechanism is not very well understood.

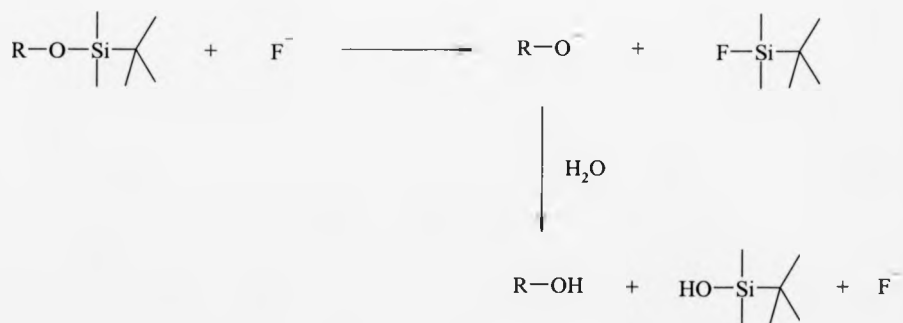


Figure 3.6.2 Proposed mechanism for the deprotection of TBDMS ethers with fluoride anion.

Desilylation of heptakis(2,3-di-*O*-acetyl-6-*O*-*tert*-butyldimethylsilyl)- β -cyclodextrin was achieved at room temperature over 24 hours with boron trifluoride etherate in dichloromethane. After the addition of water and purification by column chromatography, the product was analysed by ^{13}C and ^1H NMR spectroscopy to determine whether complete desilylation had occurred to regenerate the seven hydroxyl groups at the primary face. Inspection of the ^1H NMR spectra showed the complete disappearance of the signals at 0.86 and 0.02 ppm that correspond to the *tert*-butyl and dimethyl silyl groups respectively of the TBDMS protecting group. Furthermore, analysis of the ^{13}C NMR spectra showed the expected seven-fold symmetry that confirmed the removal of the TBDMS groups. The IR spectra showed the appearance of the OH stretch at 3250 cm^{-1} that qualitatively indicated the presence of the hydroxyl groups. The small discrepancy in the elemental analysis was attributed to difficulties in obtaining accurate molecular weight values for these high molecular weight species.

3.7 Synthesis of Heptakis(2,3-di-*O*-acetyl-6-*O*-(2-bromo-2-methylpropionyl))- β -cyclodextrin

Following the successful synthesis and characterisation of heptakis(2,3-di-*O*-acetyl)- β -cyclodextrin, the final step of the 4-stage reaction was to esterify the seven hydroxyl groups with an appropriate initiating group to generate a multifunctional initiator with seven initiation sites. Like before, a 2-bromo-2-methylpropionyl functionality was required to be attached to the primary face since this group is able to promote initiation of copper (I) mediated LRP. 2-Bromoisobutyryl anhydride was again used as the reagent to realise the esterification of heptakis(2,3-di-*O*-acetyl)- β -cyclodextrin (Figure 3.7.1).

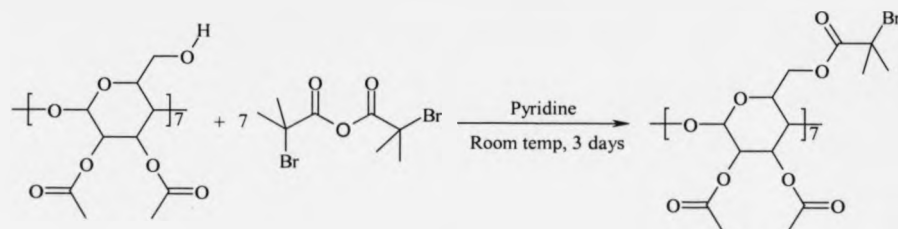


Figure 3.7.1 Synthesis of the seven-armed multifunctional initiator heptakis(2,3-di-*O*-acetyl-6-*O*-(2-bromo-2-methylpropionyl))- β -cyclodextrin.

The reaction proceeds via a nucleophilic attack of the anhydride and a long reaction time (three days) was required to ensure complete esterification had occurred and also because the anhydride reagent is only a mild reagent. High dilution ensured that any inter-molecular hydrogen bonding was minimised. After careful aqueous work-up, heptakis(2,3-di-*O*-acetyl-6-*O*-(2-bromo-2-methylpropionyl))- β -cyclodextrin was purified by column chromatography on a large column of silica gel to effectively separate any by-products. The disappointing yield of 8 % was thought to be due to the difficulty in passing such high molecular weight species ($\text{FW} = 2764 \text{ g mol}^{-1}$) through such a large column of silica gel.

Analysis of the ^1H NMR spectra of the product showed the appearance of a new signal at 1.92 ppm that corresponded to the methyl groups of the initiating unit. This signal could be distinguished from the signal at 2.02 ppm corresponding to the protons of the acetyl protecting groups at the secondary face. Integration of the new signal at 1.92 ppm was identical to the integration of the signal at 2.02 ppm and this confirmed that complete substitution of the hydroxyl groups with an initiating functionality had occurred. The absence of any absorption in the IR spectra at 3250 cm^{-1} further indicated that hydroxyl groups were not present in the final product. The discrepancy in the

elemental analysis was attributed to the difficulties in obtaining accurate molecular weight values for these high molecular weight species. The four-step strategy for the synthesis of a multifunctional initiator with seven initiating sites at the primary face of β CD had now been realised. The complete reaction scheme for the synthesis is summarised in Figure 3.7.2. Full characterisation of the intermediates in this synthetic pathway ensured that only pure products were used for subsequent stages in the strategy. The extensive use of column chromatography ensured the purification of the intermediates and isolation of any isomers. It was also noted that the high molecular weight of some of these β CD derivatives may have prevented their passing through the chromatography columns and caused lower yields to be observed.

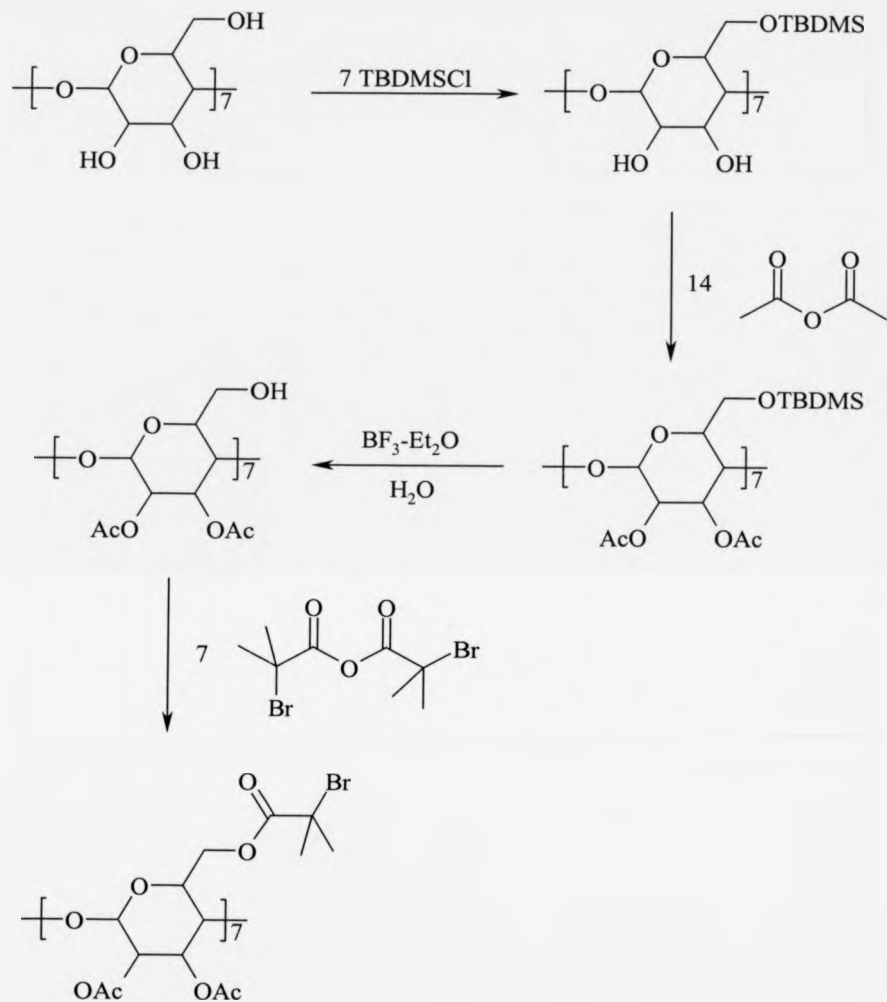


Figure 3.7.2 Synthetic strategy for the formation of heptakis(2,3-di-*O*-acetyl-6-*O*-(2-bromo-2-methylpropionyl))- β -cyclodextrin, a seven-armed multifunctional initiator.

3.8 Copper (I) Mediated LRP initiated by 14-Br-CD

The directed synthesis of the multifunctional initiator with 14 discrete initiating sites and a β CD core allows its use in copper mediated living radical polymerisation to be investigated. Living radical polymerisation has been shown to be an easy synthetic route to produce well-defined polymers¹⁸⁻³² and star-shaped polymers can be prepared using this method³³⁻³⁶. Suitable reaction conditions for the formation of well-defined star polymers using the 14-armed multifunctional initiator needed to be investigated.

3.8.1 Suitable Reaction Conditions for the LRP of MMA initiated by 14-Br-CD

The previous chapter has shown that smooth initiation of the 21-Br-CD multifunctional requires a low concentration of initiator to suppress any star-star coupling reactions. This is thought to be due to the high number of initiating sites that are in close proximity to each other thereby increasing the likelihood of irreversible termination reactions when two radicals combine. Consequently, a ratio of $[MMA]:[Cu]:[L]:[I] = 500:4:8:1$ was employed for the living radical polymerisation of MMA. This ratio found to produce well-defined star polymers using the 21-Br-CD multifunctional initiator. The polymerisation was carried out in toluene and a reaction temperature of 60 °C was used to further suppress the likelihood of any star-star coupling reactions.

Table 3.8.1 summarises the data obtained for the formation of star PMMA polymers by LRP. Under these conditions, an increase in molecular weight with increasing conversion (Figure 3.8.1) demonstrated that 14-Br-CD was initiating the polymerisation of MMA. Conversion of monomer to polymer was determined by gravimetry in preference to the use of ^1H NMR which was not appropriate due to the low concentration of initiator relative to the monomer.

Time (mins)	Conversion* (%)	M _n (SEC)	M _n (theo)	PDI
60	1.4	10200	13740	1.09
120	4.9	24300	34710	1.06
180	7.5	36100	56630	1.06
240	10.8	50000	79400	1.06
300	13.1	59800	95550	1.06
360	14.4	69300	104980	1.06
430	15.0	83200	115560	1.05

Table 3.8.1 Evolution of conversion and molecular weight in the LRP of MMA in toluene (50 % v/v) at 60 °C initiated by 14-Br-CD and mediated by Cu(I)Br / *N*-pentyl-2-pyridylmethanimine ([M]:[I]:[Cu]:[L] = 500:1:4:8). *Conversion determined by gravimetry.

The distribution of molecular weights (PDI) during the polymerisation remained remarkably low throughout (PDI < 1.09) and decreased slightly over time. It is thought that hydrodynamic volume of these star polymers compared to their linear counterparts is partly responsible for the narrow molecular weight distributions observed.

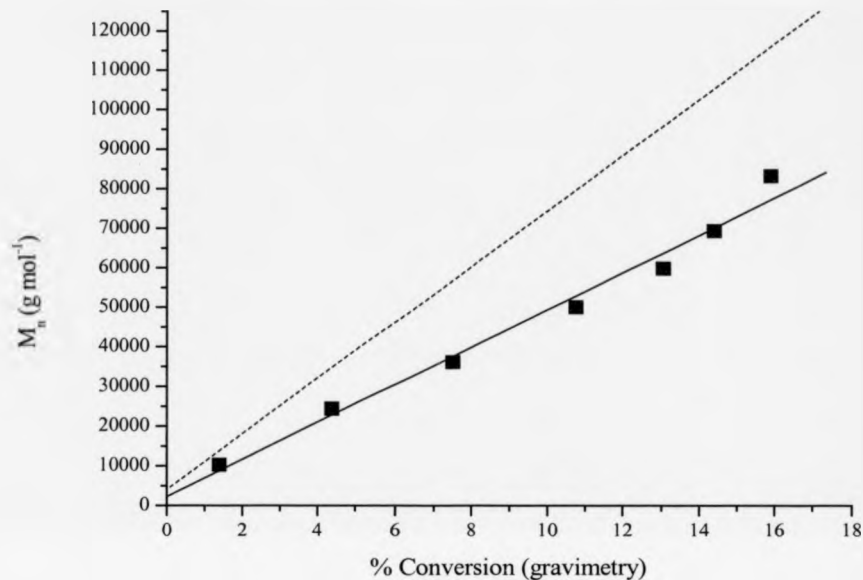


Figure 3.8.1 Evolution of molecular weight distribution with conversion for the LRP of MMA in toluene (50 % v/v) at 60 °C initiated by 14-Br-CD and mediated by Cu(I)Br / *N*-pentyl-2-pyridylmethanimine ([M]:[I]:[Cu]:[L] = 500:1:4:8). Dashed line is M_n (theo).

The first order kinetic rate plot for this polymerisation showed a straight line (Figure 3.8.2) which indicated that the concentration of radical species remained constant throughout the polymerisation. Low conversions were observed after four hours of polymerisation and this was attributed to the low polymerisation temperature chosen and also the low concentration of initiator that was used.

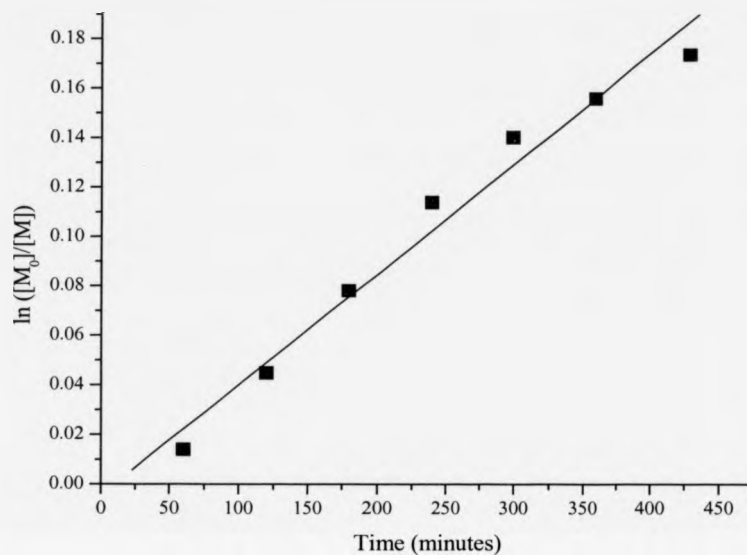


Figure 3.8.2 First order rate plot for the LRP of MMA at 60 °C initiated by 14-Br-CD and mediated by Cu(I)Br / *N*-pentyl-2-pyridylmethanimine ($[M]:[Cu]:[L]:[I] = 500:4:8:1$) in toluene (50 % v/w).

When the polymerisation temperature was increased from 60 °C to 90 °C, higher monomer conversions were observed and the molecular weight distribution remained narrow (Table 3.8.2).

Time (mins)	Conversion* (%)	M_n (SEC)	M_n (theo)	PDi
60	17.3	53800	124780	1.07
120	21.0	89300	151340	1.06
180	32.5	120000	231280	1.06
240	35.9	141000	255790	1.07
300	41.5	163000	294490	1.09

Table 3.8.2 Evolution of conversion and molecular weight in the LRP of MMA in toluene (50 % v/v) at 90 °C initiated by 14-Br-CD and mediated by Cu(I)Br / *N*-pentyl-2-pyridylmethanimine ([M]:[I]:[Cu]:[L] = 500:1:4:8). *Conversion determined by gravimetry.

The first order rate plot for the polymerisation of MMA at 90 °C (Figure 3.8.3) shows a non-linear relationship at longer reaction times. This is indicative of a gradual loss of reactive species resulting from irreversible termination. This may account for the gradual increase in molecular weight distribution.

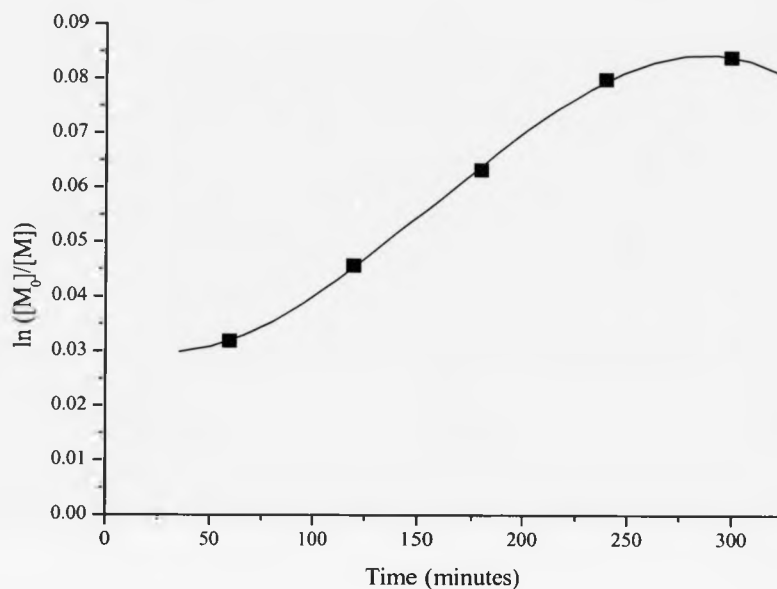


Figure 3.8.3 First order rate plot for the LRP of MMA at 90 °C initiated by 14-Br-CD and mediated by Cu(I)Br / *N*-pentyl-2-pyridylmethanimine ([M]:[Cu]:[L]:[I] = 500:4:8:1) in toluene (50 % v/w).

The evolution of molecular weight with monomer conversion (Figure 3.8.4) also shows deviation from linearity.

In general, higher polymerisation temperatures appear to affect the control over the reactions where higher temperatures lead to a loss of control. Control of the polymerisation is important if well-defined polymers are to be obtained. Loss of control is usually a result of irreversible radical-radical termination events that produces 'dead' polymer chains. The 'dead' chains cannot be further activated by the copper catalytic complex and so addition of more monomer units is prevented. Chain-end functionality

is also lost by the combining of two radical species and further modifications to the chain-end are not possible.

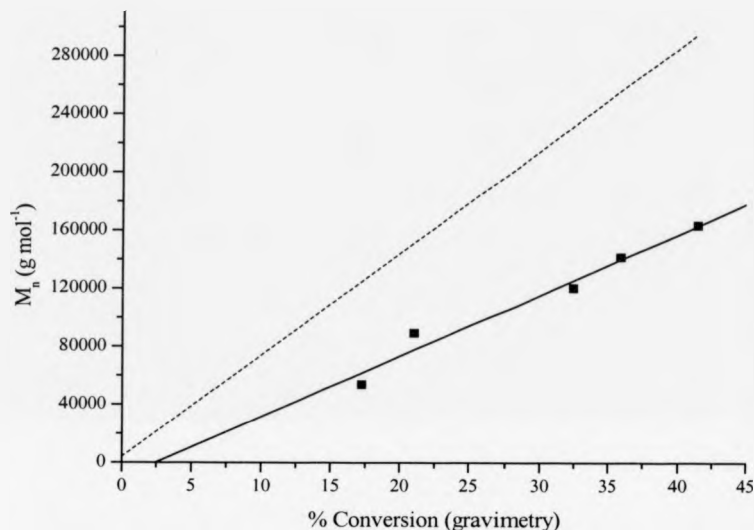


Figure 3.8.4 Evolution of molecular weight distribution with conversion for the LRP of MMA in toluene (50 % v/v) at 90 °C initiated by 14-Br-CD and mediated by Cu(I)Br / *N*-pentyl-2-pyridylmethanimine ([M]:[I]:[Cu]:[L] = 500:1:4:8). Dashed line is M_n (theo).

The number average molecular weight (M_n) of the star polymers obtained by SEC is much lower than the theoretical molecular weights as calculated by the initial ratio of MMA to initiating site and monomer conversion. The deviation becomes more significant with increasing reaction time. The differences in the theoretical molecular weights and the actual molecular weights determined by SEC may be due to the differences in hydrodynamic volume of the star polymers when compared to the linear

polymers that were used to calibrate the SEC equipment. Further studies, such as those using light scattering techniques, would determine the actual molecular weight of the star polymers.

In summary, suitable reaction conditions for the copper (I) mediated LRP of MMA initiated by 14-Br-CD have been determined. A low concentration of the multifunctional initiator prevents termination reactions and a low reaction temperature also facilitates the formation of well-defined star polymers.

3.8.2 Formation of block copolymers

Block copolymerisation is one of the most important applications of living radical polymerisation. Block copolymers are usually obtained by the sequential living polymerisation of one monomer followed by another. In metal-catalysed living radical polymerisation, the isolated halogen-capped polymer can be used as a macroinitiator, taking advantage of the stability of the dormant carbon-halogen bond. From the previous section, if well-defined star polymers were formed, it should be expected that each chain-end would have a terminal bromine atom that would be capable of initiating the polymerisation of another monomer. The isolated homopolymer was used as a macroinitiator for the block copolymerisation of *n*-butyl methacrylate (*n*BMA) that belongs to the same family as MMA (Figure 3.8.5).

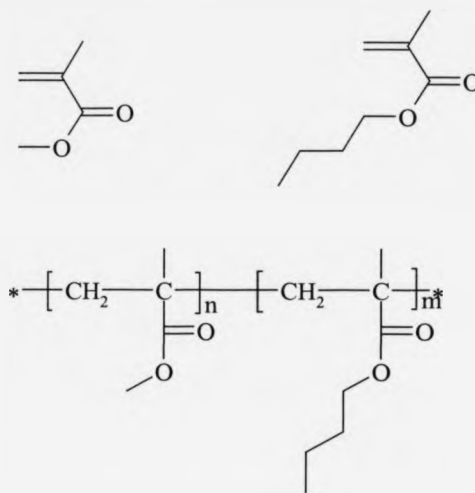


Figure 3.8.5 PMMA-*b*-PnBMA diblock copolymer.

Following the isolation of the 14-armed PMMA macroinitiator, *n*BMA was polymerised in the ratio [*n*BMA]:[Cu]:[L]:[I] = 500:4:8:1 where [I] was the concentration of the PMMA macroinitiator. The polymerisation temperature was maintained at 60 °C and the kinetic data obtained is shown in Table 3.8.3.

Time (mins)	Conversion (%)	M_n (SEC)	M_n (theo)	PDi
60	0.7	44600	36700	1.07
120	2.0	57500	49850	1.07
180	2.6	69000	56180	1.06
240	3.9	79600	68880	1.06
300	5.0	89200	79630	1.05
360	6.0	98200	90270	1.05
420	7.0	107000	99630	1.05

Table 3.8.3 Kinetic data for the synthesis of a diblock copolymer of PMMA-*b*-PnBMA using 14-armed PMMA as a macroinitiator.

Upon formation of the diblock copolymer, the molecular weight increased linearly with conversion (Figure 3.8.6) indicating that good control of the molecular weight could be attained. Very narrow molecular weight distributions ($PDI < 1.07$) were also observed during the polymerisation.

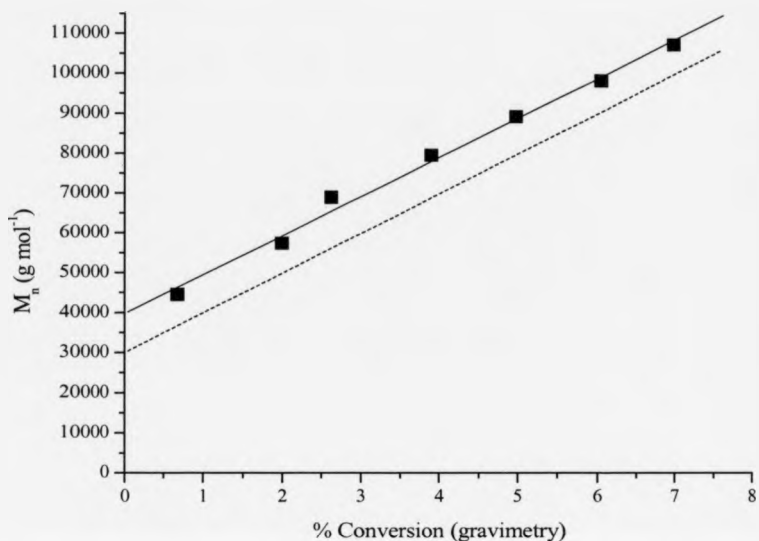


Figure 3.8.6 Evolution of molecular weight M_n with conversion for the LRP of PMMA-*b*-*n*BMA initiated by 14-Br-CD PMMA macroinitiator ($M_n \sim 30000 \text{ g mol}^{-1}$) and mediated by Cu(I)Br / *N*-pentyl-2-pyridylmethanimine ($[M]:[Cu]:[L]:[I] = 500:4:8:1$) in toluene at 60 °C. Dashed line shows M_n (theo).

There is good agreement between the molecular weight obtained by SEC and the theoretical molecular weight calculated from the ratio $[n\text{BMA}]:[\text{macroinitiator}]$ and the monomer conversion. Furthermore, the first order rate plot (Figure 3.8.7) shows that there is a constant concentration of radical species during the polymerisation suggesting that no termination events occur.

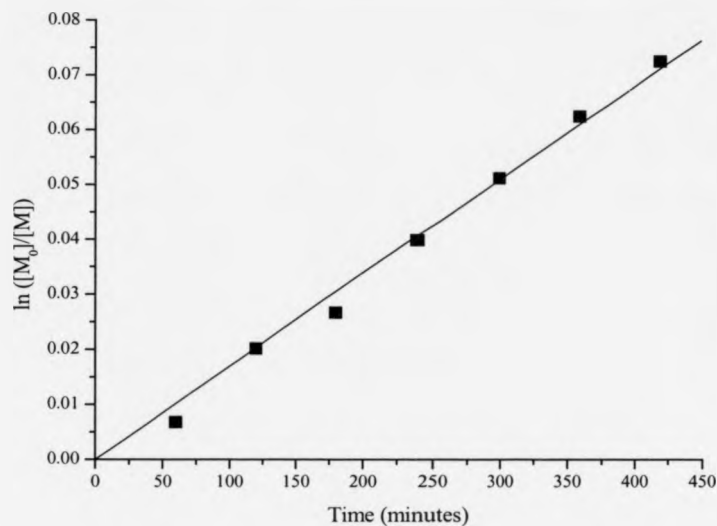


Figure 3.8.7 First order kinetic plot for the LRP of PMMA-*b*-PnBMA initiated by 14-Br-CD PMMA macroinitiator ($M_n \sim 30000 \text{ g mol}^{-1}$) in toluene at 60°C and mediated by Cu(I)Br / *N*-pentyl-2-pyridylmethanimine.

The SEC traces for the formation of the PMMA-*b*-PnBMA diblock copolymer are shown in Figure 3.8.8. The narrow peaks are symmetrical and no shoulder peaks are observed at high molecular weight which is evidence that no termination events such as star-star coupling are occurring.

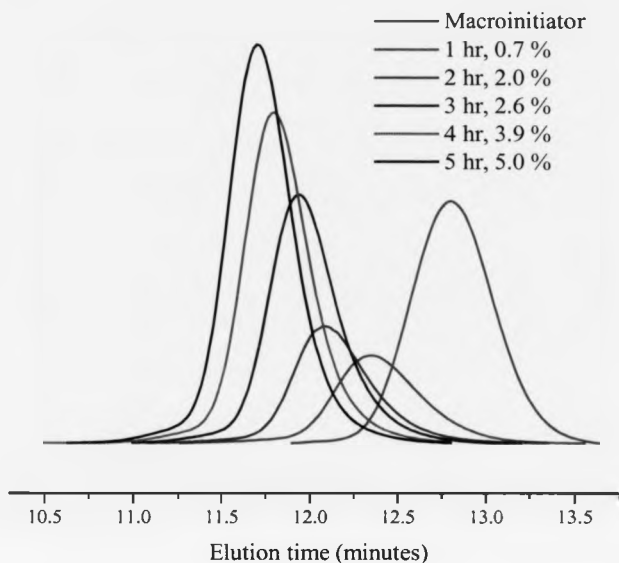


Figure 3.8.8 SEC traces for the formation of PMMA-*b*-PnBMA diblock copolymers formed from a 14-Br-CD PMMA macroinitiator.

In conclusion, it appears that the 14-armed initiator is capable of initiating the polymerisation of MMA and the halogen chain-ends are preserved so that they can participate in a further living radical polymerisation to produce diblock 14-arm star copolymers. The narrow molecular weight distributions that were observed, together with the linear increase in molecular weight with increasing conversion, confirm that well-defined star polymers can be synthesised that incorporate a β CD core. The precise synthesis of the multifunctional initiator is seen as the key step in determining the number of polymeric arms that are attached to the core.

3.8.3 Suitable Reaction Conditions for the LRP of Styrene initiated by 14-Br-CD

Suitable reaction conditions for the living radical polymerisation of styrene initiated by 21-Br-CD have been determined in the previous chapter. It was found that well-defined star polymers with 21 arms could be obtained when the concentration of initiator with respect to monomer was low ($[M]:[I] = 500:1$) and a polymerisation temperature of 100 °C was used. It was thought that similar reaction conditions would be necessary for the polymerisation of styrene using the 14-Br-CD initiator since this initiator also had a large number of initiating sites in close proximity.

Table 3.8.4 shows the kinetic data obtained from the LRP of styrene using the 14-Br-CD multifunctional initiator.

Time (mins)	Conversion (%)	M_n (SEC)	M_n (theo)	PDI
60	0.3	4360	11600	1.07
120	1.2	8710	22000	1.16
180	2.5	14700	32000	1.14
240	4.5	20700	46100	1.14
300	5.5	26200	53000	1.16
360	7.0	30700	64100	1.20
420	8.4	32100	74300	1.53
480	10.0	33900	86000	1.38

Table 3.8.4 Kinetic data for the LRP of styrene initiated by 14-Br-CD in xylene at 100 °C and mediated by Cu(I)Br / *N*-pentyl-2-pyridylmethanimine ($[M]:[I]:[Cu]:[L] = 500:1:4:8$).

The high molecular weight distribution for these reactions indicate poor control over the molecular weight. Although the molecular weight increases with increasing conversion, there is no evidence of a linear relationship (Figure 3.8.9) and the polymerisation appears to slow at about 7 % conversion. Styrene undergoes termination by combination more readily than MMA and this may be a factor that affects the control over these polymerisations. This may also explain the high molecular weight distributions ($PDI > 1.53$) that were observed.

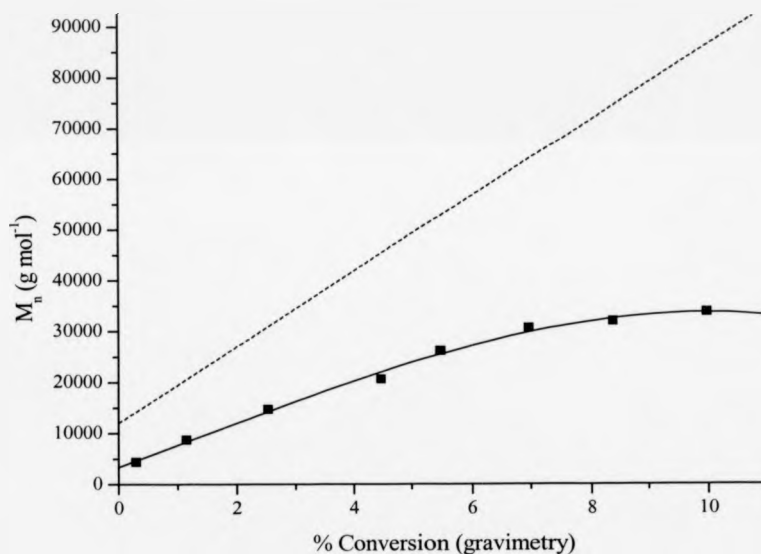


Figure 3.8.9 Evolution of molecular weight with conversion for the LRP of styrene initiated by 14-Br-CD in xylene at 100 °C and mediated by Cu(I)Br / *N*-pentyl-2-pyridylmethanimine ($[M]:[I]:[Cu]:[L] = 500:1:4:8$). Dashed line shows M_n (theo).

Although the first order kinetic plot shows linear kinetics (Figure 3.8.10), the non-linear evolution of the molecular weight with conversion means that poor control is afforded

for the LRP of styrene and this does not lead to as well-defined star polymers as with methacrylates.

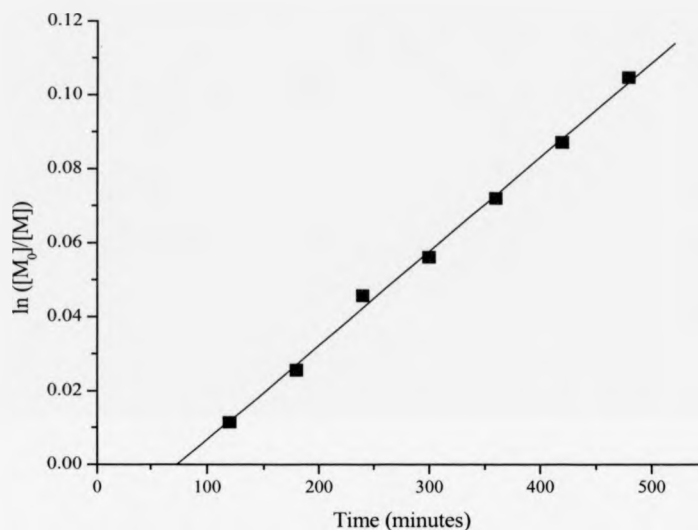


Figure 3.8.10 First order kinetic plot for the LRP of styrene initiated by 14-Br-CD in xylene at 100 °C and mediated by Cu(I)Br / *N*-pentyl-2-pyridylmethanimine.

3.8.4 LRP of *n*BMA initiated by 14-Br-CD

The formation of block copolymers that incorporates *n*-butyl methacrylate (*n*BMA) as the second block has already been demonstrated as described above and so the polymerisation of *n*BMA initiated by 14-Br-CD was considered of interest. The polymerisation rate was expected to be similar to that observed for MMA and well-defined star polymers containing precisely 14 arms should be formed. The ratio of $[n\text{BMA}]:[I]:[\text{Cu}]:[L]$ was kept the same as for the conditions determined for MMA and the kinetic data is shown in Table 3.8.5.

Time (mins)	Conversion (%)	M_n (SEC)	M_n (theo)	PDI
60	0.1	9710	4180	1.09
120	1.1	19400	15180	1.07
180	2.9	28000	32700	1.07
240	4.0	35900	43090	1.07
300	5.0	43600	53060	1.07
355	7.0	49900	72960	1.06

Table 3.8.5 Kinetic data for the LRP of *n*BMA initiated by 14-Br-CD in toluene at 60 °C and mediated by Cu(I)Br / *N*-pyridyl-2-methanimine ([M]:[I]:[Cu]:[L] = 500:1:4:8).

The molecular weight distribution remains remarkably low ($PDI < 1.07$) throughout the polymerisation which is also observed in the LRP of MMA. Analysis of the evolution of molecular weight with conversion (Figure 3.8.11) shows that the molecular weight increases linearly with increasing conversion and so it appears that good control over the molecular weight can be afforded in the LRP of *n*BMA. The theoretical values were slightly higher than the experimental values at higher conversions and this was again attributed to the differences in hydrodynamic volume of the star polymers when compared to their linear counterparts that were used to calibrate the SEC equipment.

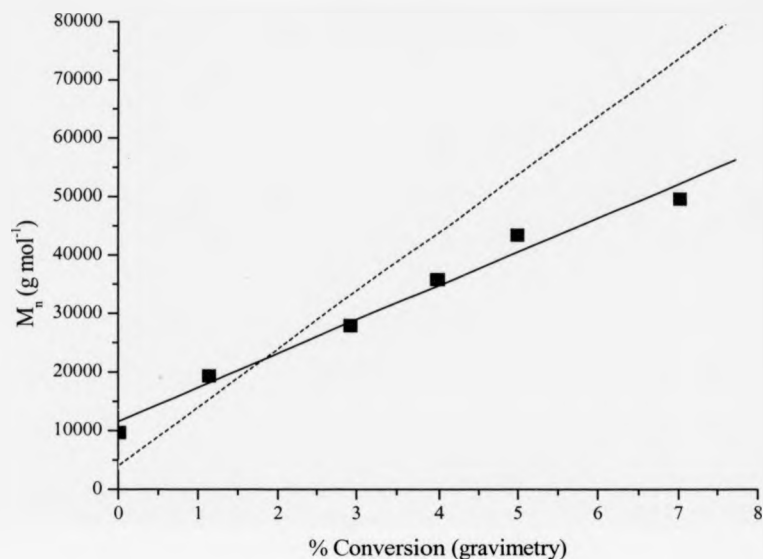


Figure 3.8.11 Evolution of molecular weight with conversion for the LRP of *n*BMA initiated by 14-Br-CD in toluene at 60 °C and mediated by Cu(I)Br / *N*-pentyl-2-pyridylmethanimine ([M]:[I]:[Cu]:[L] = 500:1:4:8). Dashed line represents M_n (theo).

There was no evidence of loss of reactive species during the polymerisation as shown in the first order rate plot (Figure 3.8.12). When compared with the similar polymerisation using MMA, the reaction rates were lower with only 7 % conversion being observed after a reaction time of six hours for *n*BMA compared to 14 % conversion after the same time for MMA. It is possible that the longer alkyl chain of *n*BMA hinders the efficiency of the polymerisation leading to lower conversions.

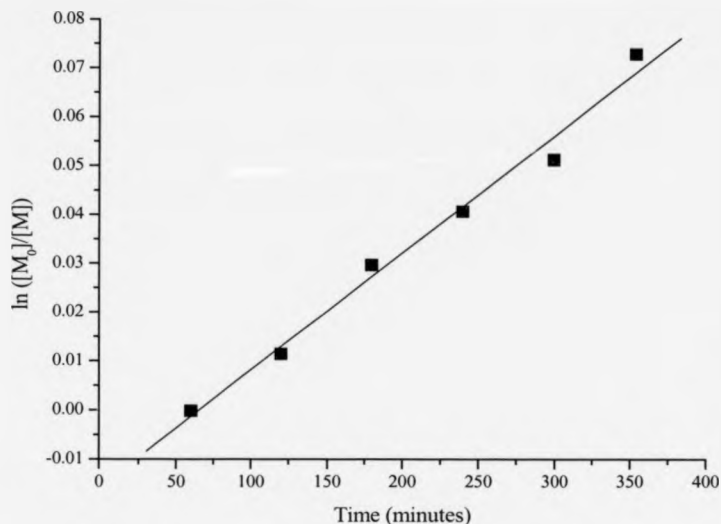


Figure 3.8.12 First order kinetic plot for the LRP of *n*BMA in toluene at 60 °C initiated by 14-Br-CD and mediated by Cu(I)Br / *N*-pentyl-2-pyridylmethanimine ([M]:[I]:[Cu]:[L] = 500:1:4:8).

3.9 Copper (I) Mediated LRP initiated by 7-Br-CD

The four-step synthesis of the multifunctional initiator incorporating seven discrete initiating sites with a β CD core allows for the investigation of its suitability in copper (I) mediated LRP. The previous section has demonstrated that well-defined star-shaped polymers with 14 arms can be synthesised in a controlled fashion using a copper catalyst and optimised polymerisation conditions. It was anticipated that star-shaped polymers with seven polymeric arms could be synthesised in a similar fashion.

3.9.1 LRP of MMA initiated by 7-Br-CD

To suppress the effects of star-star coupling and irreversible termination reactions, a low concentration of the multifunctional initiator was used. This was found to be necessary in the polymerisations involving the 21- and 14-armed multifunctional initiators to avoid the appearance of shoulder peaks at high molecular weight in the SEC spectra. The concentration ratio [M]:[I] was investigated at 500:1 and Table 3.9.1 summarises the results.

Time (mins)	Conversion* (%)	M _n (SEC)	M _n (theo)	PDI
60	1.2	8150	6820	1.12
120	4.4	11100	18120	1.31
180	8.8	17000	33540	1.08
240	14.1	49100	52150	1.07
300	16.3	60400	59840	1.07
360	20.6	70100	74950	1.08
420	23.7	75100	85880	1.08

Table 3.9.1 Evolution of molecular weight for the LRP of MMA initiated by 7-Br-CD and mediated by copper (I) / *N*-pentyl-2-pyridylmethanimine in toluene at 60 °C ([M]:[I]:[Cu]:[L] = 500:1:4:8). *Conversion determined by gravimetry.

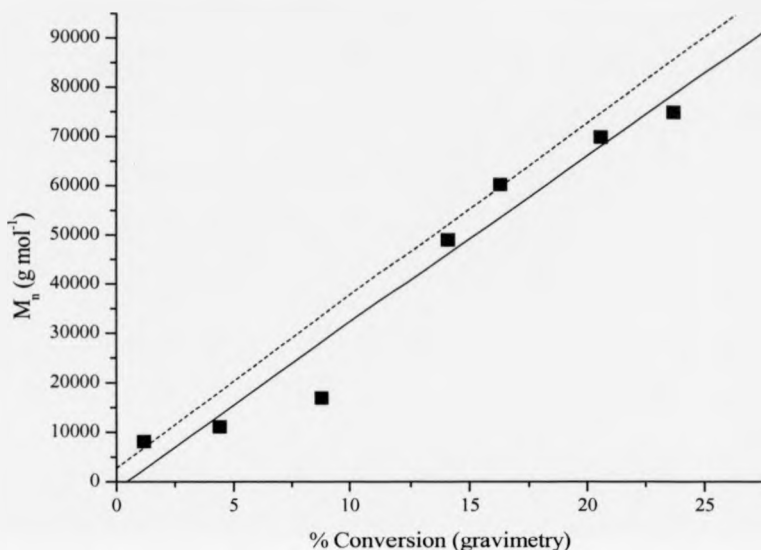


Figure 3.9.1 Evolution of molecular weight with conversion for the LRP of MMA initiated by 7-Br-CD in toluene at 60 °C and mediated by Cu(I)Br / *N*-pentyl-2-pyridylmethanimine ($[M]:[I]:[Cu]:[L] = 500:1:4:8$). Dashed line represents M_n (theo).

Figure 3.9.1 shows that there is an increase in molecular weight with increasing conversion that indicates that initiation has occurred and star polymers are being formed. The theoretical molecular weight values are generally higher than those observed by SEC and the distribution of molecular weights remained low ($PDI < 1.31$) at all stages of the polymerisation. The low molecular weight distributions over the observed conversion range provide strong evidence for the absence of significant termination events. There is some deviation from linearity but analysis of the first order rate plot for this reaction (Figure 3.9.2) does show a linear relationship indicating that the concentration of reactive species in the system remains constant.

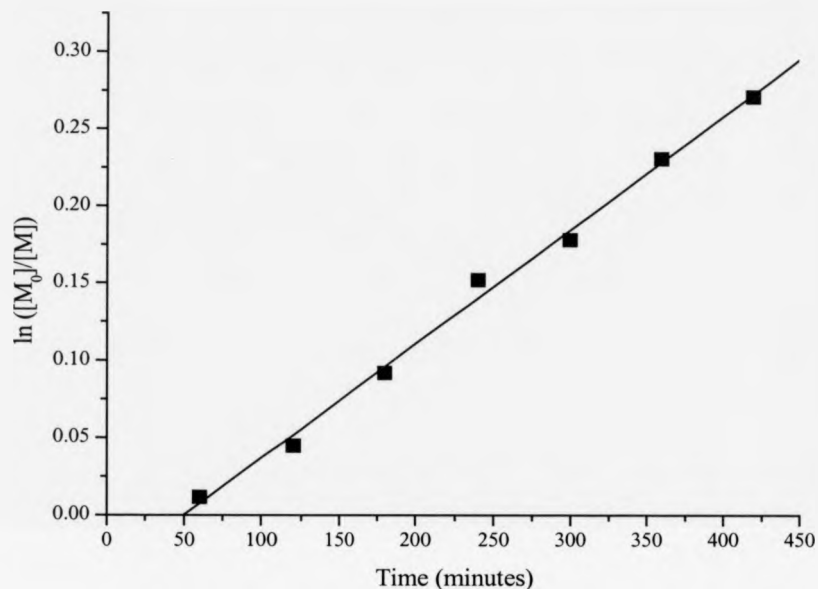


Figure 3.9.2 First order kinetic plot for the LRP of MMA in toluene at 60 °C initiated by 7-Br-CD and mediated by Cu(I)Br / *N*-pentyl-2-pyridylmethanimine ($[M]:[I]:[Cu]:[L] = 500:1:4:8$).

It is clear from Figure 3.9.1 that in the early stages of the polymerisation slower rates were observed. The reason for this is unknown and it may be a genuine feature of the reaction or caused by some impurity in the system. This effect was not observed in the polymerisations of star polymers with 21- or 14-arms. At higher conversions however, more acceptable rates of polymerisation were observed.

3.9.2 LRP of PEGMA initiated by 7-Br-CD

The living radical polymerisation of the hydrophilic monomer poly(ethylene glycol) methacrylate (PEGMA, $M_w \sim 475 \text{ g mol}^{-1}$) initiated by 7-Br-CD was investigated. Due to the low volatility and high viscosity of PEGMA, kinetic samples obtained during the polymerisation were analysed by ^1H NMR to determine the polymer conversion. This was achieved by comparing the vinylic protons of PEGMA at 6.2 ppm with the protons arising from the methoxy protons of the polymer at 3.4 ppm. Table 3.9.2 summarises the kinetic data obtained for the polymerisation.

Time(mins)	Conversion* (%)	M_n (SEC)	M_n (theo)	PDi
60	12.5	18400	23550	1.07
120	23.1	19500	41170	1.06
180	30.9	24000	54140	1.06
240	45.3	27500	78080	1.07
300	51.6	30000	88550	1.06
360	59.9	34900	102350	1.06
420	67.3	36500	114650	1.07

Table 3.9.2 Kinetic data for the LRP of PEGMA initiated by 7-Br-CD in toluene at 60 °C and mediated by copper (I) / *N*-pentyl-2-pyridylmethanimine ($[\text{M}]:[\text{I}]:[\text{Cu}]:[\text{L}] = 50:1:4:8$). *Conversion determined by ^1H NMR.

It can be seen that the molecular weight distributions remained low throughout the polymerisation and this indicated that no termination events were occurring by star-star coupling. The absence of any shoulder peaks at high molecular weight also indicated the absence of termination events by star-star coupling. The polymerisation of PEGMA

initiated by 7-Br-CD was encouraging since an increase in molecular weight with increasing conversion was observed despite the lengthy synthetic procedure required to form the multifunctional initiator. Furthermore, a linear relationship between conversion and molecular weight was observed (Figure 3.9.3) that indicated good control over molecular weight was possible.

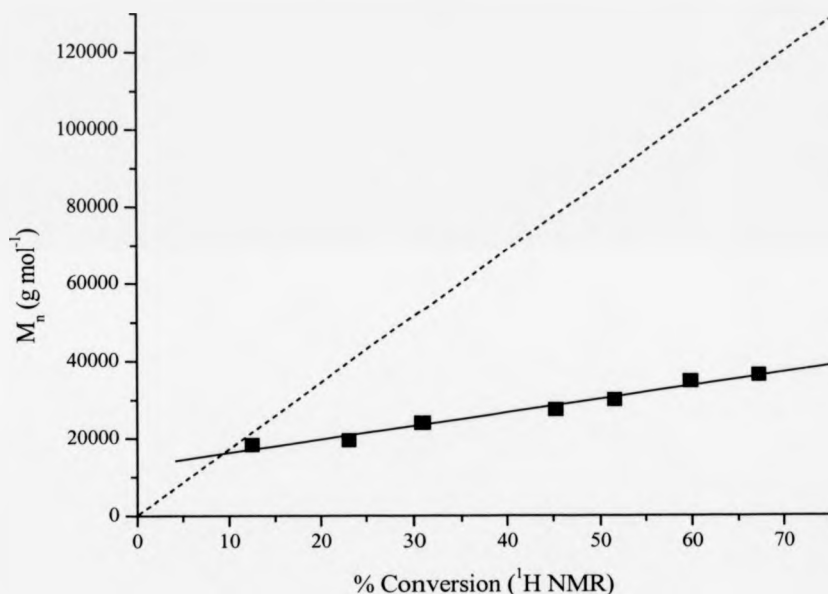


Figure 3.9.3 Evolution of molecular weight with conversion for the LRP of PEGMA initiated by 7-Br-CD in toluene at 60 °C and mediated by $\text{Cu(I)Br} / N$ -pentyl-2-pyridylmethanimine ($[\text{M}]:[\text{I}]:[\text{Cu}]:[\text{L}] = 50:1:4:8$). Dashed line represents $M_n(\text{theo})$.

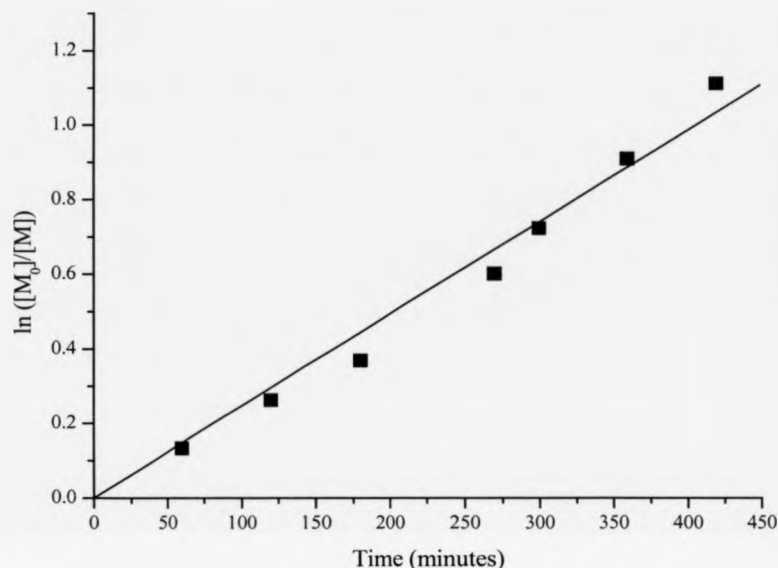


Figure 3.9.4 First order kinetic plot for the LRP of PEGMA in toluene at 60 °C initiated by 7-Br-CD and mediated by Cu(I)Br / *N*-pentyl-2-pyridylmethanimine ([M]:[I]:[Cu]:[L] = 50:1:4:8).

The first order kinetic plot (Figure 3.9.4) showed a linear relationship that again indicated that the concentration of radical species in the polymerisation remained constant. There was a large deviation of the molecular weights observed by SEC compared with the theoretical weight as calculated by the ratio [M]:[I] and monomer conversion. This deviation became more marked at higher conversions. Whilst the differences in hydrodynamic volume between the star polymers and linear polymers (used to calibrate the SEC equipment) could partly account for the observed differences, other factors may be involved. One factor could be the flexibility of the poly(ethylene

glycol) chains that are more flexible than the PMMA homopolymer chains. This would also affect the differences observed between experimental and theoretical molecular weights.

The conversions for the living radical polymerisation of PEGMA were much higher than other monomers investigated. It was thought that the determination of PEGMA conversion by ^1H NMR may have incurred a large error due to the low concentration of initiating species with respect to monomer species. This may have caused an inherent inaccuracy in calculating the conversions. Gravimetry was deemed inappropriate to determine monomer conversion since PEGMA has a low volatility and incomplete evaporation of the monomer after drying will have affected any subsequent conversion calculations.

3.10 Analysis of Polymeric Arms by Hydrolysis of Star Polymers

Although the multifunctional initiators used above have been shown to initiate polymerisations mediated by a copper (I) catalyst, it has so far been unclear as to whether all the initiating sites on the modified β CD have participated in the polymerisation. There have been indications of high initiator efficiency such as the narrow molecular weight distributions that have been observed in every polymerisation. This would indicate that the molecular weight of each arm on each β CD initiator is similar but does not confer initiation at each initiation site. The absence in the SEC spectra of the peak at low molecular weight corresponding to the initiator during the polymerisations would also indicate good initiator efficiency. The close proximity of initiating sites on each β CD molecule could hinder the ability of each initiation site to cause an initiation event. Consequently, it was necessary to further investigate the structure of the star polymers by examining the polymeric arms that were attached to the

β CD core. This would enable the precise number of arms attached to the core to be determined. In order to characterise the individual arms of the star polymers, the arms would have to be disconnected from the β CD core so that they could be investigated independently of the core. Since the polymeric arms are connected to the core via ester linkages, they can be cleaved by hydrolysis under basic conditions (Figure 3.10.1). SEC analysis of the recovered linear arms would provide a more accurate determination of molecular weight since they can be compared against the linear calibration standards. The molecular weights of the linear arms would therefore be expected to be the absolute molecular weight of the star polymer divided by its functionality.

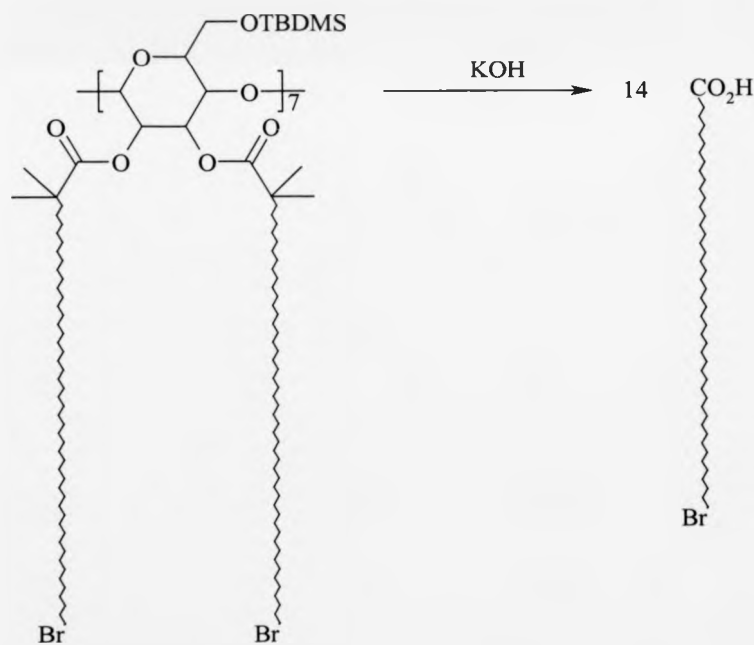


Figure 3.10.1 Disconnection of polymeric arms from β CD core by hydrolysis of ester linkages in basic conditions.

A star-shaped PMMA polymer was prepared using the 14-armed multifunctional initiator. The polymerisation was stopped at 18 % conversion and the resulting polymer was purified by passing it through a column of basic alumina to remove the copper complexes. Precipitation of the PMMA star polymer in petroleum ether and subsequent molecular weight analysis using light scattering techniques showed the absolute molecular weight M_w of the star to be $129000 \text{ g mol}^{-1}$ which was in close agreement with the theoretical molecular weight of $130000 \text{ g mol}^{-1}$. The molecular weight distribution of this star polymer was low ($\text{PDI} = 1.11$). If initiation at all 14 initiating sites had occurred, and all 14 arms propagated at the same rate, then it was anticipated that hydrolysis of the arms would yield linear PMMA polymers with a molecular weight M_n of one-fourteenth the absolute molecular weight of the star i.e. $M_n = 9210 \text{ g mol}^{-1}$. The star polymer was refluxed with potassium hydroxide in methanol and tetrahydrofuran and the resulting linear polymer arms were precipitated in petroleum ether and analysed by SEC. The SEC traces of the star polymer and the product obtained after hydrolysis are shown in Figure 3.10.2. It can be seen that there is a shift in the SEC traces to lower molecular weight following the hydrolysis which indicates that the polymeric arms have been cleaved from the β CD core and hydrolysis has occurred. Furthermore, the molecular weight M_n of the cleaved arms was found to be 10800 g mol^{-1} and a low molecular weight distribution was observed ($\text{PDI} = 1.16$). The observed molecular weight of the linear PMMA was in good agreement with the theoretical molecular weight of 9210 g mol^{-1} based on the ratio of the absolute molecular weight of the star divided by its functionality. This result was encouraging as it confirmed that all 14 of the initiating sites on 14-Br-CD were causing initiation and the linear PMMA arms were of similar molecular weight as observed by the narrow molecular weight distributions of the cleaved arms.

—

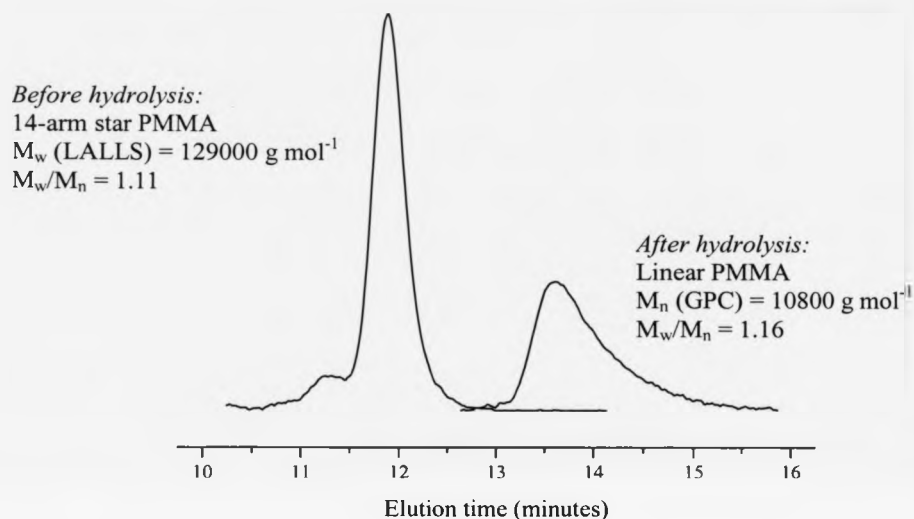


Figure 3.10.2 SEC traces of star-shaped PMMA (M_w 129000 g mol⁻¹) before hydrolysis (left trace) and linear PMMA (M_n 10800 g mol⁻¹) after hydrolysis (right trace)

The cleavage of the polymeric arms from the β CD core has enabled their independent analysis and confirms that well-defined star polymers with a discrete number of arms can be synthesised by copper (I) mediated LRP.

3.11 Conclusions

By careful modification of the primary and secondary faces of cyclodextrin, it is possible to synthesise suitable derivatives that can be employed as multifunctional initiators for the LRP of various methacrylate and styrene monomers. The β CD derived initiators with 14 and seven discrete initiating sites represent novel compounds. The precise synthesis of the initiator is the key step in predetermining the functionality of the star polymers and this was achieved using multiple protection and deprotection steps as well as extensive chromatography procedures. The reaction conditions for the formation of well-defined star polymers were determined and it was found necessary to use a low concentration of initiator to suppress any termination reactions caused by star-star coupling. This is the first time that well defined star polymers with 14 and seven arms have been prepared by copper mediated LRP. Reaction temperatures lower than that normally used for the living radical polymerisation of linear MMA and styrene were also found necessary to control the polymerisations of the star polymers. The molecular weights of the star-shaped polymers as determined by SEC were generally lower than the theoretical molecular weights and this was attributed to the differences in hydrodynamic volumes between star and linear polymers.

3.12 Chapter 3 References

- 1 L. Jicsinszky and E. Fenyvesi, in 'Comprehensive Supramolecular Chemistry', ed. J. L. Atwood and J. M. Lehn, Oxford, 1996.
- 2 W. Saenger, M. Noltemeyer, P. C. Manor, B. Hingerty, and B. Klar, *Bioorg. Chem.*, 1976, **5**, 187.
- 3 A. Hybl, R. E. Rundle, and D. E. William, *J. Am. Chem. Soc.*, 1965, **87**, 2779.
- 4 K. Takeo, K. Uemura, and H. Mitoh, *J. Carbohydr. Chem.*, 1988, **7**, 293.
- 5 K. Takeo, H. Mitoh, and K. Uemura, *Carbohydr. Res.*, 1989, **187**, 203.
- 6 M. J. Pregel and E. Bunzel, *Can. J. Chem.-Rev. Can. Chim.*, 1991, **69**, 130.
- 7 P. Fugedi, *Carbohydr. Res.*, 1989, **192**, 366.
- 8 A. W. Coleman, P. Zhang, C. C. Ling, J. Mahuteau, H. Parrot-Lopez, and M. Miocque, *Supramol. Chem*, 1992, **1**.
- 9 A. W. Coleman, P. Zhang, H. Parrot-Lopez, C. C. Ling, M. Miocque, and L. Mascrier, *Tetrahedron Lett.*, 1991, **32**, 3997.
- 10 A. R. Khan, L. Barton, and V. T. D'Souza, *J. Org. Chem.*, 1996, **61**, 8301.
- 11 W. A. Konig, D. Icheln, T. Runge, B. Pfaffenberger, P. Ludwig, and H. Huhnerfuss, *J. High Res. Chromatogr.*, 1991, **14**, 530.
- 12 T. Moriya, K. Saiko, H. Kurita, K. Matsumoto, T. Otake, H. Mori, M. Mori, N. Ueba, and N. Kunita, *J. Med. Chem.*, 1993, **36**, 164.
- 13 E. J. Corey and A. Venkateswarlu, *J. Am. Chem. Soc.*, 1972, **94**, 6190.
- 14 K. Karl, C. K. Lee, and L. Khan, *Carbohydr. Res.*, 1982, **101**, 31.
- 15 J. Farras, C. Serra, and J. Vilarrasa, *Tetrahedron Lett.*, 1998, **39**, 327.
- 16 A. S. Y. Lee, H. C. Yeh, and M. H. Tsei, *Tetrahedron Lett.*, 1995, **36**, 6891.

- 17 D. R. Kelly, S. M. Roberts, and R. F. Newton, *Synth. Commun.*, 1979, **9**, 295.
- 18 T. Ando, M. Kamigaito, and M. Sawamoto, *Kobunshi Ronbunshu*, 2002, **59**, 199.
- 19 V. Coessens, T. Pintauer, and K. Matyjaszewski, *Prog. Polym. Sci.*, 2001, **26**, 337.
- 20 V. Darcos, P. Fairclough, and D. M. Haddleton, *Abstr. Pap. Am. Chem. Soc.*, 2002, **224**, 282.
- 21 D. M. Haddleton, A. M. Heming, and A. P. Jarvis, *Abstr. Pap. Am. Chem. Soc.*, 1999, **218**, 281.
- 22 M. Kamigaito, T. Ando, and M. Sawamoto, *Chem. Rev.*, 2001, **101**, 3689.
- 23 M. Kamigaito, T. Ando, and M. Sawamoto, *Abstr. Pap. Am. Chem. Soc.*, 2002, **224**, 034.
- 24 K. Matyjaszewski, S. Gaynor, D. Greszta, D. Mardare, and T. Shigemoto, *Macromol. Symp.*, 1995, **98**, 73.
- 25 K. Matyjaszewski, *Abstr. Pap. Am. Chem. Soc.*, 2000, **219**, 263.
- 26 K. Matyjaszewski and J. H. Xia, *Chem. Rev.*, 2001, **101**, 2921.
- 27 K. Matyjaszewski, *Abstr. Pap. Am. Chem. Soc.*, 2001, **221**, 212.
- 28 K. Matyjaszewski, *Abstr. Pap. Am. Chem. Soc.*, 2002, **224**, 001.
- 29 K. Ohno, B. Wong, and D. M. Haddleton, *J. Polym. Sci. Pol. Chem.*, 2001, **39**, 2206.
- 30 M. Sawamoto and M. Kamigaito, *Abstr. Pap. Am. Chem. Soc.*, 2001, **221**, 204.
- 31 M. Sawamoto, M. Kamigaito, and T. Ando, *Abstr. Pap. Am. Chem. Soc.*, 2002, **223**, 001.

-
- 32 J. S. Wang and K. Matyjaszewski, *Macromolecules*, 1995, **28**, 7572.
- 33 J. F. Quinn, R. P. Chaplin, and T. P. Davis, *J. Polym. Sci. Pol. Chem.*, 2002, **40**, 2956.
- 34 M. H. Stenzel and T. P. Davis, *J. Polym. Sci. Pol. Chem.*, 2002, **40**, 4498.
- 35 M. H. Stenzel-Rosenbaum, T. P. Davis, V. K. Chen, and A. G. Fane, *Macromolecules*, 2001, **34**, 5433.
- 36 M. Stenzel-Rosenbaum, T. P. Davis, V. Chen, and A. G. Fane, *J. Polym. Sci. Pol. Chem.*, 2001, **39**, 2777.

Chapter 4**Preparation of Porous Membranes by Self Organisation
Of Star Shaped Polymers formed by LRP****4.0 Introduction**

The preparation of microporous architectures by the self-assembly and self-organisation of polymeric materials has been reported by several groups¹⁻⁷. The microporous architectures are typically formed from block copolymers and star polymers and consist of layers of spherical micron-sized pores that self organise as a honeycomb pattern. Such structures may have important technological applications in photonic⁸⁻¹⁰ and opto-electronic devices¹¹, catalysis, thermal insulation materials¹², biointerfaces^{13, 14} and membranes¹⁵.

Various polymers have been applied for the fabrication of these microporous polymeric membranes. Francois et al.² used a block copolymer of polystyrene-polyparaphenylene (Figure 4.0.1) and star-shaped polystyrene to prepare films with monodisperse pore size that self-organised into a hexagonal array. The thin film was fabricated by casting a dilute solution of the polymer in carbon disulfide onto a solid substrate under humid conditions and a humid airflow.

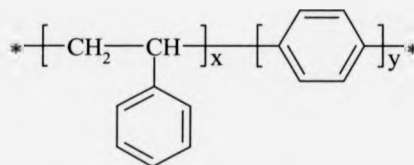


Figure 4.0.1 Polystyrene-polyparaphenylene block copolymer for the preparation of microporous polymer membranes.

The authors noted that linear polystyrene homopolymers did not lead to the formation of membranes with a regular hexagonal array of pores. Furthermore, the regular morphology of the pores was only observed when carbon disulfide was used to dissolve the polymer and not when other organic solvents were used. Honeycomb structures were observed when the length of the polystyrene block of the polystyrene-polyparaphenylene block copolymer was varied between 1500 and 50000 g mol⁻¹ with the size of the pores increasing with an increase in the molecular mass. When star-shaped polystyrene was used to form the structures, increasing the number of arms on the core was found to increase the regularity of the pores.

Patel et al.¹⁶ have also demonstrated the formation of a regular array of pores in a similar way using monochelic polystyrene (weight average molecular weight 50 000 g mol⁻¹) terminated with a carboxylic acid group. The regular morphology of the pores was not disrupted when the concentration of the polystyrene in carbon disulfide was varied between 0.1 and 5 %. Among other polymeric materials that have been used to generate honeycomb patterns are polystyrene-polyisoprene block copolymers, amphiphilic polyion complexes derivatised from polystyrene sulfonate¹⁷, amphiphilic copolymers incorporating lactose units or carboxyl groups in the side-chains, and polyion complexes composed of anionic polysaccharides¹⁴.

The presence of moisture in the surrounding atmosphere for membrane formation to occur appears to be essential. Carbon disulfide also appears to be the only solvent that is capable of promoting the regular hexagonal arrays. During the casting of the film, a humid airflow is directed over the dissolved polymer. This causes rapid evaporation of the carbon disulfide and so the solution is cooled. Due to the humid atmosphere, water droplets will condense at the air-polymer interface. Light scattering experiments have

demonstrated that water vapour condenses at the air-polymer interface in the shape of micron-sized droplets. These monodisperse spherical water droplets arrange in a hexagonal arrangement and act as a template around which the polymer can assemble. The hexagonal arrangement of the water droplets may be caused by convection. Precipitation of the polymer at the solution-water interface prevents any coagulation of the water droplets and this precipitation is essential for the hexagonal array to be maintained. The polymer layer is thought to encapsulate each water droplet and surface currents induced by the rapid evaporation of the carbon disulfide are also thought to be involved in the mechanism of pore formation. Prevention of coalescence of water droplets is essential if hexagonal structures are to be formed and this can be achieved by either thermodynamic control or by kinetic control. The thermodynamic control involves the stabilisation of the water droplets by surface-active compounds. Dynamic control is achieved by using a highly volatile solvent such as carbon disulfide so that evaporation is so rapid that water droplets have no time to coalesce before complete evaporation of the water and solvent. Once all the solvent and water has evaporated, a regular hexagonal array of pores remains.

Patel et al.¹⁶ have proposed two different hypotheses for the formation of a regular array of pores. In the first, thermocapillary convection^{18, 19} is thought to be responsible for the formation of the hexagonal packing. Convective motion coupled with the presence of a lubricating film of air between the drops will suppress the coalescence of two water droplets as long as there is a finite temperature gradient. The surface of the solution is colder due to evaporative cooling whereas the water droplets are hotter due to the latent heat of combustion. This temperature difference will lead to a thermocapillary convection and stabilise the condensing water droplets at the polymer

solution surface. In the second hypothesis, the condensing water droplets are kept apart and made to interact elastically by the vapour of the evaporating solvent as it escapes from the surface. This provides a separating layer between the two droplets and so coalescence is prevented.

The exploitation of the phenomena that creates these interesting hexagonal membranes has been severely restricted due to the synthetic routes that have been used to prepare the polymers which has generally been by anionic polymerisation. We have seen in Chapter 1 that anionic polymerisation is relatively difficult and is limited to a small number of monomers under commercially exploitable reaction conditions.

The advent of LRP techniques provides an opportunity to study the formation of these hexagonally shaped membranes with a broader variety of well-defined polymeric architectures and functionalities. This chapter will examine the formation of honeycomb structures using star-shaped β CD polymers and determine how the structure of the polymer influences the appearance and regularity of the pores. The influence of the film preparation conditions including airflow, humidity, temperature, polymer concentration, solvent and molecular weight will also be investigated.

4.1 Experimental set-up

The casting process for film formation was carried out in an incubator (Figure 4.1.1) where the temperature and humidity could be controlled and monitored. The box was equipped with a nozzle through which humid air could flow and the airflow was controlled by a flow meter. Saturation of the airflow was achieved by bubbling the air through a water reservoir before it reached the box. An additional water reservoir was placed inside the box to maintain the saturation of the atmosphere.

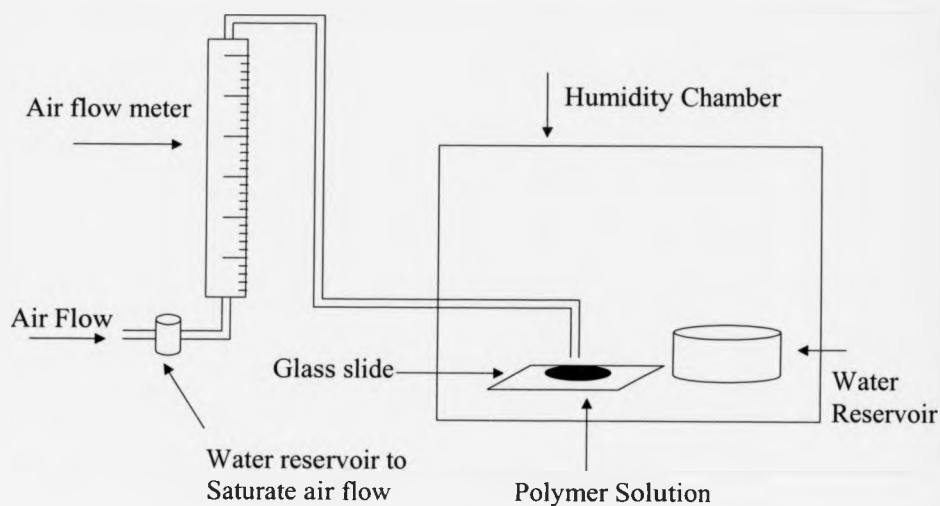


Figure 4.1.1 Schematic set-up used in the preparation of microporous membranes.

A solution of a star-shaped polymer in a volatile solvent was cast onto the glass slide and a controlled airflow was allowed to flow over the solution for a predetermined time. Once the film had been cast, the surface of the slide was analysed by scanning electron microscopy to investigate the surface morphology and, in particular, the appearance of any honeycomb-like structures.

4.2 Star-shaped polymers used in the preparation of porous membranes

The self-organisation of various star-shaped polymers with varying molecular weight and a varying number of polymeric arms was investigated for their ability to form porous membranes. The star-shaped polymers formed by LRP with a β CD core, as detailed in chapters 2 and 3, were investigated. In addition, star-shaped polymers with a D-glucose and a D-galactose core, each possessing 5 arms, were also investigated. The star-shaped polymers based on D-glucose and D-galactose were formed by copper (I)

mediated LRP and supplied with thanks by Ryan Edmonds²⁰. Both D-glucose (Figure 4.2.1) and D-galactose were derivatised to form pentafunctional initiators that could be used to initiate LRP in the formation of 5-armed star polymers.

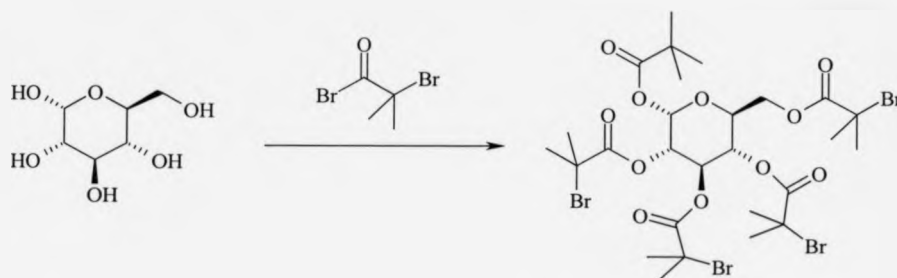


Figure 4.2.1 Synthesis of 1,2,3,4,6-penta-*O*-(2-bromo-2-methylpropionyl)-D-glucose for the formation of 5-armed star polymers by LRP.

Amphiphilic block copolymers that incorporated poly(ethylene glycol) methyl ether (MeOPEG) and polystyrene were also prepared. These linear block copolymers were blended with some of the star polymers to investigate the effect of star and linear polymer blends. This amphiphilic block copolymer was prepared by a two-step reaction. In the first step, MeOPEG was esterified with 2-bromoisobutyryl bromide in THF to form a macroinitiator (Figure 4.2.2). Due to the hydrophilic nature of MeOPEG it was necessary to dry the starting materials prior to the esterification to eliminate any side reactions between the acid bromide and water. The flexibility of the long poly(ethylene glycol) chains means that the chains are intertwined in solution at high concentration. Intermolecular hydrogen bonding therefore hinders the reaction of the terminal hydroxyl groups with the acid bromide. Consequently, it was necessary to work at high dilution to separate these polymer chains.

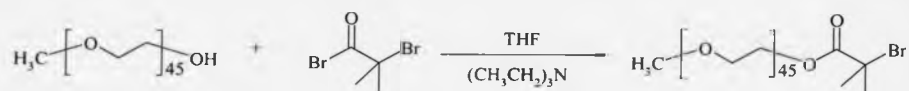


Figure 4.2.2 Esterification of MeOPEG with 2-bromoisobutyryl bromide in THF.

In the second step, the esterified MeOPEG was used as a macroinitiator for the copper (I) mediated LRP of styrene to form an amphiphilic block copolymer (Figure 4.2.3).

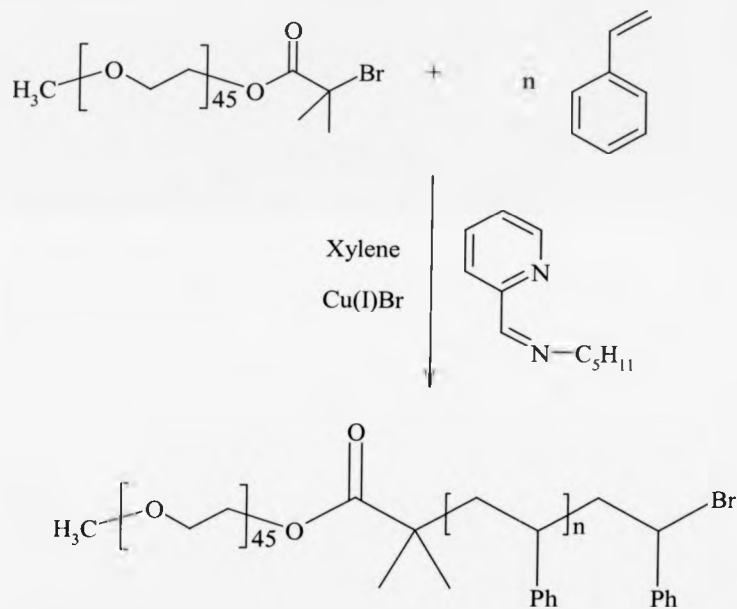


Figure 4.2.3 Copper (I) mediated LRP of styrene using MeOPEG macroinitiator in xylene.

The incorporation of linear amphiphilic block copolymers with the star-shaped polymers was thought to achieve functionality at the membrane pores. The hydrophilic portion i.e. the MeOPEG block, should preferentially migrate to the water phase and remain at the interface whilst the hydrophobic portion i.e. the polystyrene block, should remain in the bulk of the membrane. The blending process can be extended to mixtures of different polymers as a method of introducing further functionality to the membranes.

4.3 Porous membrane formation with β CD star-shaped polymers

The ability of star-shaped polystyrene with 21-arms to form honeycomb structures was investigated using star polymers with varying molecular weights. The optimum conditions required to form a regular hexagonal array of pores was determined and the factors that were considered included the airflow, humidity, temperature, solvent and evaporation time.

4.3.1 Effect of solvent on membrane formation

The effect of the solvent on the ability to generate honeycomb structures was investigated using three organic solvents; dichloromethane, toluene and carbon disulfide. A 21-armed star-shaped polystyrene with molecular weight 43000 g mol^{-1} and narrow molecular weight distribution ($\text{PDI} = 1.08$) was prepared by LRP and dissolved in the three organic solvents at a concentration of 10 g L^{-1} . The relative humidity, temperature, airflow rate and evaporation time was kept constant and films were cast on a glass slide using the three polymer solutions. Table 4.3.1 summarises the reaction conditions for these experiments.

Solvent	Relative humidity (%)	Temperature (°C)	Airflow rate (mL min ⁻¹)	Evaporation time (mins)
Toluene	71	19	1000	3
DCM	70	20	1000	3
CS ₂	72	19	1000	3

Table 4.3.1 Reaction conditions used to investigate solvent effects in the formation of membranes using a 21-armed star polystyrene ($M_w = 43000 \text{ g mol}^{-1}$, $PDI = 1.08$).

The resulting films that were cast from these three solvents were analysed by SEM to assess the surface morphology and the appearance of any porous structures. The SEM image obtained from the film cast in toluene (Figure 4.3.1) shows the appearance of a non-uniform porous structure.

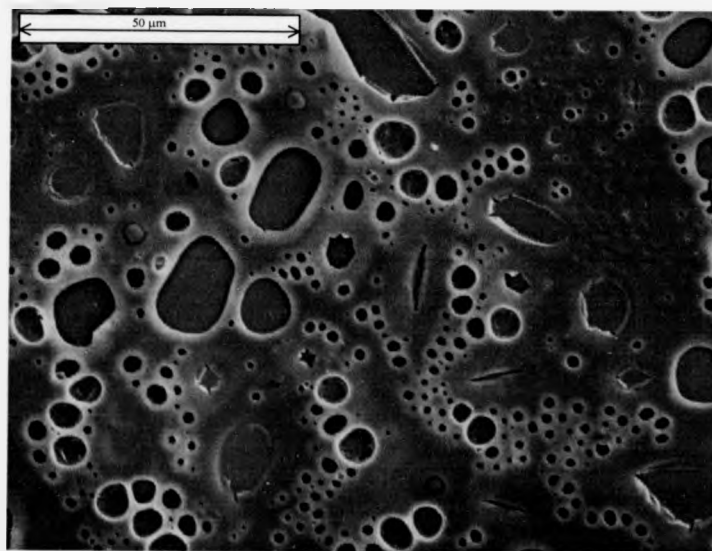


Figure 4.3.1 Surface morphology of a film of star-shaped polystyrene with 21 arms cast from a 10 g L^{-1} toluene solution.

Although pore formation is said to have occurred, the heterogeneous pore sizes and the non-hexagonal distribution of the pores means that toluene is not a good promoter of a regular honeycomb membrane. The coalescence of water droplets on the glass slide may cause the disruption of the hexagonal array. The volatility of the toluene solvent may also be a factor that affects any regular pore formation. If the toluene is slow to evaporate, then the water droplets will have more time to coalesce before all of the water and toluene are evaporated. This results in a disruption of pore formation as shown in Figure 4.3.1.

The polymer film that was cast using dichloromethane as the solvent to dissolve the 21-armed star-shaped polystyrene was analysed for pore formation by SEM and the SEM image is shown in Figure 4.3.2.

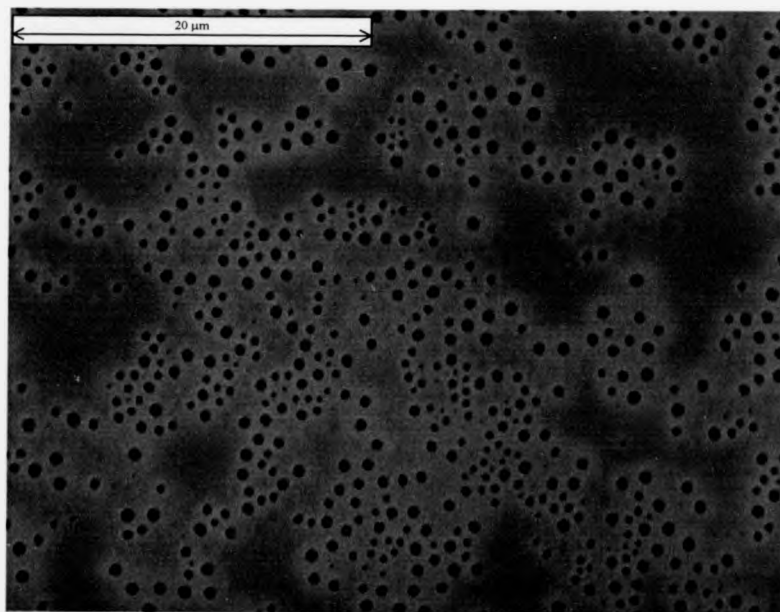


Figure 4.3.2 Surface morphology of a film of star-shaped polystyrene with 21 arms cast from a 10 g L^{-1} dichloromethane solution.

The SEM image of the surface morphology of the film cast in dichloromethane shows that pore formation occurs. The pores are generally spherically shaped and the size distribution of the pores is heterogeneous. A non-hexagonal array of the pores is also observed. When compared to the films cast in toluene, a more regular array of pores is observed and so dichloromethane seems to be a better solvent at promoting porous structures with a regular pore size. The disruption of the regularity of the pores was again attributed to the coalescence of water droplets that disrupts the hexagonal packing. The evaporation of the dichloromethane may be slower than the time taken for the water droplets to coalesce and the subsequent evaporation of the water and solvent leaves pores that have a non-hexagonal distribution.

When the solvent used to dissolve the star-shaped polystyrene was changed to carbon disulfide, the resulting film had a turbid appearance. This was in contrast to the transparent films that were obtained for the films cast from toluene and dichloromethane. The SEM image of this turbid film (Figure 4.3.3) clearly shows the formation of spherical pores with a high degree of homogeneity and a narrow size distribution. Furthermore, the pores are arranged with a hexagonal distribution and have the appearance of a honeycomb structure.

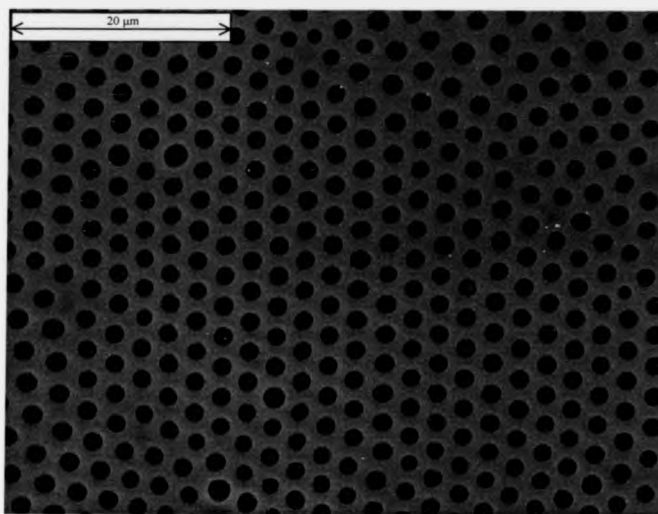


Figure 4.3.3 Surface morphology of a film of star-shaped polystyrene with 21 arms cast from a 10 g L^{-1} carbon disulfide solution. Pore diameter is $\sim 2 \mu\text{m}$.

This result was encouraging as it demonstrated that the formation of highly ordered porous membranes was possible using star-shaped polystyrenes prepared by LRP. The diameter of the pores was determined from the scale bar at the top of the SEM image and found to be $\sim 2 \mu\text{m}$.

Thus, the influence of the solvent on promoting a regular pattern of homogeneous pores appears to be very important. Toluene and dichloromethane are not good solvents for the promotion of highly ordered pores under the conditions used whereas carbon disulfide appears to be a very effective solvent at promoting the honeycomb structures.

4.3.2 Effect of the rate of airflow on membrane formation

The experimental set-up that was used to form the membranes allows the rate of saturated air entering the humidity chamber to be carefully controlled and monitored. The effect that the rate of airflow had on the formation of membranes was investigated using star-shaped polymers of molecular weight 43000 g mol^{-1} possessing 21-arms of polystyrene. It was anticipated that when air flowed across the polymer surface at a higher rate, the solvent would evaporate more rapidly leaving less time for any coalescence of the water droplets to occur. This would result in a decrease in the pore size with an increasing rate of airflow. Table 4.3.2 summarises the conditions that were employed to investigate the effect on pore formation by varying the rate of airflow.

Rate of airflow (mL min^{-1})	Relative humidity (%)	Temperature ($^{\circ}\text{C}$)	Solvent	Evaporation time (mins)
500	72	19	CS_2	3
1000	73	19	CS_2	3
1500	77	20	CS_2	3

Table 4.3.2 Reaction conditions used to investigate the effect of varying the rate of airflow in the formation of membranes using a 21-armed star polystyrene ($M_w = 43000 \text{ g mol}^{-1}$, $\text{PDI} = 1.08$).

The relative humidity and temperature inside the humidity chamber for this set of reactions was kept constant as far as was possible and carbon disulfide was selected as the solvent to dissolve the star polymers at a concentration of 10 g L^{-1} . When the rate of

airflow was set at 1500 mL min^{-1} , the resulting film that was cast showed the formation of pores (Figure 4.3.4).

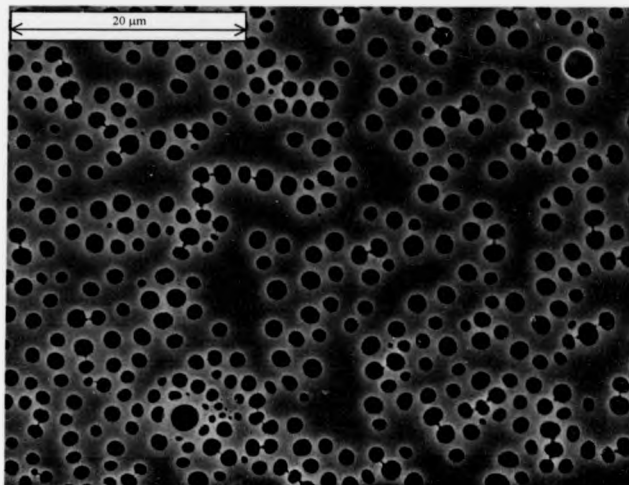


Figure 4.3.4 Surface morphology of a film of star-shaped polystyrene with 21 arms using an airflow rate of 1500 mL min^{-1} .

It is clear that, although a porous structure is observed, the distribution of the pores is not uniform and there is no evidence of a hexagonal array of pores.

When the rate of airflow was decreased to 1000 mL min^{-1} , a turbid film was formed after three minutes of the solution being subjected to the airflow. The SEM image (Figure 4.3.5) shows a highly ordered arrangement of pores that have a hexagonal distribution. The pores were homogeneous in size and the diameter of the pores was found to be $\sim 2 \mu\text{m}$.

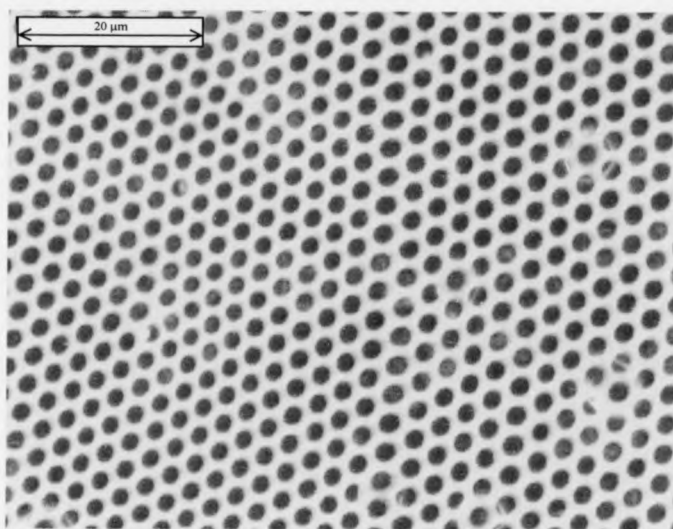


Figure 4.3.5 Surface morphology of a film of star-shaped polystyrene with 21 arms using an airflow rate of 1000 mL min^{-1} .

The pore size of the film shown in Figure 4.3.5 is the same as that shown in Figure 4.3.3. It is noted that the membrane shown in Figure 4.3.5 has a slightly higher density of pores than the membrane shown in Figure 4.3.3. The reason for this variation is unclear although it may be attributed to small differences in the precise concentration of the star polymer solution.

Finally, the rate of airflow was decreased to 500 mL min^{-1} and the resulting turbid film that was generated showed the presence of a highly ordered hexagonal array of pores (Figure 4.3.6). The pore diameter was found to be $\sim 3 \mu\text{m}$ which is larger than the pores observed when the airflow rate was higher.

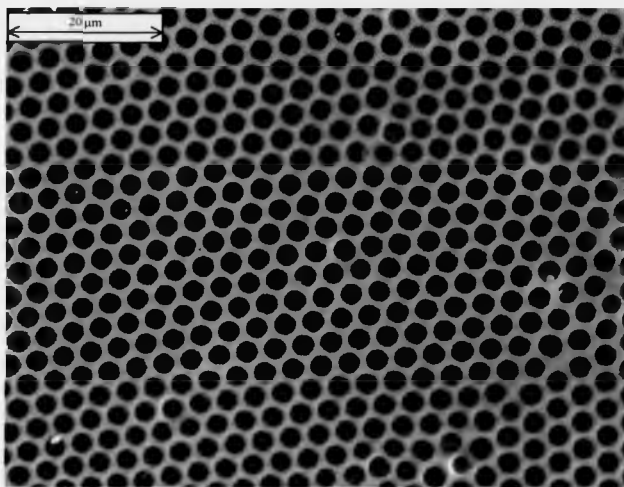


Figure 4.3.6 Surface morphology of a film of star-shaped polystyrene with 21 arms using an airflow rate of 500 mL min^{-1} .

It appears that the rate of airflow does have an effect on the formation of pores. At high rates of airflow, it appears that pore formation is disrupted whereas lower rates of air flow, typically 500 and 1000 mL min^{-1} , can promote the arrangement of highly ordered pores that are homogeneous in size. Furthermore, pore sizes with a smaller diameter are observed when the rate of airflow is increased. This may be explained by considering the rate at which the solvent evaporates from the solution surface. When the rate of airflow is increased, there will be an increased evaporation of solvent which, in this case, is carbon disulfide. The increased rate of solvent evaporation will lead to a more rapid condensation of the water droplets onto the solution surface due to a more rapid temperature drop. The subsequent rapid evaporation of all the solvent and water molecules will lead to a decreased pore size since coalescence of the water droplets is minimised.

4.3.3 Effect of temperature and relative humidity on membrane formation

Since the temperature and relative humidity inside the humidity chamber vary simultaneously, it was difficult to assess these parameters independently. Star-shaped polystyrene polymers with 14-arms ($M_n = 18000 \text{ g mol}^{-1}$, $\text{PDI} = 1.09$) and 21-arms ($M_n = 43000 \text{ g mol}^{-1}$, $\text{PDI} = 1.08$) were prepared by LRP and the effect that the relative humidity and temperature had on the formation of pores was investigated according to Table 4.3.3. The rate of airflow was kept constant at 1000 mL min^{-1} for each film that was cast.

Number of arms	Relative humidity (%)	Temperature ($^{\circ}\text{C}$)
14	69	20
14	75	20
14	82	19
21	43	18
21	53	19
21	81	19

Table 4.3.3 Reaction conditions used to assess the effect of relative humidity and temperature on pore formation. 10 g L^{-1} of 14-armed polystyrene ($M_n = 14000 \text{ g mol}^{-1}$) and 21-armed polystyrene ($M_n = 43000 \text{ g mol}^{-1}$) in CS_2 with an airflow rate of 1000 mL min^{-1} was used.

The effect of increasing the relative humidity on the 14-armed stars shows that more ordered pores are formed when the relative humidity is increased (Figure 4.3.7)

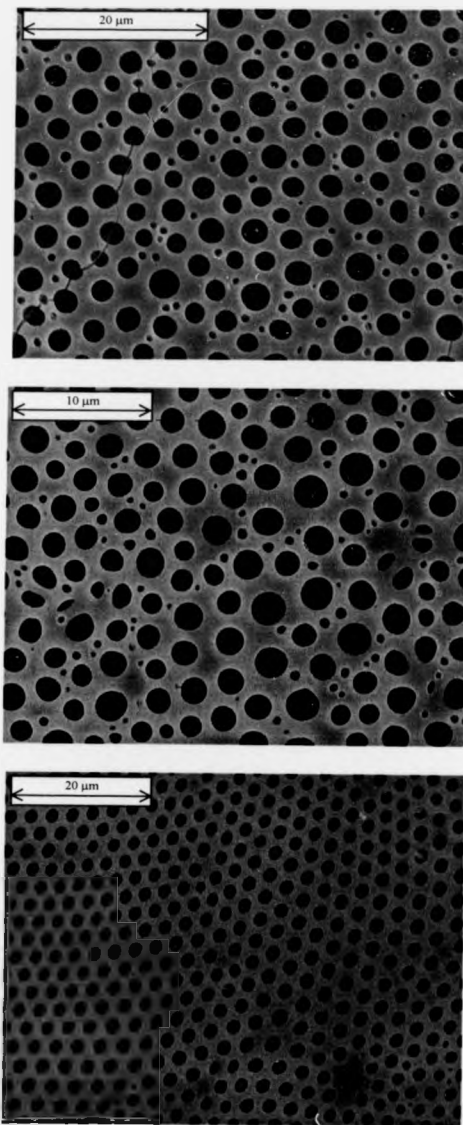


Figure 4.3.7 Pore formation with a 14-armed star polystyrene at relative humidity 69 % (top image), 75 % (middle image) and 82 % (bottom image).



When the relative humidity was low (69 %) pore formation could still occur but the pores were heterogeneous in size and a hexagonal distribution was not observed. As the relative humidity increased, the pores became more ordered and at a relative humidity of 82 %, highly ordered pores were formed where the pores were perfectly spherical, monodisperse and formed a hexagonal array. A similar effect was observed for the 21-armed star-shaped polystyrenes (Figure 4.3.8) when the relative humidity was increased.

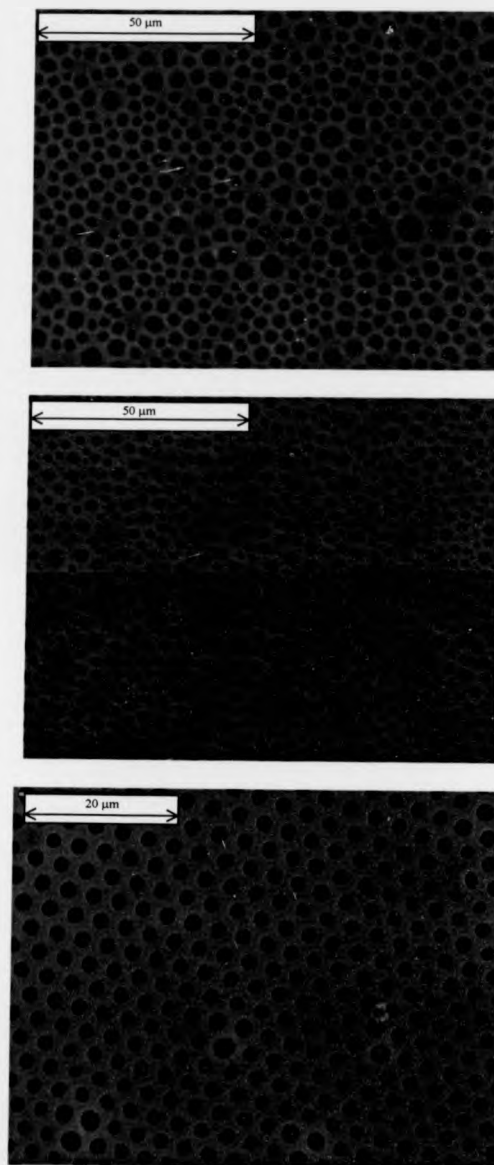


Figure 4.3.8 Pore formation with a 21-armed star polystyrene at relative humidity 43 % (top image), 53 % (middle image) and 81 % (bottom image).

The relative humidity does have a profound effect on influencing the formation of highly ordered membranes with honeycomb structures. A relative humidity of at least 70 % is required for the formation of such structures. Whilst it was difficult to independently vary the temperature of the humidity chamber, it was observed that temperatures in the range 17 – 20 °C are also required if highly ordered pores are to be formed.

4.3.4 Optimum conditions for the formation of porous membranes

From the above experiments the optimum conditions for the formation of homogeneous spherical pores that arrange in a regular hexagonal array have been determined. A humid atmosphere is required and the relative humidity must be at least 70 % for the ordered pores to be observed. Below this relative humidity a heterogeneous size distribution of pores is observed. It is thought that a high relative humidity is required so that water droplets can condense onto the cold surface at a rapid rate and the droplets allowed to self organise into the hexagonal array. It has been reported by Boer et al.²¹ that the temperature at the solution surface is –6 °C brought about by the evaporation of the solvent. This associated decrease in the solution temperature causes water from the moist air to condense on the cold solution surface. The optimum flow rate of air over the solution surface has been found to be 500 mL min⁻¹ and 1000 mL min⁻¹ if a highly ordered hexagonal array of pores is to be observed. Higher airflow rates do not give a homogenous distribution of pores. The rate of airflow over the solution surface is important as this dictates the rate of evaporation of the volatile solvent. If the airflow rate is too low, solvent cannot evaporate fast enough for the water droplets to condense onto the surface. Conversely, if the airflow rate is increased there will be faster

evaporation of the solvent and water droplets can condense more rapidly onto the solution surface due to a more rapid temperature drop.

Formation of a homogeneous size distribution of pores has been found to be dependent on the solvent that the polymer is dissolved in. The ideal solvent has been found to be carbon disulfide which is highly volatile. Carbon disulfide is able to dissolve the polystyrene star polymers used but since it is insoluble in water, the water droplets appear on the solution surface and the coalescence of the water droplets is prevented. Since the polystyrene is also insoluble in water, the polystyrene precipitates and coalescence of the water droplets is further prevented. It is possible that the polystyrene precipitates at the interface between the solution and the water droplet to form an envelope around the water droplets thus stabilising these isolated water droplets. This envelope of droplets may also prevent droplet-to-droplet coalescence and preserve any regularity of these droplets.

The subsequent evaporation of the carbon disulfide solvent from the polymer-enveloped water droplets will reduce the solution volume and the temperature of the remaining material then rises to ambient temperature. It is possible that the pressure inside the droplets then rises and the water droplets then burst through the film to form the pores.

4.4 Formation of pores with polymer blends

The previous section has shown that the formation of a regular array of pores is possible using star-shaped polystyrene polymers dissolved in an appropriate solvent and subjected to a high relative humidity. The use of star-shaped polymers appears to be essential for the formation of these pores and such structures are not observed when their linear counterparts are used. The differences in the physical properties of star polymers and linear polymers is thought to be the reason for this as star-shaped

polymers seem to precipitate instantaneously at the solution/water interface. Linear polystyrene is unable to precipitate at the interface as reported by Francois et al.⁶. To obtain some functionality of the pores, the effect on the addition of amphiphilic linear polymers was investigated. It was anticipated that the addition of low amounts of linear amphiphilic copolymers to the star polymer solution would not disrupt the hexagonal pattern. Furthermore, the hydrophilic portion of the diblock copolymer would migrate preferentially to the solution/water interface and the hydrophobic portion would remain in the bulk of the film.

4.4.1 Effect of pore formation with a blend of star and linear polystyrene

The amphiphilic block copolymer incorporating poly(ethylene glycol) as the hydrophilic block and polystyrene as the hydrophobic block was synthesised as outlined in section 4.2. A film using this linear block copolymer dissolved in carbon disulfide was cast onto a glass slide and pore formation analysed in the absence of any star polymer. It is clear from Figure 4.4.1 that pore formation is promoted when the linear block copolymer is used but there is no evidence of a highly ordered array of pores as observed for the star-shaped homopolymer counterparts. The pores are not spherically shaped and there is a random distribution of pores sizes.

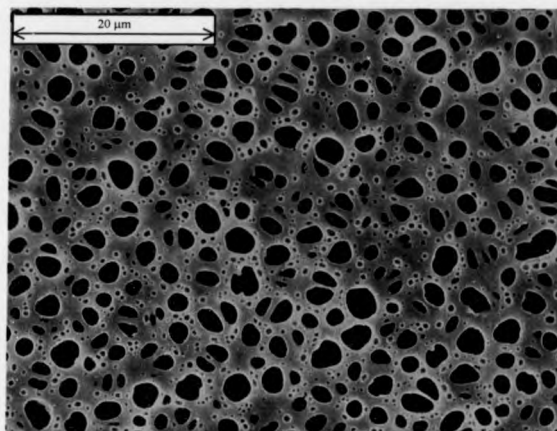


Figure 4.4.1 Surface morphology of a linear PEG-*b*-PST block copolymer after film casting from CS₂, relative humidity 71 %, 19 °C and airflow rate 500 mL min⁻¹.

Differing proportions of the amphiphilic diblock copolymer were then added to a solution of star polymer to determine what effect this had on the formation of the pores.

Table 4.4.1 illustrates the conditions used in this set of experiments.

Proportion of PEG- <i>b</i> -PST by weight (%)	Relative Humidity (%)	Temperature (°C)	Airflow rate (mL min ⁻¹)
1	72	19	500
4	76	18	500
10	74	18	500

Table 4.4.1 Experimental conditions used to investigate the effect of the addition of a linear block copolymer to a 21-armed star polystyrene polymer in CS₂.

The SEM images that were obtained when an increasing proportion of the PEG-*b*-PST linear block copolymer was added to a solution of 21-armed star shaped polystyrene show that the linear copolymer has an effect on pore formation (Figure 4.4.2).

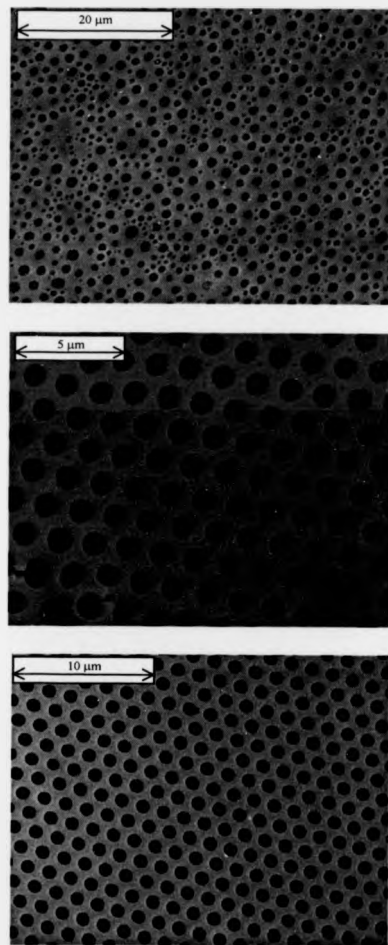


Figure 4.4.2 Surface morphology of blends of a 21-armed star-shaped polystyrene polymer with 10 % by weight PEG-*b*-PST (top), 4 % by weight PEG-*b*-PST (middle) and 1 % by weight PEG-*b*-PST (bottom).

It is clear from Figure 4.4.2 that the addition of an amphiphilic block copolymer can affect the formation of pores. By blending the star polymer with a low proportion of the linear polymer (1 % by weight linear polymer, bottom image of Figure 4.4.2) the formation of a regular array of pores is observed and a hexagonal distribution of pores is observed. The diameter of these pores was measured and found to be $\sim 1 \mu\text{m}$.

No defects in the porous structure were observed. Upon increasing the proportion of the linear block copolymer to 4 % by weight (middle image of Figure 4.4.2) pore formation is still promoted and a hexagonal distribution of pores can be observed. The pores are largely spherically shaped and a narrow size distribution of pores is obtained. Closer inspection of this image reveals that some of the pores are not perfectly spherical in shape and there are some imperfections in the film where the hexagonal distribution is interrupted and some of the pores are cracked.

When the proportion of the linear block copolymer is increased to 10 % by weight (top image of Figure 4.4.2) pore formation is observed but the hexagonal distribution is completely disrupted. Although the pores are largely spherically shaped, there is a heterogeneous size distribution of these pores.

In conclusion, blends of star and linear polymers can still promote the formation of highly ordered honeycomb structures as long as the proportion of linear polymer remains low. Increasing the proportion of linear polymer tends to disrupt the hexagonal structure and ultimately leads to the complete disappearance of this structure. By introducing linear polymers into the structure is beneficial if the pores are to be functionalised. The wide range of linear block copolymers that can be prepared by LRP will enable the relationship between the star and linear polymers and their influence on pore formation to be determined. The block copolymers would be expected to lie at the interface with the hydrophilic portion interacting with the water droplets. Thus the

internal surface of the pore will be functionalised. The effect of varying the chemical composition of each block on the amphiphilic copolymer can be investigated and this is a good way to introduce functionality into the films. For example, an amphiphilic block copolymer incorporating dimethylaminoethyl methacrylate (DMAEMA) (Figure 4.4.3) can introduce amino functionality to the pores.

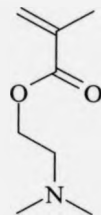


Figure 4.4.3 Chemical structure of dimethylaminoethyl methacrylate (DMAEMA).

When a star polymer was blended with 2 % by weight of linear PDMAEMA, pores were formed but there was a heterogeneous size distribution of pores (Figure 4.4.4) and so there was disruption to the hexagonal pattern.

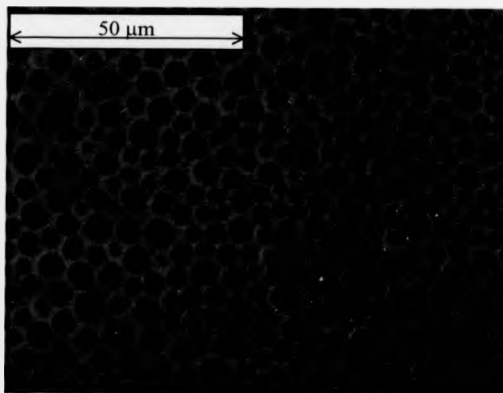


Figure 4.4.4 Pore formation with a 21-armed star polystyrene polymer blended with 2 % by weight PDMAEMA in CS₂ at 72 % relative humidity, 20 °C and airflow rate 500 mL min⁻¹.

It appears that the incorporation of polystyrene in the block copolymer is necessary to observe the hexagonal structures. Linear PDMAEMA homopolymers blended with the star polymer does not give a good porous structure, despite the optimum pore-forming conditions being employed. The synthesis of block copolymers by LRP that incorporates polystyrene and PDMAEMA is possible but this synthesis was not carried out for this work.

4.5 Effect of molecular weight on the formation of pores

The ability to control the pore size of these highly ordered porous structures would be highly beneficial and would enable the membranes to be used for different applications. For example, a micron-sized porous film would be appropriate for cell growth studies while nanometre-sized pores in the dimensions of visible light may be applicable for photonic band gap materials. The molecular weight of the star polymer is likely to influence the pore size. The optimum conditions for the formation of the ordered structures has already been investigated and so the effect that the molecular weight of the star polymers has on this formation can now be assessed. Star polymers with 14 and 21 arms were investigated as detailed in Table 4.5.1.

Number of arms	Molecular weight M_n (g mol^{-1})	PDi	Relative humidity (%)	Temperature ($^{\circ}\text{C}$)	Rate of airflow (mL min^{-1})
14	18000	1.09	78	19	1000
14	43000	1.74*	71	19	1000
14	54000	1.18	68	18	1000
21	19000	1.08	74	19	1000
21	43000	1.08	75	19	1000
21	79000	1.17	83	19	1000

Table 4.5.1 Experimental conditions to investigate the effect of molecular weight on pore formation. A 10 g L^{-1} solution in CS_2 was used in all experiments. *Shoulder peak at high molecular weight observed in SEC trace.

The SEM images obtained from the 21-armed star polystyrenes are shown in Figure 4.5.1. In all images, spherical pores are formed that have a narrow size distribution and the regular honeycomb structure is observed. Measurement of the pore diameter (Table 4.5.2) shows that there is a small increase in pore size as the molecular weight of the star increases.

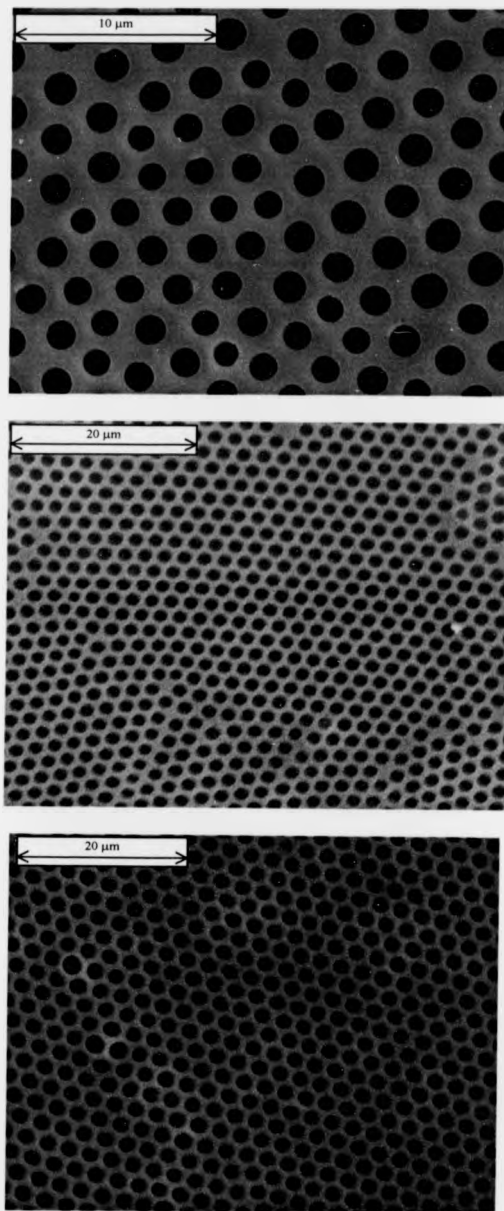


Figure 4.5.1 SEM images showing the surface morphology of 21-armed star polystyrene with increasing molecular weight; 18600 g mol^{-1} (top), 43000 g mol^{-1} (middle) and 79000 g mol^{-1} (bottom).

Number of arms	Molecular weight M_n (g mol^{-1})	Average pore diameter (μm)
21	18600	1.5
21	43000	1.8
21	79000	2.5

Table 4.5.2 Measurement of average pore diameter of 21-armed polystyrene with differing molecular weights.

Similarly, the SEM images obtained for the differing molecular weights of the 14-armed star polystyrenes are shown in Figure 4.5.2 and the measurement of the average pore diameter is shown in Table 4.5.3.

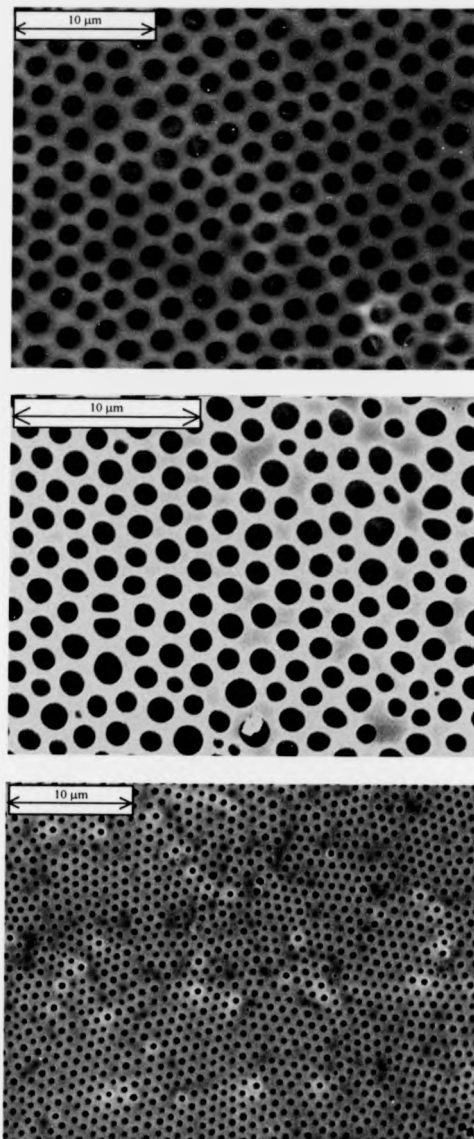


Figure 4.5.2 SEM images showing the surface morphology of 14-armed star polystyrene with increasing molecular weight; 18000 g mol⁻¹ (top), 43000 g mol⁻¹ (middle) and 79000 g mol⁻¹ (bottom).

Number of arms	Molecular weight M_n (g mol^{-1})	Average pore diameter (μm)
14	18000	1.3
14	43000	1.5
14	54000	1.5*

Table 4.5.3 Measurement of average pore diameter of 21-armed polystyrene with differing molecular weights. *Heterogeneous pore sizes.

The effect that the molecular weight has over the control of pore size is more marked when considering the results of the 21-armed star polystyrenes. The optimum conditions for film casting were used in all experiments and the formation of highly ordered pores was observed in all cases. As the molecular weight of the star increased, the diameter of the pore also increased. It appears that pore size can be directly controlled over the molecular weight of the polymer and can be altered in the range 1.5-2.5 μm . This result is quite interesting as it indicates that small changes at the molecular level can influence the structure on the micron scale.

When considering the 14-armed star polystyrenes, pore formation was observed for the three molecular weights investigated and honeycomb structures were observed. Problems were encountered when attempting to cast films from the high molecular weight structure since the hexagonal array appeared slightly disrupted and a heterogeneous size distribution of pores meant that it was not appropriate to include these results in this discussion. When the molecular weight of the 14-armed star polystyrene is increased from 18000 g mol^{-1} to 43000 g mol^{-1} , the average pores size increases slightly from 1.3 μm to 1.5 μm .

It seems that increases in molecular weight have the effect of increasing the pore size provided the optimum casting conditions are used to form pores with a homogeneous size distribution. Furthermore, an increase in the number of arms on the star polymer also has the effect of increasing the pore size. A five-armed star polystyrene with a galactose core and molecular weight 12000 g mol^{-1} has been found to have an average pore diameter of $0.83 \mu\text{m}$ and this further confirms that a lower number of arms confers a smaller pore size.

In summary, the pore size increases with increases in molecular weight although the pore size appears to be dependent on the polymer architecture. While it seems possible to create pores of a uniform size distribution, the prediction of the pore size seems difficult as this is dependent on the structure of the star polymer. A correlation between the polymer architecture, the number of polymeric arms attached to a core, the molecular weight and pore diameter would enable the precision synthesis of highly ordered pores whose size can be predetermined. The ability to predict the pore sizes would be highly advantageous for many industrial applications such as synthetic membranes and medical devices.

4.6 Conclusions

The formation of highly ordered porous structures from star polymers synthesised by copper-mediated LRP has been demonstrated. Star-shaped polymers with a β CD core possessing 21- and 14-arms can promote the formation of honeycomb structures under appropriate film casting conditions. The optimum film casting conditions have been determined and there are a number of variables that can be controlled to optimise the formation of pores. There is a necessity for a high relative humidity (>70 %) to promote a homogeneous size distribution of pores and temperatures above 17 °C are also required. The rate of airflow over the solution surface also affects pore formation and it was found that a rate of 500 mL min⁻¹ or 1000 mL min⁻¹ achieves the best results. Carbon disulfide seems to be the only solvent that is capable of promoting the highly ordered structures. Furthermore, the pore size can be controlled to a certain extent by varying the molecular weight of the star polymer and also by varying the number of arms on the core. Increases in molecular weight confer an increase in pore diameter. Linear polymers do not appear to promote ordered structures and it is thought that the unique properties of spherical-shaped materials such as star polymers are essential to obtain the highly ordered porous films. One of the characteristics of spherical materials is the ability for them to instantaneously precipitate at the solution/water interface. Linear homopolymers do not have this ability and precipitation does not occur. It is probable that this property of star polymers assists in forming a polymer envelope around the water droplets and stabilising their arrangement before the droplets evaporate leaving behind the honeycomb structure. Blending small proportions of linear polymers with the star polymers does not disrupt the porous structure and this can provide a route to introduce functionality to the pores. Experiments using fluorescent monomers (Figure 4.6.1) incorporated into the

hydrophilic portion of an amphiphilic block copolymer and subsequent analysis of the pores with a confocal microscope may assist in confirming the hydrophilic nature of the pores.

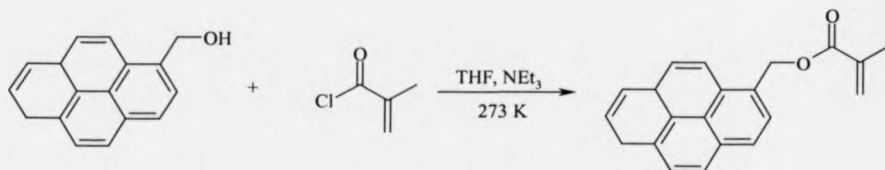


Figure 4.6.1 Synthesis of a fluorescent monomer based on pyrene.

The mechanism for the pore formation is not well understood. It is understood that the process involves the condensation of water droplets onto the solution surface since in the absence of a humid atmosphere, a regular array of pores is not observed.

Furthermore, the polymer is required to be dissolved in a volatile solvent that is immiscible with water so that the polymer can precipitate at the water/solution interface to form an envelope around the condensed water droplet. This prevents the coalescence of the water droplets and the hexagonal array formed by convection currents and capillary interactions is stabilised. Once all the solvent and water has evaporated from the surface, this leaves behind the hexagonal array of pores.

4.7 Chapter 4 References

- 1 S. A. Jenekhe and X. L. Chen, *Science*, 1999, **283**, 372.
- 2 G. Widawski, M. Rawiso, and B. Francois, *Nature*, 1994, **369**, 387.
- 3 B. Francois, O. Pitois, and J. Francois, *Adv. Mater.*, 1995, **7**, 1041.
- 4 S. A. Jenekhe and X. L. Chen, *Science*, 1998, **279**, 1903.
- 5 B. Francois, Y. Ederle, and C. Mathis, *Synth. Met.*, 1999, **103**, 2362.
- 6 O. Pitois and B. Francois, *Eur. Phys. J. B*, 1999, **8**, 225.
- 7 M. H. Stenzel-Rosenbaum, T. P. Davis, A. G. Fane, and V. Chen, *Angew. Chem.-Int. Edit.*, 2001, **40**, 3428.
- 8 O. Painter, R. K. Lee, A. Scherer, A. Yariv, J. D. O'Brien, P. D. Dapkus, and I. Kim, *Science*, 1999, **284**, 1819.
- 9 J. Wijnhoven and W. L. Vos, *Science*, 1998, **281**, 802.
- 10 E. Yablonovitch, T. J. Gmitter, R. D. Meade, A. M. Rappe, K. D. Brommer, and J. D. Joannopoulos, *Phys. Rev. Lett.*, 1991, **67**, 3380.
- 11 M. Imada, S. Noda, A. Chutinan, T. Tokuda, M. Murata, and G. Sasaki, *Appl. Phys. Lett.*, 1999, **75**, 316.
- 12 T. Bitzer, 'Honeycomb Technology', Chapman and Hall, London 1997.
- 13 T. Nishikawa, J. Nishida, R. Ookura, S. I. Nishimura, S. Wada, T. Karino, and M. Shimomura, *Mater. Sci. Eng. C-Biomimetic Supramol. Syst.*, 1999, **10**, 141.
- 14 T. Nishikawa, J. Nishida, R. Ookura, S. I. Nishimura, S. Wada, T. Karino, and M. Shimomura, *Mater. Sci. Eng. C-Biomimetic Supramol. Syst.*, 1999, **8-9**, 495.

-
- 15 R. E. Kesting, 'Synthetic Polymer Membranes', Wiley, New York 1985.
- 16 M. Srinivasarao, D. Collings, A. Philips, and S. Patel, *Science*, 2001, **292**, 79.
- 17 O. Karthaus, N. Maruyama, X. Cieren, M. Shimomura, H. Hasegawa, and T. Hashimoto, *Langmuir*, 2000, **16**, 6071.
- 18 P. D. Aversana, J. R. Banavar, and J. Koplik, *Phys. Fluids*, 1996, **8**, 15.
- 19 P. D. Aversana, V. Tontodonato, and L. Carotenuto, *Phys. Fluids*, 1997, **9**, 2475.
- 20 R. Edmonds, 'Ph.D Thesis', University of Warwick, 2002.
- 21 B. d. Boer, U. Stalmach, H. Nijland, and G. Hadziioannou, *Adv. Mater.*, 2000, **12**, 1581.
- 22 S. Pascual, *Personal Communication*, 2001.

Chapter 5**Further Modifications of Star-shaped β CD Polymers
for the Synthesis of Diblock Copolymers****5.0 Introduction**

The previous chapters have shown that cyclodextrin can be modified in a number of ways to enable it to be employed as a multifunctional initiator used to form well-defined star polymers containing 7-, 14- and 21-arms by copper (I) mediated living radical polymerisation. As an extension to those polymerisations, it may be possible to form more complex architectures whereby the polymer at one face of the cyclodextrin will differ from the polymer at the other face. This provides an interesting synthetic challenge since polymerisations will have to be directed at either of the two faces without affecting the other face. Polymers prepared by LRP use an organometallic complex to establish an equilibrium between active and dormant chain ends and all chains will be terminated by halogens (dormant species). Since these chain ends can be re-activated it will be necessary to deactivate these chain ends to prevent further polymerisation occurring at this face when polymerisation at the other face is required. By modifying each face of the cyclodextrin with a different polymer, the formation of diblock copolymers may be possible. For example, the formation of a cyclodextrin amphiphilic diblock copolymer that possesses a hydrophobic polymer at one face and a hydrophilic polymer at the other face may exhibit surfactant behaviour. These types of compounds are used extensively in household products such as shampoo and conditioners¹⁻⁵, laundry detergents^{6, 7}, general cleaning products and in food preparations⁸⁻¹⁰. Furthermore, the cavity of the cyclodextrin may be exploited so that

host-guest interactions can be investigated and release of the guest from the inclusion complex may be mediated by the structure of the polymer at either of the faces. In this chapter, the modification of star-shaped polymers with a cyclodextrin core for the synthesis of diblock copolymers is investigated.

5.1 Modification of the ω -Bromo end groups

The star-shaped polymers prepared by living radical polymerisation all possess relatively stable carbon-bromine terminal linkages that originate from the multifunctional initiator. The equilibrium between the dormant carbon-halogen species and the active radical species lies towards the dormant species and so the majority of polymer terminals exist as the stable carbon-bromine bond. Due to the stable nature of this covalent bond, the isolated polymers possess the carbon-bromine bond that is intact at the ω end. Although this bond is stable, it is potentially active and may affect the stability of further products. In this section, the ability to effectively quench the terminal carbon-halogen bonds to form more stable carbon-carbon bonds will be investigated. By deactivating the ω -terminals of polymer chains at one face of the β CD star polymers may allow further and directed chemical modification at the other face of the β CD. A number of research groups have investigated quenching reactions of metal-catalysed living radical polymerisations. Among these, Sawamoto et al. investigated the use of silyl enol ethers such as α -(trimethylsiloxy)styrene and *p*-methoxy- α -(trimethylsiloxy)styrene (Figure 5.1.1) and found them to be efficient end-capping agents for polymers prepared by Ru(II)-mediated polymerisation^{11, 12}.

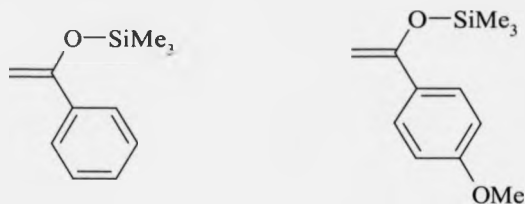


Figure 5.1.1 Chemical structures of α -(trimethylsilyloxy)styrene and *p*-methoxy- α -(trimethylsilyloxy)styrene for the quenching of metal-catalysed LRP.

Matyjaszewski et al. have reported ω -dehalogenation using tributyltin hydride¹³. The trialkyltin hydrides are common dehalogenation reagents and can react with organic halides via a free radical chain mechanism. The trialkyl tin radical can be generated by the copper (I) bromide / ligand complex and this radical can abstract the halogen atom from the ω -terminus of the polymer to generate a polymer radical. This radical then subsequently reacts with a trialkyl tin hydride to form the reduced product and a new trialkyltin radical (Figure 5.1.2).

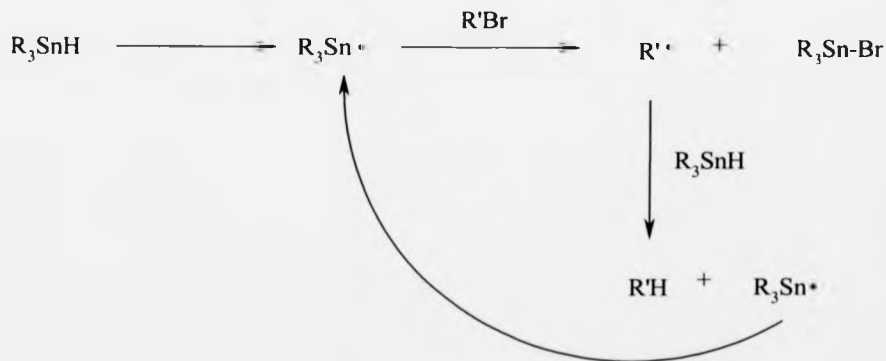


Figure 5.1.2 Dehalogenation of an alkyl halide $R'X$ with trialkyl tin hydride.

Before investigating any dehalogenation reactions using the star-shaped β CD polymers, the end-capping was performed on linear homopolymers and the effectiveness of the silyl enol ethers as quenching agents was investigated. Low molecular weight linear PMMA was synthesised using ethyl-2-bromoisobutyrate as an initiator and the process mediated by a copper (I) / *N*-pentyl-2-pyridylmethanimine complex in toluene at 90 °C. The polymerisation was stopped at 25 % conversion and the resulting polymer was purified and found to have a molecular weight of 2500 g mol⁻¹ and relatively narrow molecular weight distribution (PDI ~ 1.25). This polymer, with its characteristic carbon-bromine ω -terminus, was used as a macroinitiator to initiate the quenching reaction using α -(trimethylsiloxy)styrene. A 10-fold excess of the silyl enol ether was used to ensure complete dehalogenation at the PMMA ω -terminal and the reaction was mediated by a copper (I) bromide / *N*-pentyl-2-pyridylmethanimine complex in toluene at 90 °C. After four hours of reaction the copper complexes were removed by filtration through basic alumina and the resulting polymer isolated by precipitation in cold petroleum ether. SEC analysis of the isolated polymer showed the molecular weight of the polymer to be 2500 g mol⁻¹ as expected. Inspection of the ¹H NMR spectra was used to investigate the end-group structure. The ¹H NMR spectra of linear PMMA prepared by LRP with a carbon-bromine terminus shows characteristic signals at 2.5 ppm and 3.8 ppm that correspond to the methylene protons and methoxy protons respectively of the terminal MMA unit. Analysis of the ¹H NMR spectra of the quenched polymer shows the disappearance of these signals that correspond to the bromine terminal. New signals were observed downfield at 7.5 ppm that presumably correspond to the protons on the aromatic ring of the silyl enol ether. To further verify that the chain ends were dehalogenated, a chain extension polymerisation with MMA was performed. If the terminal carbon-bromine bond was still present, the polymer would function as a

macroinitiator and MMA would propagate to yield higher molecular weight species. However, this was not the case and after four hours of polymerisation, no increase in molecular weight was observed. This led to the conclusion that the silyl enol ether had dehalogenated the polymer chain ends thus causing them to be deactivated. The mechanism for this deactivation is thought to proceed via a radical pathway where the radical species is generated by the activation of the carbon-halogen bond by the copper (I) catalytic complex (Figure 5.1.3).

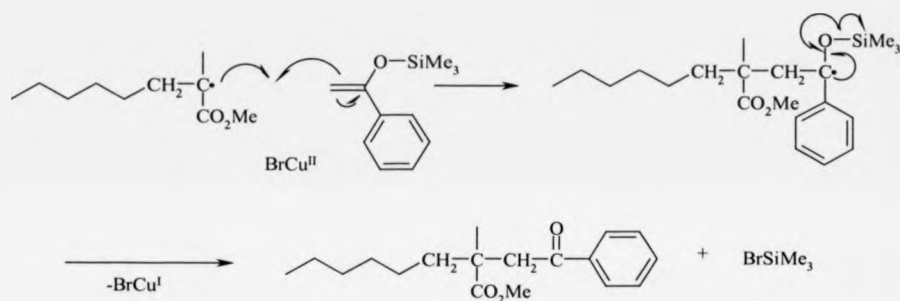


Figure 5.1.3 Possible mechanism of reaction of silyl enol ethers with PMMA for the deactivation of chain ends.

The successful dehalogenation of the linear PMMA was not observed when applied to the deactivation of chain ends of the star-shaped polymers. Deactivation of the carbon-halogen chain ends of 14-armed PMMA stars could not be verified since the signals in the ^1H NMR spectra corresponding to the silyl enol ether group were not observed. This made the analysis of the end-group structure non-trivial. The difficulty in synthesising well-defined star polymers of low molecular weight was also a factor in assessing the incorporation of the silyl enol ether.

Subsequently, the use of trialkyl tin hydride was investigated to replace the terminal halogen of the polymer chains with a hydrogen atom. Linear PMMA initiated by ethyl-

2-bromoisobutyrate was again investigated and the simultaneous polymerisations with and without the addition of tri *n*butyl tin hydride were performed. The addition of tri *n*butyl tin hydride seemed to quench the rate of polymerisation compared with the control experiment (Figure 5.1.4).

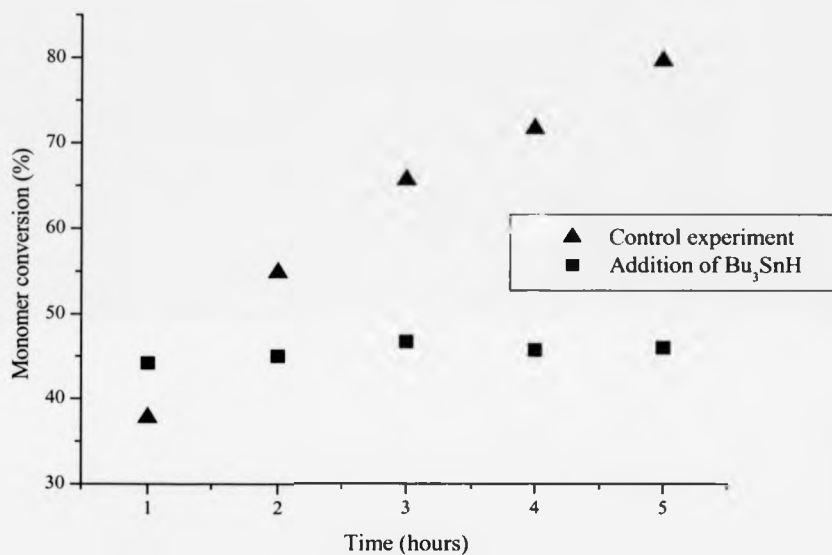


Figure 5.1.4 Effect of the addition of tri *n*butyl tin hydride on the LRP of MMA initiated by ethyl-2-bromoisobutyrate.

The linear PMMA polymer with dehalogenated chain ends was isolated and a chain extension reaction was performed to confirm that the carbon-bromine chain ends had been replaced with a carbon-hydrogen bond. Since there was little increase in molecular weight with increasing time it was assumed that the dehalogenation was successful. The linear PMMA that was not subjected to any quenching showed an increase in molecular

weight during the chain extension reaction (Figure 5.1.5) as expected since the terminal carbon-bromine groups were able to reinitiate the polymerisation of MMA.

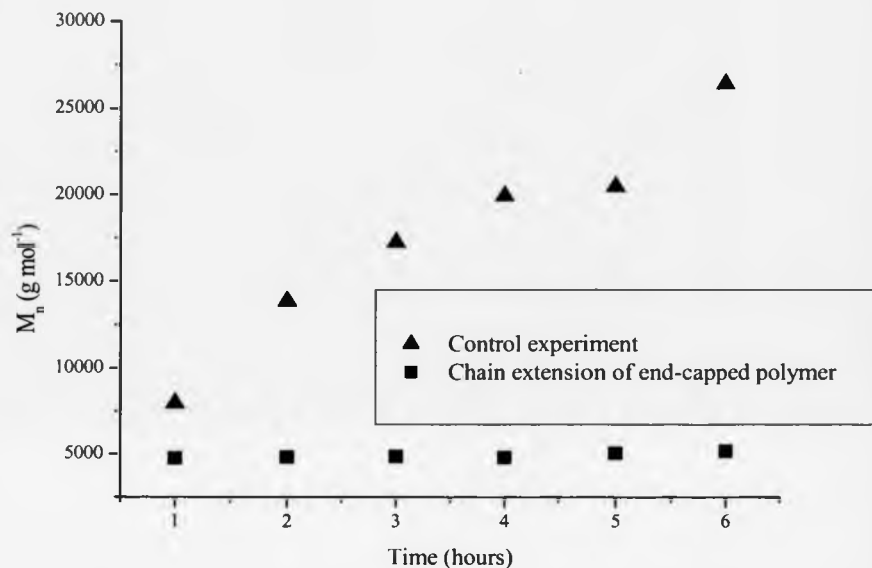


Figure 5.1.5 Chain extension reaction with MMA of PMMA quenched with Bu_3SnH .

Following the successful end-capping of linear PMMA with a hydrogen atom by quenching with trialkyl tin hydride, the dehalogenation was extended to a star polymer with 14 arms. To achieve this, a 14-armed star PMMA was synthesised with molecular weight $M_n = 27000 \text{ g mol}^{-1}$. A further reaction was then performed using a six-fold excess (with respect to each carbon-halogen terminus) of tri *n*butyl tin hydride and the copper (I) / *N*-pentyl-2-pyridylmethanimine complex was employed to generate the radical species. After allowing the quenching reaction to continue overnight, the resulting polymer was isolated and found to have a molecular weight $M_n = 29000 \text{ g mol}^{-1}$ which is similar to the original molecular weight as expected. The ^1H NMR spectra

(Figure 5.1.6) shows the absence of the signals at 2.5 ppm and 3.8 ppm that correspond to the protons of the methylene and methoxy respectively of the terminal MMA unit α to the bromine atom.

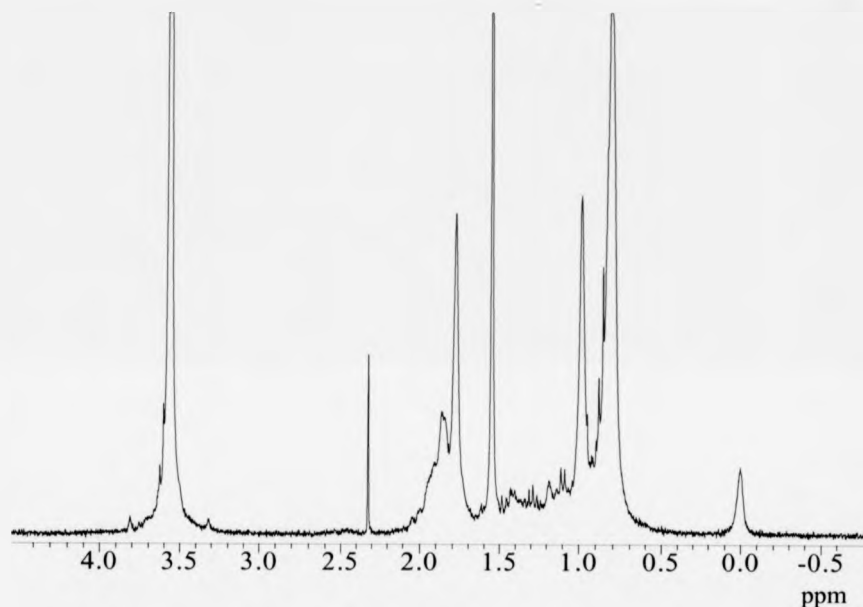


Figure 5.1.6 ^1H NMR spectra of star-shaped PMMA with carbon-hydrogen bonds at the ω -terminal.

To ensure that the carbon-bromine chain-ends were deactivated a chain extension reaction was performed with a fresh feed of MMA monomer and after 20 hours reaction time, no significant increase in molecular weight was observed ($M_n = 31000 \text{ g mol}^{-1}$). It was concluded that all 14 carbon-bromine bonds at the ω -terminal of the 14-armed PMMA star polymer had been deactivated and replaced with a stable carbon-hydrogen bond (Figure 5.1.7).

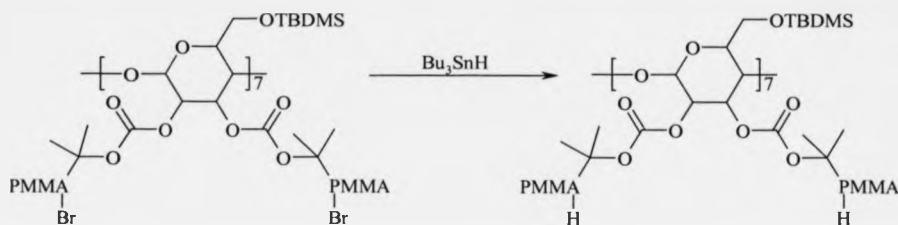


Figure 5.1.7 Dehalogenation of a 14-armed PMMA star polymer with Bu_3SnH .

5.2 Deprotection of *tert*-butyl dimethylsilyl groups

To regenerate the seven hydroxyl groups at the primary face of β CD required the deprotection of the TBDMS groups. This has previously been described in the synthesis of 7-Br-CD where the deprotection was realised using boron trifluoride etherate. It was anticipated that this same approach could be applied to the deprotection of TBDMS groups from a star polymer (Figure 5.2.1).

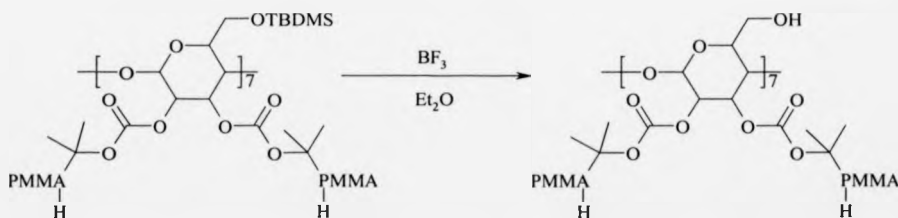


Figure 5.2.1 Deprotection of TBDMS groups from a 14-armed PMMA star polymer.

The reaction was stirred for 24 hours at room temperature and after this time, inspection of the ^1H NMR spectra (Figure 5.2.2) showed the disappearance of the signals at 0.02 ppm and 0.86 ppm that correspond to the dimethyl silyl protons and *tert*-butyl protons respectively of the TBDMS group. Since a very small amount of product was

obtained, this was not purified and was subsequently used in crude form to esterify the hydroxyl groups with an initiating functionality (see next section below).

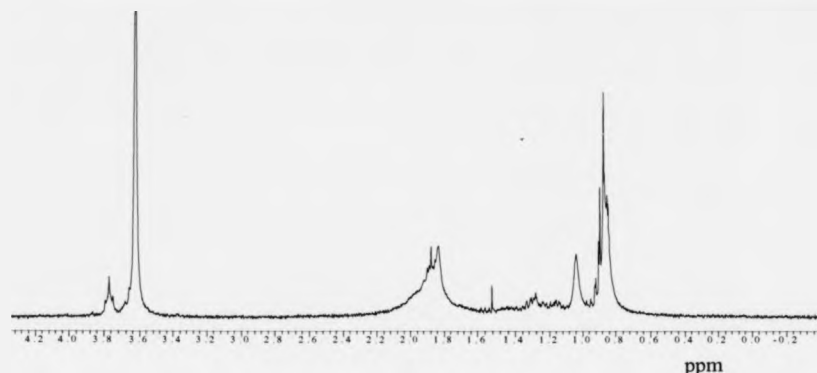


Figure 5.2.2 ¹H NMR spectra of a 14-armed star PMMA polymer with TBDMS groups deprotected at the primary face.

5.3 Modification at the primary face of a 14-armed PMMA star polymer with deactivated chain ends

The crude star-shaped β CD PMMA polymer with deactivated chain ends and hydroxyl groups regenerated at its primary face was used in the attempted synthesis of a 14-armed star-shaped β CD PMMA polymer with seven initiating sites at the primary face. This modification represents the seventh reaction step that the β CD has undergone. Esterification of this crude product with 2-bromoisobutyryl bromide was expected to proceed via the reaction shown in Figure 5.3.1.

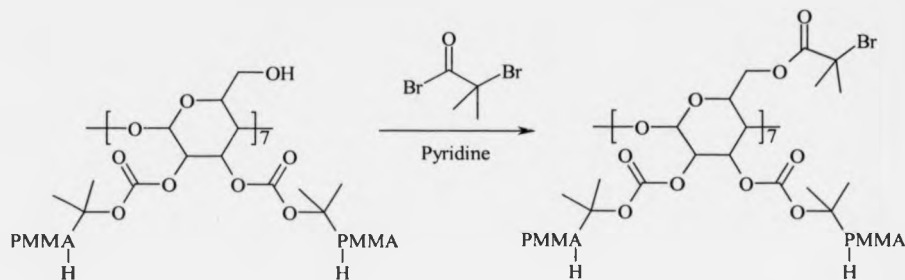


Figure 5.3.1 Esterification of a 14-armed PMMA star polymer at the primary face with 2-bromoisobutyryl bromide.

Due to the very small amount of product that this reaction produced, it was not considered appropriate to thoroughly wash the product in a rigorous aqueous work-up as was the case for the synthesis of previous initiators. Instead, the product was precipitated in water and dried in a desiccator at room temperature. The ^1H NMR spectra (Figure 5.3.2), although quite noisy, showed the presence of a signal at 1.9 ppm and this was attributed to the incorporation of the tertiary bromide moiety at the primary face of the 14-armed star-shaped β CD.

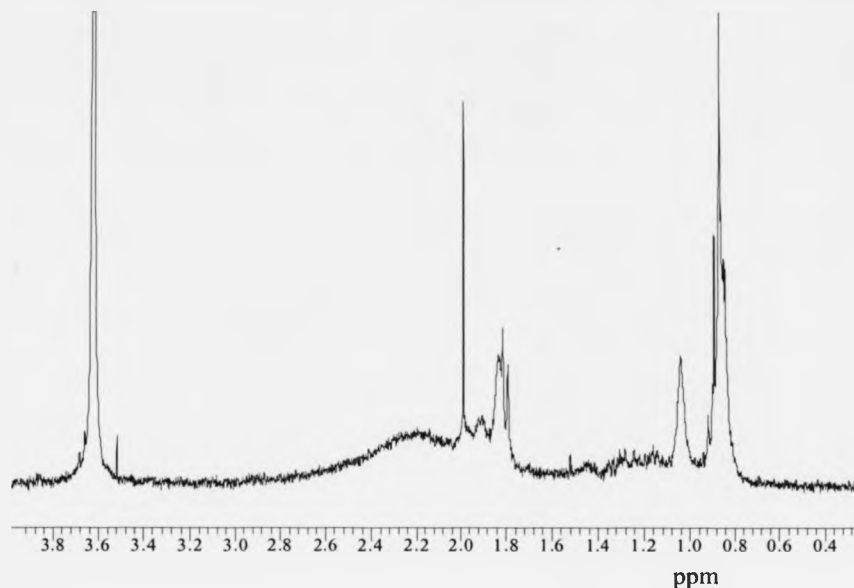


Figure 5.3.2 ^1H NMR spectra of a 14-armed PMMA star polymer with alkyl bromide initiating sites at the primary face of β CD.

It was tentatively thought that this compound would be able to initiate the living radical polymerisation of a monomer to form a diblock star polymer where each face would be polymerised independently.

5.4 Living radical polymerisation of a 14-armed PMMA star β CD polymer functionalised at the primary face with alkyl bromide moieties

The appearance in the ^1H NMR spectra of the initiator signal at 1.9 ppm was encouraging since it indicated the possibility of forming diblock star polymers where one monomer could be polymerised at one face of the β CD and a second monomer could then be polymerised at the other face of β CD. MMA was used to investigate whether polymerisation could occur at the primary face of β CD. Since the polymer

chain-ends of the PMMA at the secondary face had been previously deactivated by reaction with the tri *n*butyl tin hydride to form carbon-hydrogen chain-ends, the propagation of the second feed of MMA would not occur at these chain-ends. Instead, propagation would be directed towards the primary face.

Using this polymer as a macroinitiator ($M_n = 16000 \text{ g mol}^{-1}$, $PD_i = 1.19$), the LRP of MMA in toluene at $60 \text{ }^\circ\text{C}$ was investigated. It was found that the molecular weight increased very slowly over time (Table 5.4.1) indicating that either the initiator efficiency was low or the esterification of the hydroxyl groups with the alkyl bromide was incomplete. Conversions were not calculated due to the low volume of the polymerisation mixture and the uncertainty of the number of initiating sites that were present. The SEC curves (Figure 5.4.1) for the polymerisation show unimodal peaks although the molecular weight distributions broaden with increasing molecular weight.

Time (hours)	M_n (SEC)	PDI
4	18000	1.34
22	26500	1.45
30	29000	1.61
50	33000	1.71

Table 5.4.1 Evolution of molecular weight for the formation of diblock star polymers.

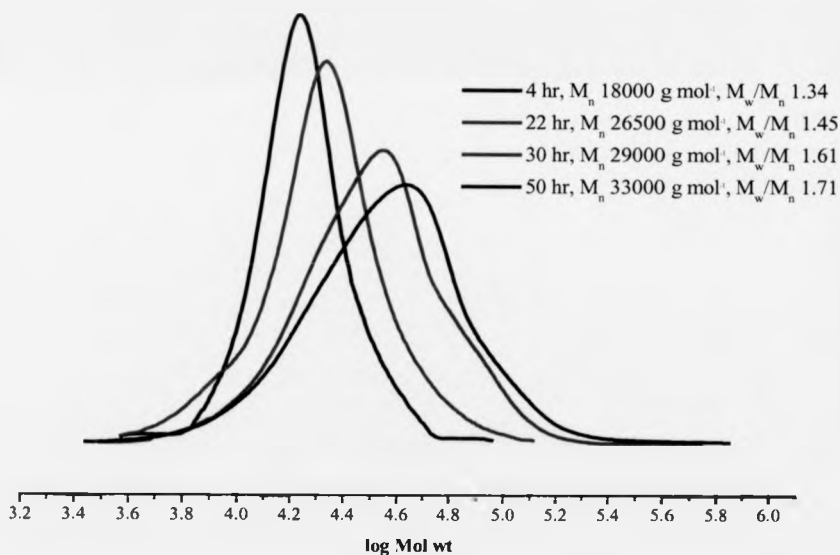


Figure 5.4.1 SEC curves for the formation of a diblock star polymer with 14 PMMA arms at the secondary face and PMMA arms at the primary face.

5.5 Conclusions

In summary, it does appear feasible that block copolymers can be synthesised where one monomer can propagate at one side of β CD and a second monomer can subsequently be synthesised at the other side of β CD. Although the synthetic pathway to accomplish this is labour intensive and involves multiple purification, protection and deprotection stages, it nonetheless shows that these types of polymeric structures are possible. There are many ways in which these initial studies can be further developed to achieve more efficient reactions where the intermediate products can be more fully characterised. Alternative end-capping reagents can be investigated to avoid the need for highly toxic tin compounds. Perhaps the reaction conditions for the silyl enol ethers as quenching agents could be optimised for their application in quenching star polymers. These reactions do, however, provide an insight into the possibilities of more complex polymeric architectures involving β CD and allows for any structure-relationship properties to be further investigated.

5.6 Chapter 5 References

- 1 V. Andre, R. Norenberg, P. Hossel, and A. Pfau, *Macromol. Symp.*, 1999, **145**, 169.
- 2 W. W. Schmidt, D. R. Durante, R. Gingell, and J. W. Harbell, *J. Am. Oil Chem. Soc.*, 1997, **74**, 25.
- 3 H. Rushton, C. L. Gummer, and H. Flasch, *Skin Pharmacol.*, 1994, **7**, 78.
- 4 L. J. Nehmsmann, *J. Soc. Cosmet. Chem.*, 1986, **37**, 288.
- 5 M. W. Heliouff, *Drug & Cosmetic Industry*, 1988, **142**, 38.
- 6 R. L. Burns and E. P. Duliba, *J. Surfactants Deterg.*, 2000, **3**, 361.
- 7 E. Smulders, P. Krings, and H. Verbeck, *Tenside Surfactants Deterg.*, 1997, **34**, 386.
- 8 N. Garti, V. Clement, M. Fanun, and M. E. Leser, *J. Agric. Food Chem.*, 2000, **48**, 3945.
- 9 N. Garti, A. Aserin, and M. Fanun, *Colloid Surf. A-Physicochem. Eng. Asp.*, 2000, **164**, 27.
- 10 P. C. Schulz, M. S. Rodriguez, L. F. Del Blanco, M. Pistonesi, and E. Agullo, *Colloid Polym. Sci.*, 1998, **276**, 1159.
- 11 K. Tokuchi, T. Ando, M. Kamigaito, and M. Sawamoto, *J. Polym. Sci. Pol. Chem.*, 2000, **38**, 4735.
- 12 T. Ando, M. Kamigaito, and M. Sawamoto, *Macromolecules*, 1998, **31**, 6708.
- 13 V. Coessens and K. Matyjaszewski, *Macromol. Rapid Commun.*, 1999, **20**, 66.

Chapter 6

Experimental

6.0 General Characterisation

^1H and ^{13}C NMR spectra were recorded on Bruker DPX 300 or DPX 400 spectrometers using deuterated solvents obtained from Aldrich or CEA. Elemental analyses were performed on a Leeman Labs CE 440 elemental analyser. Infrared absorption spectra were performed on a Bruker Vector 22 FTIR spectrometer fitted with a Golden Gate diamond attenuated total reflection (ATR) sample platform. Scanning electron microscopy (SEM) images were recorded using a JEOL JSM-6100 field emission microscope working at 10 kV. Prior to imaging by SEM, the samples were coated with a thin (~3 nm) layer of gold using a JEOL JFC 1100E gold sputterer. Static light scattering (SLS) measurements of star-shaped polymers were performed on a Malvern Autosizer 4800 instrument fitted with a 150 mW Nd/YAG green laser operating at a wavelength of 532 nm and an avalanche photodiode (ADP). SLS measurements were performed at 30 °C in THF at 12 independent angles between 30 and 140° with 60 separate 1 s measurements made over 60 s before averaging for each angle. Mass spectra were recorded on a Kratos MS80 or Micromass Autospec spectrometer using chemical ionization (CI) or electrospray ionization (EI) techniques.

SEC analysis was measured at ambient temperature using a Polymer Laboratories (PL) system equipped with a PL-gel 5 μm (50 x 7.5 mm) guard column and two PL-gel 5 μm (300 x 7.5 mm) mixed D columns. Data was collected at 1 point s^{-1} using a differential refractive index detector or UV detector eluted with THF at 1 mL min^{-1} . Absolute weight-average number (M_w) measurements by SEC were measured with a PL modular

SEC equipped with a low angle laser light scattering (LALLS; 5°, 2 mW HeNe laser) detector and a concentration detector linked in series with a PL-gel guard column and two PL-gel 5 μm (300 x 7.5 mm) mixed C columns with THF at 1 mL min⁻¹ as an eluent. The equipment was calibrated with narrow MWD PMMA or PST standards obtained from PL. Values obtained for M_n were subject to an error of 2-3 % while M_w values varied between 4-5 % between successive runs.

6.1 Reagents

Methyl methacrylate (Aldrich, 99 %) and styrene (Aldrich, 99 %) were passed through a short column of activated basic alumina to remove inhibitors and acidic impurities, degassed by bubbling with dry nitrogen for at least 30 minutes and stored at 0 °C prior to use. Toluene (BDH, 98 %), xylene (Aldrich, 98 %) and THF (Romil "Hi-Dry", 99.99 %) were degassed by bubbling with dry nitrogen for at least 30 minutes prior to use. Triethylamine was stored over sodium hydroxide pellets prior to use. β CD hydrate (Avocado, 98 %) was dried under vacuum at 80 °C over phosphorus pentoxide overnight prior to use. Pyridylmethanimine ligands were prepared as described previously¹. Silica gel with particle size 40-60 μm and pore diameter 60 Å (FluoroChem) was used for column chromatography. All other reagents not specifically mentioned were purchased from Aldrich and used as received.

6.2 Purification of copper (I) bromide

Copper (I) bromide (Avocado, 98 %) was purified by adapting the method used by Keller and Wycoff² for the purification of copper (I) chloride. Typically, copper (I) bromide (50 g, 0.35 mol) was ground to a fine powder in a mortar to which was added dilute sulfuric acid (2 M, 5 mL) to form a paste. This was added to a stirred solution of

sodium sulfite (2 M, 2 L) to give a fine white suspension in a blue solution of the copper (II) species. The white suspension was collected by careful vacuum filtration under a blanket of nitrogen whilst taking care not to expose the powder to air. The solid was washed with glacial acetic acid (250 mL), absolute ethanol (250 mL) and anhydrous diethyl ether (250 mL). Care was taken with each wash to ensure that the solid had minimum exposure to oxygen. The cream coloured product was isolated by removal of volatiles at 150 °C under vacuum for 12 hours and stored in a dark container prior to use. Yield = 83.4 %.

6.3 Synthesis of *N*-pentyl-2-pyridylmethanimine

The Schiff base ligand was prepared via modification to the method used by Bähr and Thamlitz³.

Pentylamine (25.0 mL, 0.22 mol) was slowly added dropwise to a stirred solution of pyridine-2-carboxaldehyde (20.6 mL, 0.22 mol) in diethyl ether (40 mL) at 0 °C. Dry magnesium sulfate (5 g) was added and the solution was stirred at room temperature for five hours. The solution was filtered under gravity and the diethyl ether was removed by rotary evaporation. The resulting orange oil was purified by distillation under reduced pressure. The product was obtained as a clear orange oil (bp. 81-83 °C at 4.4 mbar). Yield = 63.2 %.

¹H NMR (CDCl₃, 298 K, 300 MHz) δ (ppm from TMS) = 8.6 (d, J = 4.0 Hz, 1H, Pyr-H), 8.31 (s, 1H, N=CH), 7.92 (d, J = 7.7 Hz, 1H, Pyr-H), 7.65 (t, J = 7.7 Hz, 1H, Pyr-H), 7.26 (t, J = 5.0 Hz, 1H, Pyr-H), 3.61 (t, J = 5.6 Hz, 2H, N-CH₂), 1.69 (m, 2H, CH₂), 1.30 (t, 4H, CH₂CH₂), 0.87 (t, J = 7.3 Hz, 3H, CH₃).

^{13}C NMR (CDCl_3 , 298 K, 75 MHz) δ (ppm from TMS) = 160.66 ($\text{HC}=\text{N}$), 150.44, 138.91, 128.12, 126.76, 122.55 (Pyr-C), 62.73, 31.49, 30.40, 22.98 ($-\text{CH}_2-\text{CH}_2-\text{CH}_3$), 16.05 ($-\text{CH}_2-\text{CH}_3$).

IR absorption ν (cm^{-1}) = 3056, 3007 (Ar. C-H stretch), 2968-2853 (Alk. C-H stretch), 1650 (C=N stretch), 1588, 1567, 1467, 1438 (Ar. C-C stretch).

Mass spectrum: m/z = 177 (M + H).

Elemental analysis: 74.43 %C, 9.12 %H, 15.91 %N; (theoretical; 74.95 %C, 9.15 %H, 15.90 %N).

6.4 Synthesis of 2-bromoisobutyryl anhydride

2-Bromoisobutyric bromide (133.5 g, 581 mmol) was added dropwise at 0 °C to a cooled solution of 2-bromoisobutyric acid (80.9 g, 484 mmol) in anhydrous THF (800 mL) with triethylamine (80.7 mL, 581 mmol) and stirred at room temperature for five hours. The resulting triethylammonium bromide was removed by suction filtration and THF removed under reduced pressure to give a slightly dark solid. This residue was dissolved in dichloromethane (500 mL) and washed with a saturated NaHCO_3 solution (3 x 500 mL), dried over MgSO_4 , filtered and the solvent removed under reduced pressure to give a white solid that was recrystallised from cold *n*-hexane.

Yield = 85 %, mp = 63-65 °C.

^1H NMR (CDCl_3 , 298 K, 300 MHz) δ (ppm from TMS) 1.89 (s, 12H, 2-C-(CH_3)₂).

^{13}C NMR (CDCl_3 , 298 K, 75 MHz) δ (ppm from TMS) 172.9 (C=O), 40.3 (C-Br), 24.3 (C- CH_3).

IR absorption ν (cm^{-1}) = 2950 (Alk. C-H stretch), 1810 and 1740 (C=O stretch), 1050 (C-O stretch).

Mass spectrum: m/z = 317 (M + H).

6.5 Synthesis of heptakis(6-*O*-*tert*-butyldimethylsilyl)- β -cyclodextrin

β CD modified at the primary face was prepared via modification of the method used by Fügedi⁴.

To a stirred solution of dry β CD (19.2 g, 17 mmol) in anhydrous pyridine (150 mL) at 0 °C was added dropwise a solution of *tert*-butyldimethylchlorosilane (23.0 g, 152 mmol) in anhydrous pyridine (50 mL). The solution was stirred at room temperature overnight before being precipitated in a stirred mixture of ice and water (1500 mL) and collected by suction filtration as a white precipitate. The precipitate was purified by flash chromatography on a column of silica gel using a 16:2:1 ethyl acetate/ethanol/water mixture as eluent. The solvent was removed and the product dried under vacuum at 60 °C to give a white solid.

Yield = 85.3 %, mp = 315-320° (dec.)

¹H NMR (CDCl₃, 298 K, 300 MHz) δ (ppm from TMS) = 5.23-3.54 (63H, sugar residues), 0.86 (s, 63H, 7C-(CH₃)₃), 0.03 (s, 42H, 7Si-(CH₃)₂).

¹³C NMR (CDCl₃, 298 K, 75 MHz) δ (ppm from TMS) = 102.1 (C-1), 81.2 (C-4), 72.6-73.5 (C-2, C-3, C-5), 61.2 (C-6), 25.9 (C-(CH₃)₃), 18.3 (C-(CH₃)₃), -5.0 (Si-(CH₃)₂).

IR absorption ν (cm⁻¹) = 3300 (broad OH stretch), 2900 (Alk. C-H stretch), 1250 (Si-CH₃ stretch), 1000 (Si-O stretch).

6.6 Synthesis of heptakis(2,3-di-O-(2-bromo-2-methylpropionyl)-6-O-(tert-butyl dimethylsilyl))- β -cyclodextrin

To a stirred solution of heptakis(6-O-tert-butyl dimethylsilyl)- β -cyclodextrin (4.0 g, 2.1 mmol) in anhydrous pyridine (70 mL) and a catalytic amount of 4-(dimethylamino)pyridine was added 2-bromoisobutyric acid anhydride (27.7 g, 87 mmol). The solution was stirred at room temperature for three days. After this time, the pyridine was removed *in vacuo* to give a dark orange oil that was dissolved in dichloromethane (200 mL). The organic layer was washed successively with an HCl solution (1 N, 2 x 300 mL), saturated NaHCO₃ solution (2 x 300 mL), saturated brine (2 x 300 mL) and water (2 x 300 mL). The organic phase was dried over MgSO₄, filtered and the dichloromethane removed under reduced pressure to afford a pale yellow solid that was purified by flash chromatography on a column of silica gel using a 6:1 toluene/ethyl acetate mixture as eluent. The solvent was removed to give a white powder that was recrystallised from ethanol.

Yield = 27.0 %

¹H NMR (CDCl₃, 298 K, 300 MHz) δ (ppm from TMS) = 5.22-3.68 (49H, sugar residues), 1.91 (m, 84H, 14C-(CH₃)₂), 0.86 (s, 63H, 7C-(CH₃)₃), 0.03 (s, 42H, 7Si-(CH₃)₂).

¹³C NMR (CDCl₃, 298 K, 75 MHz) δ (ppm from TMS) = 172.4 and 170.6 (C=O), 102.1 (C-1), 82.1 (C-4), 73.2-72.5 (C-2, C-3, C-5), 60.8 (C-6), 56.8 and 55.6 (C-Br), 31.6-30.9 (C-CH₃), 24.6 (C-(CH₃)₃), 17.8 (C-(CH₃)₃), -5.0 (Si-(CH₃)₂).

Elemental analysis: 44.38 %C, 6.62 %H; (theoretical; 41.82 %C, 5.97 %H)

IR absorption ν (cm⁻¹) = 2900 (Alk. C-H stretch), 1740 (C=O stretch), 1250 (Si-CH₃ stretch), 1000 (Si-O stretch).

6.7 Synthesis of heptakis(2,3,6-tri-*O*-(2-bromo-2-methylpropionyl)- β -cyclodextrin

To a solution of dry β CD (2.3 g, 2 mmol) in anhydrous pyridine (20 mL) was added a solution of 2-bromoisobutyryl anhydride (40 g, 128 mmol) in anhydrous pyridine (20 mL) together with a catalytic amount of 4-(dimethylamino)pyridine. The mixture was stirred at room temperature for four days and the resulting orange solution was concentrated under reduced pressure and diluted with dichloromethane (150 mL). The organic layer was washed successively with an HCl solution (1 N, 2 x 150 mL), saturated NaHCO₃ (2 x 150 mL), saturated brine (2 x 200 mL) and water (2 x 150 mL). The organic phase was dried over MgSO₄, filtered and the dichloromethane removed under reduced pressure to give a dark orange oil that was purified by flash chromatography on a column of silica gel using a 3:1 toluene/ethyl acetate mixture as eluent. The resulting clear yellow oil was crystallised from cold *n*-hexane to give a white solid.

Yield = 17 %, mp = 230-240 °C (dec.)

¹H NMR (CDCl₃, 298 K, 300 MHz) δ (ppm from TMS) = 5.4-3.5 (m, 49H sugar residues), 1.81 (s, 126H, CH₃).

¹³C NMR (CDCl₃, 298 K, 75 MHz) δ (ppm from TMS) = 171.4 (C=O), 97.7, 81.5, 73.8-70.4, 64.3 (sugar carbons), 56.4 (C-Br), 31.3-30.8 (C-CH₃).

IR absorption ν (cm⁻¹) = 2970, 2930 (Alk. Stretch), 1740 (C=O stretch).

Elemental analysis: 35.73 %C, 4.22 %H; (theoretical; 35.49 %C, 4.15 %H).

6.8 Synthesis of heptakis(2,3-di-*O*-acetyl-6-*O*-*tert*-butyldimethylsilyl)- β -cyclodextrin

This β CD derivative was prepared via modification of the procedure used by Takeo *et al.* for the α CD analogue⁵.

To a solution of heptakis(6-*O*-*tert*-butyldimethylsilyl)- β -cyclodextrin (21.0 g, 11 mmol) in anhydrous pyridine (40 mL) was added acetic anhydride (43 mL, 0.46 mol) together with a catalytic amount of 4-(dimethylamino)pyridine. The solution was stirred for three days after which time the pyridine was removed under reduced pressure. The resulting orange oil was diluted with dichloromethane (200 mL) and washed successively with an HCl solution (1 N, 2 x 300 mL), saturated NaHCO₃ (2 x 300 mL), saturated brine (2 x 300 mL) and water (2 x 300 mL). The organic phase was dried over MgSO₄, filtered and the dichloromethane removed under reduced pressure to give a white solid that was dried under vacuum at room temperature.

Yield = 61 %

¹H NMR (CDCl₃, 298 K, 300 MHz) δ (ppm from TMS) = 5.30-3.66 (49H, sugar residues), 2.20 and 2.21 (2s, each 21H, 14-OC(CH₃)), 0.86 (s, 63H, 7-C(CH₃)₃), 0.02 (s, 42H, 7-Si(CH₃)₂).

¹³C NMR (CDCl₃, 298 K, 75 MHz) δ (ppm from TMS) = 171.0 and 169.2 (C=O), 96.5 (C-1), 75.3 (C-4), 71.9-71.3 (C-2, C-3, C-5), 61.9 (C-6), 25.9 (C-(CH₃)₃), 20.8 (COCH₃), 18.3 (C-(CH₃)₃), -5.0 (Si-(CH₃)₂).

IR absorption ν (cm⁻¹) = 2850 (Alk. C-H stretch), 1720 (C=O), 1050 (C-O stretch).

Elemental analysis: 53.62 %C, 8.12 %H; (theoretical; 53.31 %C, 7.83 %H).

6.9 Synthesis of heptakis(2,3-di-*O*-acetyl)- β -cyclodextrin

To a solution of heptakis(2,3-di-*O*-acetyl-6-*O*-*tert*-butyldimethylsilyl)- β -cyclodextrin (15.0 g, 6 mmol) in anhydrous dichloromethane (180 mL) was added a 50 % solution of BF₃ in anhydrous diethyl ether (15 mL). The solution was stirred at room temperature for 24 hours then diluted with dichloromethane (200 mL) and washed with water (400 mL) before being dried over Na₂SO₄, filtered and the dichloromethane removed under reduced pressure. The resulting white solid was purified by flash chromatography on a column of silica gel using a 16:2:1 ethyl acetate/ethanol/water as eluent and dried under vacuum at room temperature.

Yield = 57 %, mp = 191-196 °C

¹H NMR (CDCl₃, 298 K, 300 MHz) δ (ppm from TMS) = 5.38-3.72 (56H, sugar residues), 2.06 (s, 42H, 14-CH₃).

¹³C NMR (CDCl₃, 298 K, 75 MHz) δ (ppm from TMS) = 170.1 and 169.3 (C=O), 96.3 (C-1), 75.2 (C-4), 72.0 (C-2), 71.3 (C-3), 70.3 (C-5), 61.2 (C-6), 20.5 (COCH₃).

IR absorption ν (cm⁻¹) = 3250 (broad O-H stretch), 1720 (C=O stretch), 1050 (C-O stretch).

Elemental analysis: 49.86 %C, 5.31 %H; (theoretical; 48.78 %C, 5.73 %H).

6.10 Synthesis of heptakis(2,3-di-*O*-acetyl-6-*O*-(2-bromo-2-methylpropionyl))- β -cyclodextrin

To a solution of heptakis(2,3-di-*O*-acetyl)- β -cyclodextrin (5.0 g, 3 mmol) in anhydrous pyridine (70 mL) was added 2-bromoisobutyric acid anhydride (19.0 g, 60 mmol) together with a catalytic amount of 4-(dimethylamino)pyridine. The solution was stirred at room temperature for three days. Removal of the pyridine under reduced pressure gave an orange oil that was diluted with dichloromethane (200 mL) and washed

successively with an HCl solution (1 N, 200 mL), saturated NaHCO₃ (200 mL), saturated brine (200 mL) and water (200 mL). The organic phase was dried over MgSO₄, filtered and the dichloromethane removed under reduced pressure to give a slightly yellow solid that was precipitated twice from petroleum ether (bp 40-60 °C) and dried under vacuum at room temperature.

Yield = 8 %

¹H NMR (CDCl₃, 298 K, 300 MHz) δ (ppm from TMS) = 5.32-3.81 (49H, sugar residues), 2.02 (s, 42H, 14-CH₃), 1.92 (s, 42H, 7-(CH₃)₂).

¹³C NMR (CDCl₃, 298 K, 75 MHz) δ (ppm from TMS) = 171.5, 170.2 and 169.5 (C=O), 96.3 (C-1), 72.0 (C-2), 71.3 (C-3), 70.3 (C-5), 61.2 (C-6), 20.5 (COCH₃).

IR absorption ν (cm⁻¹) = 1730 (C=O stretch), 1050 (C-O stretch).

Elemental analysis: 46.26 %C, 5.63 %H; (theoretical; 42.55 %C, 4.85 %H).

6.11 Polymerisation procedure

All polymerisations were carried out using Schlenk apparatus under dry nitrogen. In a typical polymerisation, the solid reagents and a dry magnetic follower were charged to a pre-dried Schlenk tube. The tube was sealed with a rubber septum and the tube evacuated and flushed with nitrogen three times. The degassed monomer and degassed solvent were then added via oven-dried degassed syringes and the Schlenk tube was subjected to three freeze pump thaw degassing cycles. The tube was brought to reaction temperature in a stirred, thermostatted oil bath and held for five minutes for the reagents to reach equilibrium before the complexing ligand was added under nitrogen. Samples were removed periodically using degassed syringes under a blanket of nitrogen for conversion analysis and molecular weight analysis. PMMA and PST samples were diluted with THF and passed down a short column of basic alumina to remove copper

complexes prior to molecular weight analysis. Conversion was determined using gravimetry by accurately weighing a sample into a pre-weighed aluminium pan and removing the volatile monomer and solvent in a vacuum oven thermostatted at 60 °C until a constant sample weight was achieved. For samples involving non-volatile monomers, conversion was determined using ^1H NMR by integrating the appropriate regions of the spectrum.

6.12 Isolation and purification of polymers

Polymers in kinetic experiments were prepared by LRP using copper (I) bromide and *N*-pentyl-2-pyridylmethanimine as a complexing ligand. The copper complex was fully soluble in a mixture of either monomer/toluene or monomer/xylene at the reaction temperature but relatively insoluble at room temperature. Once a polymerisation was complete, the solution was allowed to cool to room temperature and passed down a column of basic alumina to remove the copper complexes and precipitated in either petroleum ether (bp. 40 – 60 °C) for PMMA or cold methanol for PST. The polymer was collected by filtration under gravity and dried under vacuum at room temperature. Polymers prepared in this way were usually white for PMMA and pale green for PST.

6.13 Copper mediated LRP of MMA initiated by heptakis(2,3,6-tri-*O*-(2-bromo-2-methylpropionyl)- β -cyclodextrin ([M]:[Cu]:[L]:[I] = 500:2:4:1)

To a pre-dried Schlenk tube was added copper (I) bromide (28 mg, 0.20 mmol), heptakis(2,3,6-tri-*O*-(2-bromo-2-methylpropionyl)- β -cyclodextrin (20 mg, 4.7×10^{-3} mmol) and a dry stirrer bar. The tube was sealed with a rubber septum and evacuated and filled with nitrogen three times. Toluene (5.5 mL, 50 % w/v) and MMA (5.3 mL, 49 mmol) were added under a blanket of nitrogen and the Schlenk

tube was subjected to three freeze pump thaw degassing cycles and subsequently heated to 60 °C in a thermostatted oil bath with magnetic stirring. Once this reaction temperature had been maintained for five minutes, *N*-pentyl-2-pyridylmethanimine (58 mg, 0.392 mmol) was added under nitrogen ($t = 0$). Samples were removed periodically using a degassed syringe for molecular weight and conversion analysis.

6.14 Copper mediated LRP of MMA initiated by heptakis(2,3-di-*O*-(2-bromo-2-methylpropionyl)-6-*O*-(*tert*-butyldimethylsilyl))- β -cyclodextrin ([M]:[Cu]:[L]:[I] = 500:4:8:1)

To a pre-dried Schlenk tube was added copper(I)bromide (30 mg, 0.21 mmol), heptakis(2,3-di-*O*-(2-bromo-2-methylpropionyl)-6-*O*-(*tert*-butyldimethylsilyl))- β -cyclodextrin (15 mg, 4.98×10^{-3} mmol) and a dry stirrer bar. The tube was sealed with a rubber septum and evacuated and filled with nitrogen three times. Toluene (3.0 mL, 50 % w/v) and MMA (2.8 mL, 26 mmol) were added under a blanket of nitrogen and the Schlenk tube was subjected to three freeze pump thaw degassing cycles and subsequently heated to 60 °C in a thermostatted oil bath with magnetic stirring. Once this reaction temperature had been maintained for five minutes, *N*-pentyl-2-pyridylmethanimine (0.08 mL, 0.42 mmol) was added under nitrogen ($t = 0$). Samples were removed periodically using a degassed syringe for molecular weight and conversion analysis.

6.15 Copper mediated LRP of MMA initiated by heptakis(2,3-di-*O*-acetyl-6-*O*-(2-bromo-2-methylpropionyl))- β -cyclodextrin ([M]:[Cu]:[L]:[I] = 500:4:8:1)

To a pre-dried Schlenk tube was added copper(I)bromide (30 mg, 0.21 mmol), heptakis(2,3-di-*O*-acetyl-6-*O*-(2-bromo-2-methylpropionyl))- β -cyclodextrin (21 mg,

7.5×10^{-3} mmol) and a stirrer bar. The tube was sealed with a rubber septum and evacuated and filled with nitrogen three times. Toluene (3.1 mL, 48 % w/v) and MMA (3.0 mL, 28 mmol) were added under a blanket of nitrogen and the Schlenk tube was subjected to three freeze pump thaw degassing cycles and subsequently heated to 60 °C in a thermostatted oil bath with magnetic stirring. Once this reaction temperature had been maintained for five minutes, *N*-pentyl-2-pyridylmethanimine (0.08 mL, 0.42 mmol) was added under nitrogen ($t = 0$). Samples were removed periodically using a degassed syringe for molecular weight and conversion analysis.

6.16 Copper mediated LRP of PMMA-*b*-PBMA initiated by heptakis(2,3-di-*O*-(2-bromo-2-methylpropionyl)-6-*O*-(*tert*-butyldimethylsilyl))- β -cyclodextrin ([M]:[Cu]:[L]:[I] = 500:4:8:1)

To a pre-dried Schlenk tube was added copper(I)bromide (24.2 mg, 0.17 mmol) and a dry stirrer bar. The tube was sealed with a rubber septum and evacuated and filled with nitrogen three times. A solution of star-shaped PMMA initiated by heptakis(2,3-di-*O*-(2-bromo-2-methylpropionyl)-6-*O*-(*tert*-butyldimethylsilyl))- β -cyclodextrin (90.4 mg, 3×10^{-3} mmol, macroinitiator $M_n = 27\,000 \text{ g mol}^{-1}$), ⁿBMA (3.2 mL, 21 mmol) and toluene (3.2 mL, 50 % w/v) was added under a blanket of nitrogen and the tube was subjected to three freeze pump thaw degassing cycles. The tube was heated to 60 °C in a thermostatted oil bath and maintained at this temperature for five minutes. After this time, *N*-pentyl-2-pyridylmethanimine (0.06 mL, 0.34 mmol) was added under nitrogen ($t = 0$). Samples were removed periodically using a degassed syringe for molecular weight and conversion analysis.

6.17 Copper mediated LRP of MMA initiated by ethyl-2-bromoisobutyrate followed by dehalogenation of end groups ([M]:[Cu]:[L]:[I] = 100:1:2:1)

To a pre-dried Schlenk tube was added copper(I)bromide (72 mg, 0.51 mmol) and a stirrer bar. The tube was sealed with a rubber septum and evacuated and filled with nitrogen three times. A solution of MMA (5.4 mL, 50.4 mmol), ethyl-2-bromoisobutyrate (0.08 mL, 0.52 mmol) and toluene (6.2 mL, 53 % w/v) was added under a blanket of nitrogen and the tube was subjected to three freeze pump thaw degassing cycles. The tube was heated to 90 °C in a thermostatted oil bath and maintained at this temperature for five minutes. After this time, *N*-pentyl-2-pyridylmethanimine (0.2 mL, 1.1 mmol) was added under nitrogen ($t = 0$). After 30 minutes a sample was taken and 1-phenyl-1-(trimethylsilyloxy)ethylene (1.0 mL, 5.1 mmol) was added to the reaction to quench the polymerisation. Samples were taken periodically over 20 hours for molecular weight analysis. After this time the dehalogenated PMMA was isolated as described previously.

6.18 Synthesis of (poly(ethylene glycol) methyl ether)-2-bromoisobutyrate (MeOPEG-I₄₅)

Poly(ethylene glycol) methyl ether ($x = 45$, 20 g, 10 mmol) was dissolved in anhydrous THF (300 mL) and triethylamine (1.7 mL, 12 mmol). 2-Bromoisobutyryl bromide (1.5 mL, 12 mmol) was added dropwise under an atmosphere of dry nitrogen. The reaction mixture was stirred for 48 hours at room temperature and the triethylammonium bromide salt filtered. The organic phase was dissolved in dichloromethane (200 mL) and washed successively with saturated NaHCO₃ solution (2 x 200 mL), dried over MgSO₄, filtered and the solvent removed under vacuum. The

product was precipitated in cold diethyl ether and collected by filtration under gravity to give a white solid.

Yield = 82 %

^1H NMR (CDCl_3 , 298 K, 300 MHz) δ (ppm from TMS) = 4.27 (t, $J = 4.9$ Hz, 2H, $\text{CH}_2\text{-O-CO-}$), 3.69 (t, $J = 4.9$ Hz, 2H, $-\text{CH}_2\text{-CH}_2\text{-O-CO-}$), 3.59 (m, 180H, $(\text{CH}_2\text{-CH}_2\text{-O})_{45}$), 3.41 (s, 3H, $-\text{O-CH}_3$), 1.84 (s, 6H, $\text{C-(CH}_3)_2$).

^{13}C NMR (CDCl_3 , 298 K, 100.6 MHz) δ (ppm from TMS) = 171.2 (C=O), 77.1, 67.7, 64.1, 53.9, 29.7.

IR absorption ν (cm^{-1}) = 2860 (Alk. C-H stretch), 1730 (C=O), 1465, 1275, 1090 (C-O stretch).

Elemental analysis: 53.01 %C, 8.92 %H; (theoretical; 52.74 %C, 8.81 %H).

6.19 Copper mediated LRP of ST initiated by MeOPEG- I_{45} macroinitiator

To a pre-dried Schlenk tube was added copper (I) bromide (36 mg, 0.25 mmol) together with a stirrer bar and the tube maintained under an atmosphere of nitrogen. A mixture of deoxygenated ST (27.6 mL, 0.24 mol), deoxygenated xylene (12 mL, 33 % w/v) and (poly(ethylene glycol) methyl ether)-2-bromisobutyrate (5 g, 2.3 mmol) was added to the tube at room temperature and the mixture was deoxygenated by three freeze-pump-thaw cycles. *N*-pentyl-2-pyridylmethanimine (0.09 mL, 0.5 mmol) was added using a degassed syringe and the tube was immersed in an oil bath thermostatted at 110 °C. Samples were removed periodically for molecular weight analysis and conversion calculations. After a typical reaction time of 24 h, the solution was cooled to room temperature, passed over a column of basic alumina, and the solvent removed under vacuum. The product was precipitated in cold methanol and filtered on sintered glassware to give a slightly green powdered product.

6.20 Hydrolysis of star-shaped PMMA polymers

To a pre-dried round bottom flask fitted with a condenser, nitrogen inlet and a stirrer bar was added the star-shaped PMMA (100 mg, M_w (LALLS) = 129 000 g mol⁻¹). The polymer was dissolved in THF (10 mL). Then, KOH (1 mL, 1 M solution in methanol) was added. The solution was refluxed for 18 hours. After this time the solvent was removed under vacuum and the resulting polymer was precipitated in water and dried under vacuum at room temperature to yield a white solid.

$$M_n = 11\ 000\ \text{g mol}^{-1}, \text{PDI} = 1.12$$

6.21 Hydrolysis of star-shaped PST polymers

To a round bottom flask fitted with a condenser, nitrogen inlet and a stirrer bar was added the star shaped PST (150 mg, M_w (LALLS) = 220 000g mol⁻¹). The polymer was dissolved in THF (10 mL). Then, KOH (3 mL, 1 M solution in ethanol) and water (0.33 mL) was added and the solution was refluxed for three days. After this time any remaining solvent was removed under vacuum and the resulting polymer was dissolved in THF, precipitated in methanol and dried under vacuum at room temperature to yield a white solid.

$$M_n \text{ (SEC)} = 10\ 500\ \text{g mol}^{-1}, \text{PDI} = 1.09$$

6.22 Copper mediated LRP of MMA initiated by heptakis(2,3-di-*O*-(2-bromo-2-methylpropionyl)-6-*O*-(*tert*-butyldimethylsilyl))- β -cyclodextrin ([M]:[Cu]:[L]:[I] = 500:4:8:1) followed by dehalogenation of end groups

To a pre-dried Schlenk tube was added copper(I)bromide (229 mg, 1.6 mmol), heptakis(2,3-di-*O*-(2-bromo-2-methylpropionyl)-6-*O*-(*tert*-butyldimethylsilyl))- β -cyclodextrin (115 mg, 0.03 mmol) and a stirrer bar. The tube was sealed with a rubber septum and evacuated and filled with nitrogen three times. A solution of MMA (21 mL, 0.2 mol) and toluene (21 mL, 50 % w/v) was added under a blanket of nitrogen and the tube was subjected to three freeze pump thaw cycles. The tube was placed in an oil bath thermostatted at 60 °C and maintained at this temperature for five minutes prior to *N*-pentyl-2-pyridylmethanimine (0.61 mL, 3.2 mmol) being added ($t = 0$). After one hour a sample was taken, the reaction stopped, and the star-shaped polymer was isolated and purified as described previously.

$$M_w = 35\,000 \text{ g mol}^{-1}, \text{ PDI} = 1.11$$

The isolated star-shaped PMMA (0.2 g, 0.007 mmol) was charged to a Schlenk tube together with copper(I)bromide (56 mg, 0.4 mmol) and a stirrer bar. The tube was sealed with a rubber septum and evacuated and filled with nitrogen three times. 1-phenyl-1-(trimethylsilyloxy)ethylene (0.383 mL, 1.88 mmol) and toluene (1.7 mL, 40 % w/v) was added under a blanket of nitrogen. The tube was placed in an oil bath thermostatted at 60 °C and maintained at this temperature for five minutes prior to *N*-pentyl-2-pyridylmethanimine (0.15 mL, 0.8 mmol). Samples were taken periodically for molecular weight analysis to ensure that the 1-phenyl-1-(trimethylsilyloxy)ethylene had quenched the reaction.

6.23 Deprotection of TBDMS groups from star-shaped PMMA with deactivated end groups

To a pre dried round bottom flask was added heptakis(2,3-di-*O*-(poly(methyl methacrylate)-6-*O*-(*tert*-butyldimethylsilyl))- β -cyclodextrin with deactivated chain ends as described previously (0.5 g, 0.02 mmol), dry DCM (8 mL), boron trifluoride diethyl etherate (1.5 mL) and a stirrer bar. The solution was magnetically stirred overnight before being diluted with dichloromethane (20 mL) and washed with water (2 x 20 mL). The organic layer was dried over Na₂SO₄, filtered, and the dichloromethane was removed under reduced pressure. The resulting solid was precipitated in petroleum ether (bp. 40 – 60 °C) and freeze-dried from benzene to yield an off-white solid.

It was noted that the shifts at 0 ppm corresponding to the Si(CH₃)₂ in the ¹H NMR spectra had disappeared.

IR absorption ν (cm⁻¹) = 3250 (broad OH stretch)

6.24 Attempted Synthesis of heptakis(2,3-di-*O*-(poly(methyl methacrylate)-6-*O*-(2-bromo-2-methylpropionyl))- β -cyclodextrin

To a pre dried round bottom flask was added heptakis(2,3-di-*O*-(poly(methyl methacrylate)- β -cyclodextrin with deactivated chain ends (0.56 g, 0.03 mmol), anhydrous pyridine (8 mL) and a stirrer bar. 2-Bromoisobutyryl bromide (0.08 mL, 0.6 mmol) was added to the solution at 0 °C and the mixture was magnetically stirred at room temperature for five hours. After this time the pyridine was removed under vacuum and the resulting product dissolved in acetone and precipitated in water.

6.25 Preparation of microporous polymeric membranes

A solution of either star-shaped PST in carbon disulfide (10 mg mL^{-1}) or star-shaped PMMA in chloroform (10 mg mL^{-1}) was prepared and a thin film of this solution was cast onto a glass support inside a humidity chamber maintained between 60 – 80 % relative humidity and between 17 – 20 °C. The solution was dried with a humid air flow for three minutes via a nozzle positioned 1 – 2 cm above the polymer solution. The rate of air flow was measured with a flow meter and was typically 1000 mL min^{-1} . Saturation of the air flow was achieved by bubbling the air through a water reservoir. The resulting polymeric films had a turbid appearance. The glass supports containing the polymeric films were then mounted onto carbon stubs and coated in a thin layer ($\sim 3 \text{ nm}$) of gold using a sputterer. The morphology of these membranes were then examined using SEM.

6.26 Determination of absolute molecular weight of star-shaped polymers using static light scattering (SLS)

A stock solution of star-shaped PST in THF (2 g L^{-1} , THF filtered three times through $0.02 \mu\text{m}$ membrane filters in a laminar flow cabinet) was prepared and left to stand overnight. Three further concentrations of 1.5 g L^{-1} , 1.0 g L^{-1} and 0.5 g L^{-1} were prepared from this stock solution and also left to stand overnight. Each of the four concentrations of star-shaped PST were filtered twice through $0.02 \mu\text{m}$ membrane filters in a laminar flow cabinet and again left to stand overnight. Prior to any measurements being made the vat of the SLS spectrometer was purged with distilled water for one hour and the laser allowed to stabilize for one hour. The spectrometer was calibrated with toluene filtered three times through $0.02 \mu\text{m}$ membrane filters into a quartz Burchard cell in a laminar flow cabinet. For each of the four concentrations of star-

shaped PST, measurements were recorded at 12 angles between 30 and 140° with 60 separate 1 s measurements made over 60 s before averaging for each angle. The Zimm Plot subsequently obtained shows the variation in intensity with change in angle and concentration. The intercept of a double extrapolation to zero concentration and zero angle is proportional to the reciprocal of the absolute molecular weight and hence the absolute molecular weight of the sample can be determined.

6.27 Chapter 6 References

- 1 D. M. Haddleton, D. J. Duncalf, D. Kukulj, M. C. Crossman, S. G. Jackson, S. A. F. Bon, A. J. Clark, and A. J. Shooter, *Eur. J. Inorg. Chem.*, 1998, 1799.
- 2 R. N. Keller and H. D. Wycoff, *Inorganic syntheses*, 1946, **2**, 1.
- 3 V. G. Bahr and Z. Thamlitz, *Anorg. Allg. Chem*, 1955, **282**, 3.
- 4 P. Fügedi, *Carbohydr. Res.*, 1989, **192**, 366.
- 5 K. Takeo and H. Maeda, *J. Carbohydr. Chem.*, 1988, **7**, 309.